CHALMERS
UNIVERSITY OF TECHNOLOGY

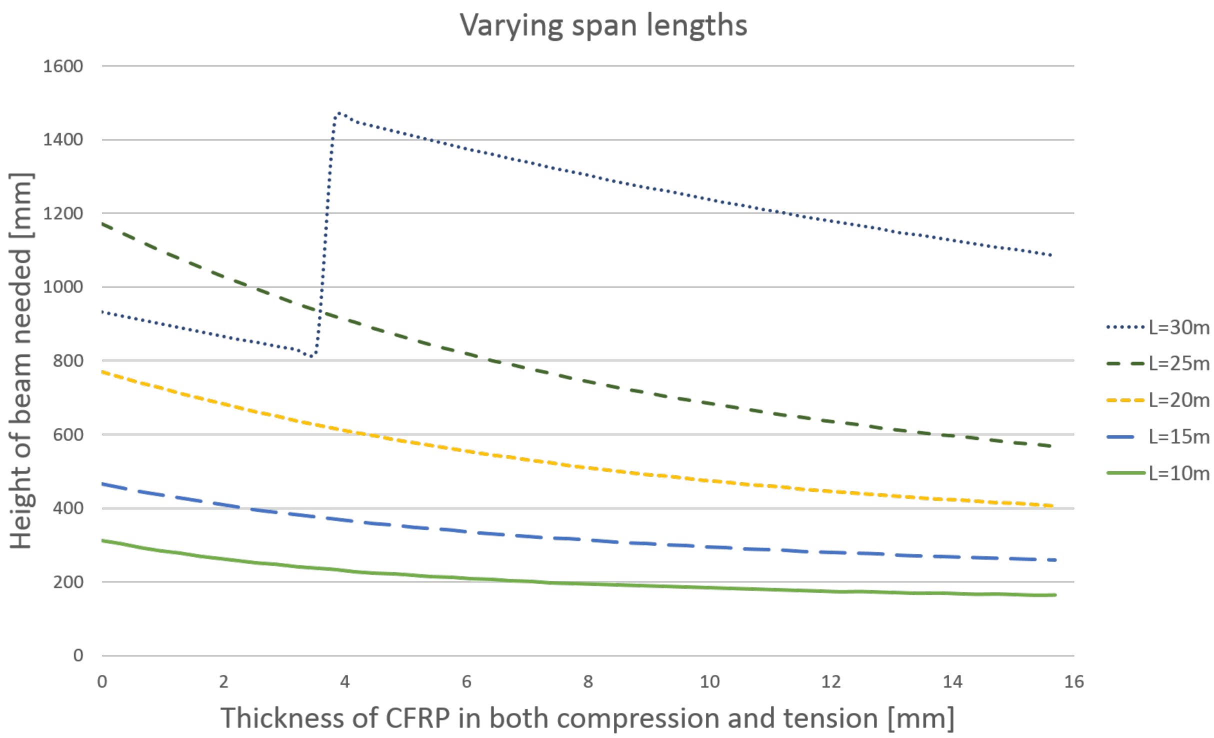

Assessment and Optimisation of CFRP Reinforced Glulam Beams

A feasibility study in design stage reinforcement configurations for pedestrian bridge applications

Master's Thesis in Master Program Structural Engineering and Building Technology

Adam Lennell

Christoffer Jonsson

Department of Architecture and Civil Engineering
Division of Structural Engineering
Lightweight Structures
CHALMERS UNIVERSITY OF TECHNOLOGY
Master's Thesis ACEX30-19-104
Gothenburg, Sweden 2019

Master's thesis ACEX30-19-104

Assessment and Optimisation of CFRP Reinforced Glulam Beams

A feasibility study in design stage reinforcement configurations for pedestrian bridge applications

Adam Lennell

Christoffer Jonsson

Department of Architecture and Civil Engineering
Division of Structural Engineering
Lightweight Structures Group
Chalmers University of Technology
Gothenburg, Sweden 2019

Assessment and Optimisation of CFRP Reinforced Glulam Beams
A feasibility study in design stage reinforcement configurations for pedestrian bridge applications

Adam Lennell

Christoffer Jonsson

Supervisor: Magnus Bäckström and Georgi Nedev, Structural Engineers at Sweco Civil AB, Gothenburg
Examiner: Associate Professor Reza Haghani Dogaheh, Department of Architecture and Civil Engineering

Master's Thesis ACEX30-19-104
Department of Architecture and Civil Engineering
Division of Structural Engineering
Lightweight Structures Group
Chalmers University of Technology
SE-412 96 Gothenburg
Telephone +46 31 772 1000

Cover: The result of the parametric study regarding varying span.

Typeset in LaTeX
Department of Architecture and Civil Engineering
Gothenburg, Sweden 2019

Assessment and Optimisation of CFRP Reinforced Glulam Beams
A feasibility study in design stage reinforcement configurations for pedestrian bridge applications
Adam Lennell
Christoffer Jonsson
Department of Architecture and Civil Engineering
Chalmers University of Technology

Abstract

Timber has throughout history been a widely used construction material due to high availability and easy access. For civil engineering structures, the technical advancement and increased loads have made other materials, such as concrete and steel, more suitable. However, with a rising environmental concern, timber structures can serve as a more sustainable alternative. To address the growing demands, Carbon Fibre Reinforced Polymer (CFRP) laminas can be used to increase the flexural strength and stiffness in timber structural elements. By embedding the reinforcement in Glued Laminated Timber (Glulam) in the production stage, the structure can be designed with higher capacity or smaller dimensions. Further on, embedding the CFRP laminas gives a better protection towards moisture and UV-radiation, which otherwise might lead to chemical deterioration and loss of structural integrity.

In this thesis, the concept of embedding CFRP in glulam beams was evaluated for pedestrian bridge applications. In design of timber pedestrian bridges, frequency and deflection demands are often governing, which usually results in structures with relatively large dimensions. Focus was therefore put on decreasing the structural height of the beams, making the concept applicable in cases where plain timber otherwise is not an option. In extension, the concept could also be used to decrease floor heights in timber high-rise buildings or create longer spans in warehouses, industrial halls and indoor arenas.

Analytic calculations were performed to evaluate two beam configurations and to perform a preliminary sizing of a stress-laminated deck bridge. The concept was then evaluated with finite element analyses, where the purpose was to evaluate the shear stresses between timber and CFRP. To investigate the economic viability, an economic comparison with two pedestrian bridges in glulam and steel was performed.

The analytic analysis showed that it was possible to reduce the height with at least 25% using a small amount of CFRP. Since CFRP is more expensive than timber, it is of interest to optimise this relation. It was shown that reinforcing the glulam beam with a small amount of CFRP is not significantly more expensive compared to an unreinforced beam, regarding material cost. The FE-analyses showed that the shear stresses between timber and CFRP would not cause a problem and that adding a pre-camber does not increase these stresses significantly.

In conclusion, it was found that reinforcing the beam did reduce the height without compromising the structural capacity or economic feasibility. Further on, it was shown that it can compete within the same field as other lightweight structures.

Keywords: CFRP Reinforcement, Timber, Pedestrian Bridge, Glulam, Composite.

Acknowledgements

We, the authors, are greatly humble for the fantastic opportunity we had to work on this inspiring project and produce this thesis. The thesis marks the ending of a journey embarked on by us six years ago, the autumn of 2013. From this day on, a new journey embarks and launches us into new challenges and future adventures. Of course, we could not have been able to do it all by ourselves, which is why we would like to take this page to direct some recognition.

To begin with, we would like to direct our gratitude to Associate Professor Reza Haghani Dogaheh, not only responsible for making sure that this thesis held up to the academic standards of Chalmers, but also for being a great support throughout our work.

Additionally, we would like to thank Sweco AB for providing us with an office space and generously sharing the knowledge of their employees. Especially we would like to thank our two supervisors Magnus Bäckström and Georgi Nedev, whom have been an invaluable help to us by making this work progress.

We would like to give our thanks to Emil Martinson, Structural Engineer at Martinsons Trä, and Martinsons Trä for arranging an interesting study visit to their factories, and the sites of some of their creations. The great support when it came to practical questions about glulam and timber bridge production were also highly valued.

Further on, we would like to thank our opponents Jonathan Söderqvist and Lars Scheidegger for a continuous fine cooperation and great discussions.

Finally we would like to thank our friend August Jansson for reminding us about when to take a coffee break.

Adam Lennell
Christoffer Jonsson
Gothenburg, June 2019

Contents

Nomenclature

The list explains several symbols, letters and variables that will be later used within the body of the document.

Upper case letters

E	Modulus of elasticity
$E_{0.05}$	Modulus of elasticity 5th procentile
E_{CFRP}	Modulus of elasticity CFRP
E_L	Modulus of elasticity longitudinal direction
E_{mean}	Mean modulus of elasticity
E_R	Modulus of elasticity radial direction
E_T	Modulus of elasticity transversal direction
G	Shear modulus
G_{LR}	Shear modulus longitudinal/radial direction
G_{LT}	Shear modulus longitudinal/transversal direction
G_{RT}	Shear modulus radial/transversal direction
I	Second moment of area
L	Length of beam or free span
Q	Axis load from service vehicle
S	First moment of area

Lower case letters

a	Acceleration
f	Frequency
$f_{.d}$	Design material parameter
$f_{.k}$	Characteristic material parameter
g	Self-weight

h_{CFRP}	Height of the CFRP in either compression or tension
h_{glulam}	Height of the glulam part
k_{cr}	Factor considering cracks for shear resistance
k_{def}	Factor considering deformations of glulam
k_h	Factor considering size effects for glulam
k_{mod}	Factor considering duration of load and service class
q	Uniformly distributed load

Greek letters

α	Transformation factor for composite cross section
α_e	Temperature expansion coefficient
δ	Deflection
γ	Partial material safety factor
μ	Frictional coefficient
ν_{CFRP}	Poisson's ratio CFRP
ν_{LR}	Poisson's ratio logitudinal/radial direction
ν_{LT}	Poisson's ratio longitudinal/transversal direction
ν_{RT}	Poisson's ratio radial/transversal direction
π	The value of Pi
ψ_{red}	Reduction factor for traffic load in deflection calculations
ρ	Density
σ	Stress
τ	Shear
ε	Strain
ζ	Damping coefficient

List of Figures

List of Tables

1 Introduction

Timber has throughout history been a widely used construction material, especially in Scandinavia where the amount of accessible forest is high. However, with an increasing demand for high-rise buildings and long span bridges, more suitable materials such as concrete and steel were introduced in a larger scale. The structural capacity of plain timber is limited and therefore its suitability in the field of construction is diminished (Johansson, 2016). Thereby, to increase the area of application, Engineering Wood Products (EWP) and methods to strengthen them arrived (Schober et al., 2015). The first EWP to ever be used was Glued Laminated Timber (Glulam) in 1906 (Gentile, 2000), which increased the possible span for timber bridges and introduced a possibility to design taller buildings.

Today there is an increasing demand for sustainable materials, which makes timber structures an alternative to mitigate environmental problems. However, due to mentioned limitations when it comes to strength and also dynamic performance, timber was never a competitor for long span bridges (Pousette, 2001). Because of this, a highly relevant topic within structural engineering is how to strengthen timber. Strengthening can make it possible to use timber in more advanced structures, where the material itself (e.g. plain timber, EWPs) does not possess the needed strength or stiffness properties.

The general demands for sustainable structures make concepts for strengthening timber structures applicable worldwide. In a more local perspective, the city of Gothenburg, Sweden, has expressed a will to build more crossings over the canal in the centre of the city (Eurenius, 2017). These crossings are mainly to increase the capacity of the existing walking and bicycling paths. It is not necessarily a long span or a challenging site that is limiting, but rather availability with regard to structural height. Therefore, it is of interest to strengthen these bridges so that a lower structural height of the main beams can be achieved. Carbon Fibre Reinforced Polymers (CFRP) is an alternative which has been used in practice and evaluated in many studies (Schober et al., 2015). CFRP has mainly been used to strengthen already existing structures, such as steel-, concrete- or timber beams. The strengthening is usually done by adding plates, strips or weaves which are glued onto the exterior of the timber beam (Frankhauser and O'Connor, 2015). However, attaching the CFRP on the exterior means that the adhesives and the CFRP are exposed to natural elements and wear and tear. The method also puts high demands on the preparations of the contact surface. By including the CFRP in the production and design stage of a glulam beam, the CFRP is protected from the outside elements. The beams can be manufactured in a controlled environment, meaning that the risks involved with preparation work decreases. With this approach, the flexural strength and stiffness can be increased. In extension, the concept could also be used to decrease floor heights in timber high-rise buildings or create longer spans in warehouses, industrial halls and indoor arenas.

1.1 Project Aim and Objectives

The main purpose of this thesis was to investigate the behaviour of glulam timber beams subjected to pedestrian loading, internally reinforced with embedded CFRP laminas. Focus was put on the possibility to reduce the structural height of the beam and still obtain sufficient structural capacity. Further on, the economic viability of this reinforcement concept was evaluated through a comparison with glulam and steel alternatives. The producibility was investigated in collaboration with a glulam manufacturer, *Martinsons Trä*.

1.2 Limitations

To be able to keep within the main aim of the master thesis, certain limitations were necessary. Only commercially available solutions, regarding CFRP (fibres and matrix), glulam beams and adhesives, that are viable within the field of civil engineering were used. Thereby, no further investigation on different materials was made. Other aspects that were not covered in the thesis are:

- Assessment or strengthening of existing structures.
- Experimental validation of the suggested reinforcement configurations.
- Advanced economic and environmental simulations.
- Changes of structural behaviour due to moisture induced effects.

1.3 Scope of Study

Trying to reduce the structural height of the beam with CFRP reinforcement raises some additional questions, such as:

- To what extent does the placement of CFRP-laminas influence the strength of the beam. Which parameters have the largest influence?
- Once the beam is strengthened for flexural failure, can other failure modes occur such as: shear, tension failure perpendicular to the grain or cracks in grain direction and in interfacial layers?
- How large is the increase in structural capacity compared with the increase of cost? What is the optimum amount of CFRP?
- How does pre-cambering the beam influence the behaviour?

1.4 Methodology

The work was divided into two separate phases. The first phase included an extensive literature study, where information about the existing knowledge and current implementation in the field was gathered. The literature study was largely based on publications by scientists, companies and universities, ensuring a wide perspective. This knowledge was complemented through gathering experience from the engineers at SWECO AB (Sweco) and Martinsons Trä.

The second phase involved identifying possible solutions and different configurations based on a fixed span of 20 meters. First, analytic calculations, based on the design standards in Eurocode 5, were carried out for a straight beam without any reinforcement. This first calculation was to obtain a reference behaviour of a straight glulam beam. The structural behaviour was then evaluated by investigating the most common failure modes. CFRP laminas were introduced in the material in various ways (quantity, placement) to mitigate the different failure modes. The procedure was then iterated, through analytic calculations, aiming for an optimal solution. The same procedure was later repeated for a T-beam. To further strengthen the concept, a preliminary sizing of a stress laminated deck bridge was performed. Based on the result of the analytic analysis, a FE-model was created, where focus was to investigate the shear stresses between the timber and CFRP and to study the effects of adding a pre-camber to the beam. The economic competitiveness of the suggested reinforcement method was then investigated based on a comparison with glulam and steel pedestrian bridges.

The FE-software used in this project to perform the finite element analysis was Brigade/Plus 6.2. For the analytic analysis, Mathcad Prime 4.0 and Matlab R2017b was used.

2

Background

The theory presented in this chapter acts as a baseline for the knowledge needed to understand the thesis. In the first sections, the materials and their properties are presented. Further on, dynamic aspects of timber bridges are described. In the end, examples of common applications of glulam beams in civil engineering structures are presented. The examples presented also give an additional insight on how the reinforcement method of embedding Carbon Fibre Reinforced Polymers (CFRP) in timber can be implemented.

2.1 Sawn Timber

Trees are divided into softwood and hardwood species (Johansson, 2016). Hardwoods are trees with leaves, including for instance beech, chestnut and alder. Softwoods on the other hand are trees with needles, for instance spruce, pine and larch. Sawn products are usually refined from softwood trees, and called timber or wood. Wood describes a relatively small piece without any defects and usually refers to test specimens. Timber refers to a larger piece of wood, usually the actual construction material, where natural defects such as knots, spiral grain angles, reaction or juvenile wood occur (Johansson, 2016). Sawn timber has the limitation that the boards cannot be produced longer or thicker than the available tree trunk, see Figure 2.1.

Figure 2.1: *A profile of a common tree trunk and which parts that can be produced (Brundin and Fröbel, 2016).*

Timber is a structural material with a long and cultural heritage in the northern countries. Since it is a naturally growing material, it has a highly anisotropic behaviour (Johansson, 2016). The anisotropy means that the strength of solid timber is dependent on the direction of loading versus the direction of the fibres. The three directions which are used to describe the orientation related to the fibre orientation is longitudinal, tangential and radial. However, the difference in properties between tangential and radial directions are often neglected. Instead the terms parallel and perpendicular to the grain direction are often used, see Figure 2.2.

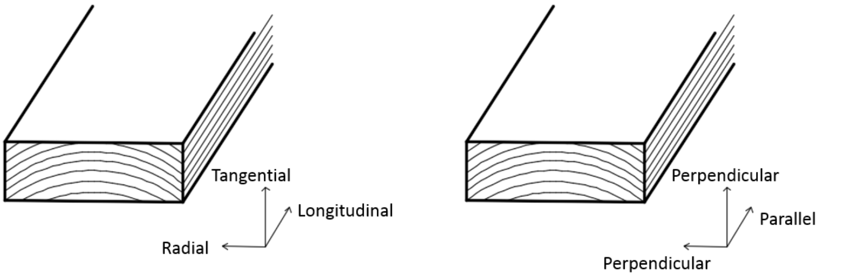

Figure 2.2: *The strength parameters in different directions of a wooden board are often simplified to parallel and perpendicular.*

2.1.1 Mechanical Properties

Being a natural construction material, timber is often more prone to dispersion of the strength, compared to steel or concrete. Therefore, there is also a greater risk for failure due to natural defects in the material (Fröbel and Crocetti, 2016). As the strength of timber varies with the actual surroundings where the tree has grown, the grading of timber is an estimate of the strength. The graded strength is based on the bending stiffness of the specific timber board (Johansson, 2016). However, there is an evident correlation between the existing defects in a timber board and the actual strength, why it is often sufficient to visually inspect the board. To ensure the quality of the product, the visual grading is complemented with mechanical testing of a few samples. Since the strength is highly dependent on the number of defects, it is possible to obtain timber boards with various strength classes from the same tree.

2.2 Glued Laminated Timber

Glued Laminated Timber (Glulam) is part of the group of structural timber called Engineering Wood Products (EWP). In fact, it is the oldest EWP, dating back to 1906 (Johansson, 2016). Examples of common shapes of glulam beams can be seen in Figure 2.3.

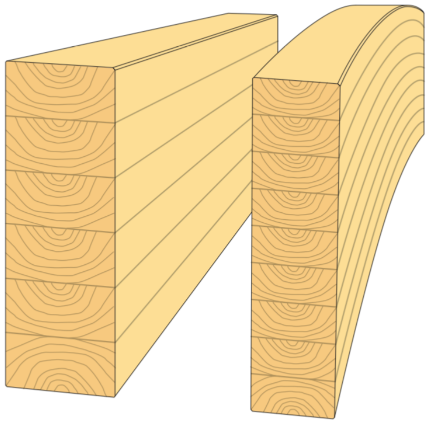

Figure 2.3: *Common shapes of a straight and a pre-cambered glulam beam (Fröbel and Crocetti, 2016).*

A glulam element consists of at least 4 lamellas that are bonded together with adhesives. The lamellas are usually around 45 millimeter for straight beams and 33 millimeter for arched or pre-cambered beams (Fröbel and Crocetti, 2016). According to E.Martinson (Personal communication, Martinsons Trä, March 11 2019), the size might also differ depending on the chosen material. The lamellas are often made from spruce, which is a member of the softwood family (Fröbel and Crocetti, 2016). To some extent, pinewood can also be used. Standard production sizes go up to 215 millimeter wide, wider beams can be achieved by joining two beams. In the same way thinner beams can be achieved by splitting a wider beam (Johansson, 2016). Experiments have shown that the mean strength of a glulam beam is not significantly higher than a sawn timber beam, but the variability of the strength is much lower due to the smearing out of natural defects (Fröbel and Crocetti, 2016), see Figure 2.4.

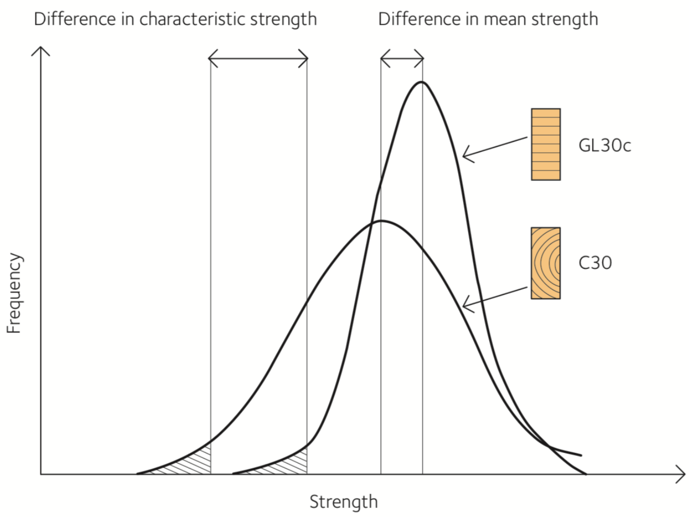

Figure 2.4: *Mean strength distribution of a sawn timber board and a glulam beam (Johansson, 2016).*

Finger jointing is a commonly used technique in glulam production to produce longer boards, and in extension longer beams, see Figure 2.5. It is also frequently used in furniture or carpentry work. Nowadays, finger joints are done by an automated machine. The length of the glue line can with this method be increased to 1.2 meters, instead of only the width of the board (Per Johansson, Personal communication, Martinsons Trä, March 11 2019).

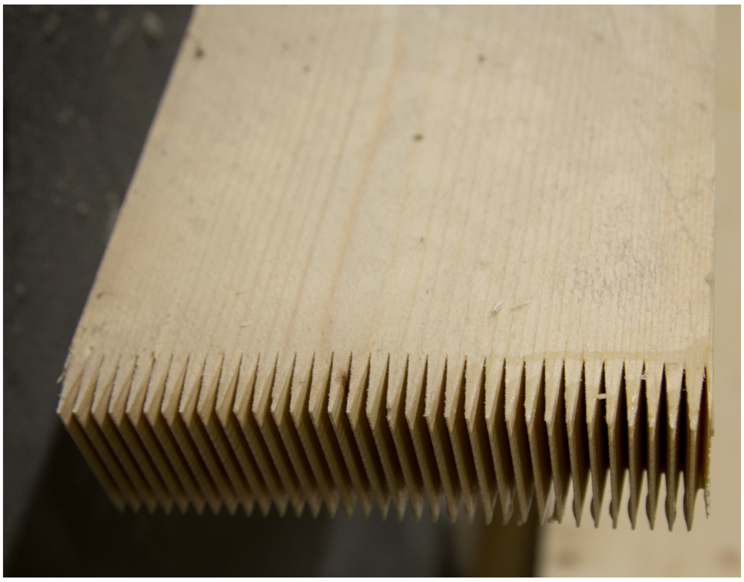

Figure 2.5: *Illustration of a finger joint in the production line at Martinsons Trä.*

According to Johansson (2016), the most common failure mode for a glulam beam is tension failure of the outermost lamella in the member. Most often, it starts from a natural defect or in the finger joint. A finished finger joint and natural defects can be seen in Figure 2.6. Shear failure is also possible in glulam beams. In curved beams, tensile failures perpendicular to the grain must also be considered.

Figure 2.6: *Illustration of a finished finger joint before planing in the production line at Martinsons Trä. It is also possible to see natural defects like knots.*

2.2.1 Production Methods

A glulam beam usually consists of timber lamellas with higher strength in the top and bottom of the beam, and with a lower strength in the middle (Johansson, 2016). However, this can be optimised and tailored to the specific needs by choosing the timber specimens with desired qualities. By gluing them together, a higher order of homogeneity is achieved compared to plain timber. Making more homogeneous members reduces the statistical deviation of the strength, see Figure 2.4, which means that the characteristic strength for a glulam member will be higher, whilst the average strength does not experience the same increase.

The strength of a glulam beam is highly dependent on the individual lamellas. Therefore, the process of choosing the correct lamellas and treating them well before joining is of high importance (Fröbel and Crocetti, 2016). The process is ensured by inspecting the timber lamellas and curing them. The lamellas are dried to approximately 12% moisture content before being glued together (Angst-Nicollier, 2012). After drying, the lamellas are planed and a constant layer of glue is applied. Whilst the glue is hardening, the pieces are pressed together in a controlled environment. It is during this time pressure can be applied to shape the beam to a camber or an arch. An illustration of the production process of a straight beam can be seen in Figure 2.7. After the hardening process is completed, the glulam beam can be treated with wax or protective coating depending on the demands (Angst-Nicollier, 2012). The most common treatment is to plane all sides and cover up smaller deficiencies.

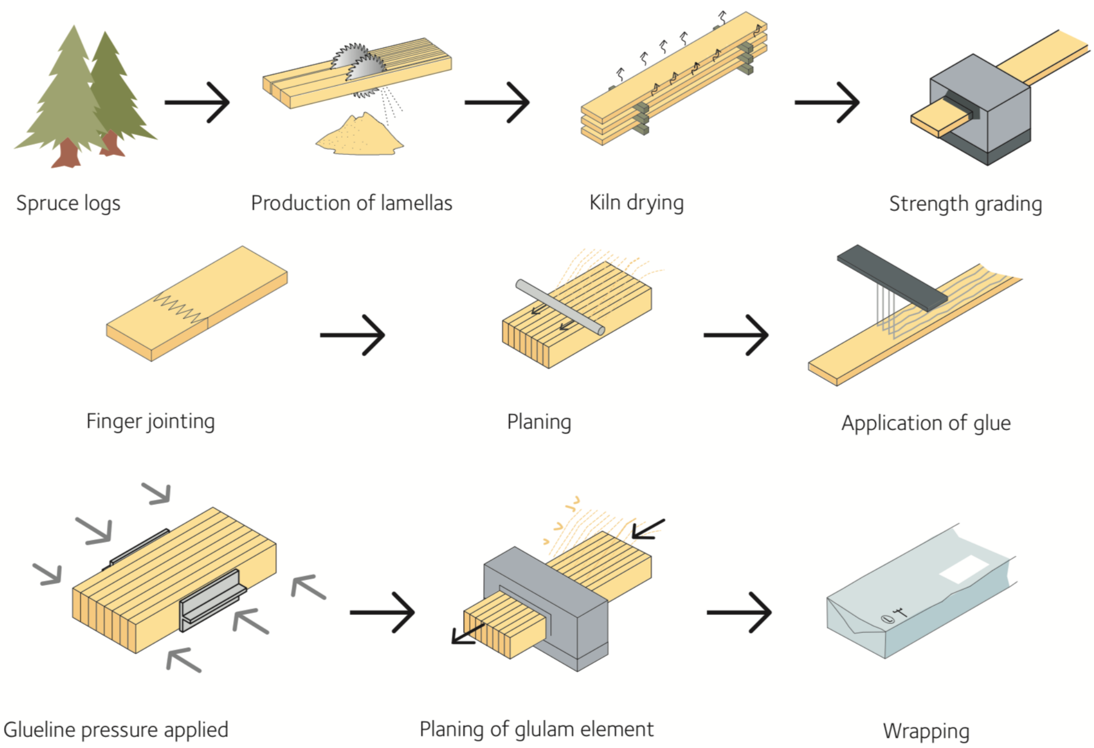

Figure 2.7: *The production process for straight glulam beams (Johansson, 2016).*

2.2.2 Mechanical Properties

The strength of a glulam beam is graded in a similar way as described in Section 2.1.1. The grading depends on the height of the beam, but also on the strength of the timber boards included (Fröbel and Crocetti, 2016). According to the Swedish manufacturing standard of glulam beams, there are four different types of glulam strength classes, exemplified here with a strength class of GL32 (SIS, 2013):

- GL32c, combined glulam beam
- GL32cs, combined split glulam beam
- GL32h, homogeneous glulam beam
- GL32hs, homogeneous split glulam beam

Combined refers to when different strength classes or timber types of the lamellas have been used to optimise the load carrying capacity, see Figure 2.8. Split refers to the fact that a wider beam has been split into thinner pieces (Fröbel and Crocetti, 2016). In a homogeneous beam, the same strength class is used for all lamellas, see Figure 2.9.

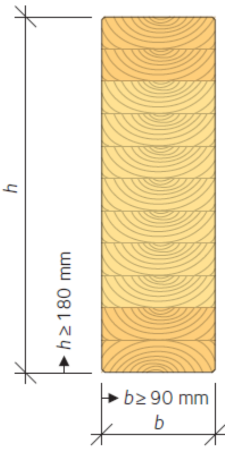

Figure 2.8: *Combined glulam beam (Fröbel and Crocetti, 2016).*

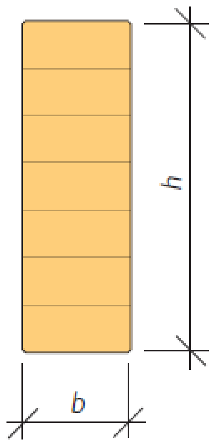

Figure 2.9: *Homogeneous glulam beam (Fröbel and Crocetti, 2016).*

2.2.3 Long Term Effects of Timber

As most civil engineering structures are built for a lifespan of up to 100 years, it is important to know and account for how the material behaves over a longer period of time. Long term effects usually lead to increased deformations and reduced strength, why it is important to consider them in both assessment and design.

Glulam beams are usually delivered at a reference moisture content corresponding to 16% (Angst-Nicollier, 2012). When mounted on site, the beams adapt to the surrounding relative humidity and temperature until equilibrium is reached. Glulam beams swell with an increasing amount of moisture and shrinks with a decreasing amount of moisture, although less when compared to sawn timber (Fröbel and Crocetti, 2016). The tendency to deform less is partly because the beams are being produced in a controlled environment, and partly due to the higher resistance of the cross section (Fröbel and Crocetti, 2016).

Creep is an ongoing deformation that occurs in the material over time. Increased moisture content in a element leads to an increase of the creep, which in turn gives increased deformations and decreased modulus of elasticity (Johansson, 2016). Creep is also dependent on the applied load. If the load varies over time it may increase the creep deformations, which is why creep is important to consider in design (Johansson, 2016).

In comparison with steel and concrete, timber has small temperature movements, which reduce the risk for temperature induced stresses in the structure (Johansson, 2016). The changes in strength and stiffness within normal temperature ranges is negligible, and are often disregarded in design standards.

As glulam beams consist of organic material, it is important to protect the structure from the surrounding environment and treat it in a correct way (Fröbel and Crocetti, 2016). Without proper treatment, the beams can be attacked by intrusive microorganisms that damage the structural integrity. The microorganisms can either affect the aesthetics by discolouring the timber (e.g. mold- or blue fungi) or they can also have more of a disruptive character and reduce the structural integrity of the material (e.g. rot fungi) (Fröbel and Crocetti, 2016). Timber is also susceptible to attacks from certain wood eating insects, which can completely destroy the structure. Glulam can also be exposed to deterioration from sunlight when left unprotected against the sun's UV-radiation. Protection can be achieved either by constructive cladding, smart connections or by impregnating the timber.

2.2.4 Failure modes

Johansson (2016) describes the failure modes of timber. They are usually classified as:

- Parallel to the grain
  - Tension failure
  - Compression failure
- Perpendicular to the grain
  - Tension failure
  - Compression failure

Tension failure parallel to the grain exhibits a brittle response, while compression failure is ductile. When the fibres buckle due to compression loads parallel to the grain, stresses can still be carried and the response will have a plastic behaviour.

The tensile strength perpendicular to grain is substantially lower. True compression strength perpendicular to grain is difficult to evaluate, since after crushing of the fibres, the stress can still accumulate.

2.3 Fibre Reinforced Polymers

Fibre Reinforced Polymers (FRP) is a structural composite material consisting of two components, a fibre and a matrix, in turn consisting of a polymer-based resin, additives and fillers (Hollaway and Teng, 2008; Potyrala et al., 2011). The fibre is the element that creates strength in the composite, possessing a high-strength and high-modulus component. The matrix has low-strength and low-modulus and is used by the fibre to transfer stresses through a plastic flow, which in turn creates a high-strength material. To achieve optimal strength in the material, the matrix should have a failure strain greater than the failure strain of the fibres, in order for the fibres to reach their ultimate strength capacity (Potyrala et al., 2011). Other properties that effect the strength of the composite is the fibre alignment, the fibre content and the strength of the interface. Being able to influence these properties, the material can be tailored to specific needs.

There are many types of fibres that can be used for FRP composites. The most common ones are glass, aramid and carbon (Hollaway and Teng, 2008). Due to its relatively high strength and stiffness properties, compared with glass and aramid, carbon is more used for flexural and shear strengthening of civil infrastructures. Research has also been carried out regarding the usage of natural fibres, such as cotton or hemp. Since these fibres consist of organic materials, they are prone to decay when exposed to the harsh environment of civil engineering structures (Allann, 2006). Combined with the fact that most of the tested fibres had a low load carrying capacity, Allann (2006) drew the conclusion that they are mostly suitable in protected non-structural elements, for instance, in cars.

In general, the matrices can be categorised into two groups, thermoplastic and thermosetting binders. According to Hollaway and Teng (2008), thermosetting polymers are mainly used for rehabilitation of structures. Thermosetting polymers are not only there to transfer stresses between the fibres, they also serve as a protection for the fibres, which otherwise can experience degradation due to abrasion and environmental corrosion. Due to their high chemical and thermal compatibility with the fibres, epoxy and vinylester matrices are most commonly used.

2.3.1 Production Methods

In general, FRPs can be produced in various ways depending on the purpose of the produced product, ranging from simple hand procedures to pressurized vacuum chambers with a controlled environment (Potyrala et al., 2011). For civil engineering purposes, there are five production methods commonly used, which are described below (Nedev, 2019).

The simplest method is called lay-up, which can be performed either with a manual roller (hand lay-up) or with a spray nozzle (spray lay-up). Hand lay-up requires extensive labour work, where the fibres and the resin are laid out in a pre-made mould, and then set to harden after applying manual pressure with a roller to remove air pockets (Potyrala et al., 2011), see Figure 2.10. Spray lay-up is an easier method, in which the resin and fibres are sprayed onto the mould, and then left to harden (Potyrala et al., 2011; Gurit, 2018), see Figure 2.11. Spray lay-up is also quicker, less expensive and more flexible regarding the shape of the mould than hand lay-up. It is however difficult to achieve high-strength materials using spray lay-up.

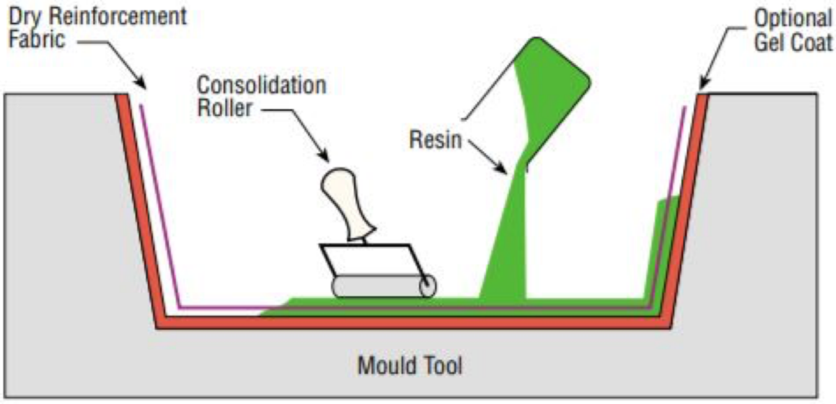

Figure 2.10: *Hand lay-up production process (Gurit, 2018).*

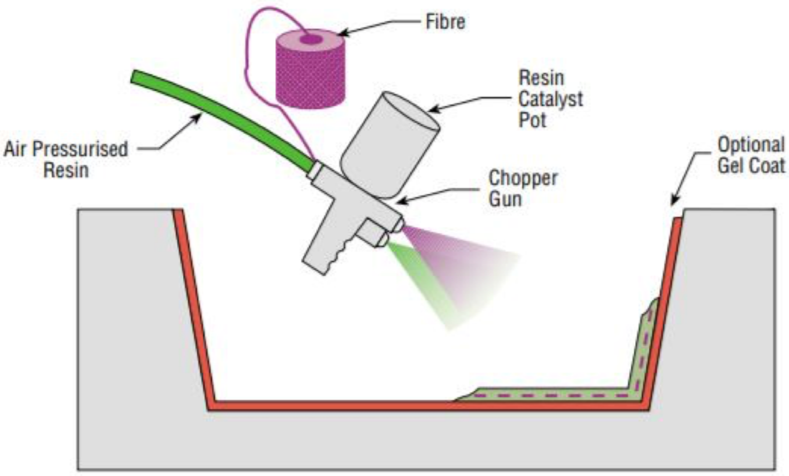

Figure 2.11: *Spray lay-up production process (Gurit, 2018).*

The most common method for load-carrying structural members in civil engineering is pultrusion, see Figure 2.12. Pultrusion is a method where the fibres are pulled through a mould with constant velocity, whilst applying resin, pressure and temperature (Gurit, 2018). On the other side, a beam with a cross sectional shape exits the mould. This method is similar to the process of hot or cold rolled steel beams. With pultrusion, it is possible to create high-strength beams with a consistent cross section. It also gives the opportunity to create common shapes like I/U/T/box-beams which makes it possible to build up composite cross sections of a bridge (Potyrala et al., 2011). For the specific case of internal reinforcement laminas, which was studied in this thesis, pultruded FRP laminas are the most suitable. The laminas have a constant cross section shape and properties and can thereby easily be produced by pultrusion.

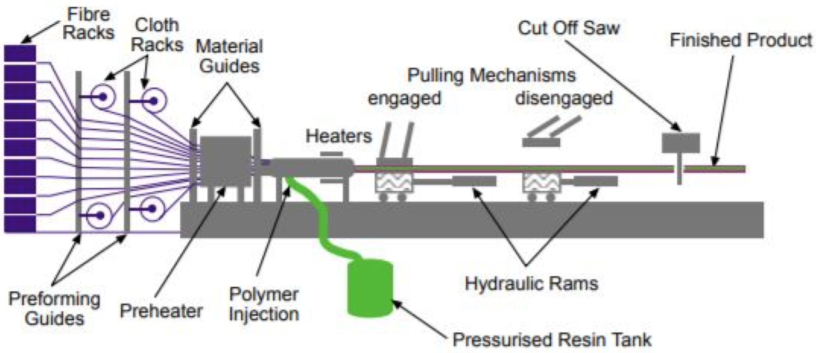

Figure 2.12: *Pultrusion production process (Gurit, 2018).*

For creating columns or pipes, a more common method to use is filament winding, see Figure 2.13. A roller with the desired cross section is rotating at a constant velocity whilst fibres coated in resin are spun around it (Gurit, 2018). It is similar to winding up a thread on a spool. The roller is then cured in a controlled environment until hardening (Potyrala et al., 2011).

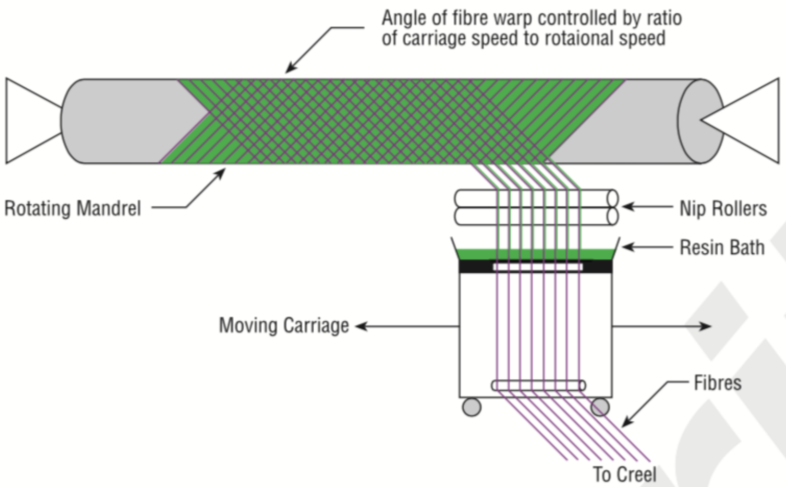

Figure 2.13: *Filament winding production process (Gurit, 2018).*

Another commonly used method is Resin Transfer Moulding (RTM), see Figure 2.14. It shares a lot of its characteristics with the more simple lay-up methods, but with an automatic press holding the two halves of the mould tool together. First the fibre is laid out in the mould, after which the air is sucked out in one end with a vacuum pump. From the other end, resin is sucked into the mould, and thereby filling every available air pocket inside the fabric (Gurit, 2018).

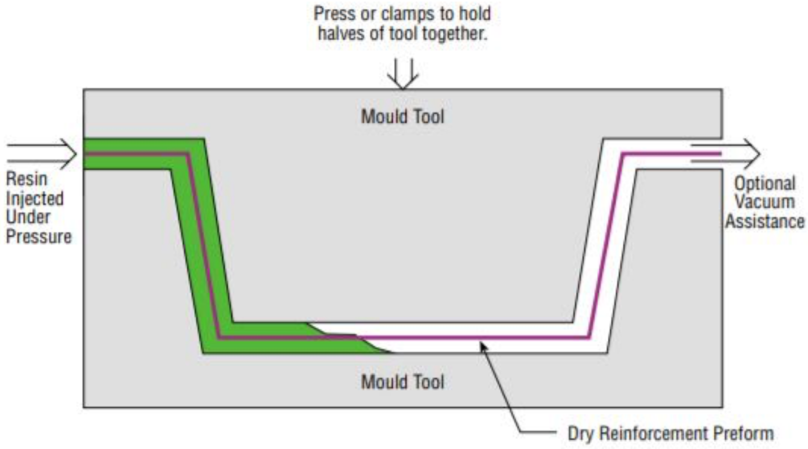

Figure 2.14: *Resin transfer moulding (RTM) production process (Gurit, 2018).*

A variant of the RTM method is the Vacuum Assisted Resin Transfer Moulding (VARTM). Here the mould is enclosed in a vacuum sealed compartment (Gurit, 2018), see Figure 2.15. Afterwards, the process continues in the same way as described for the RTM method. RTM, and the different variants, create a material with a high level of homogeneity. However, this process is rather expensive and difficult and is therefore better suited for smaller parts or structures (Potyrala et al., 2011).

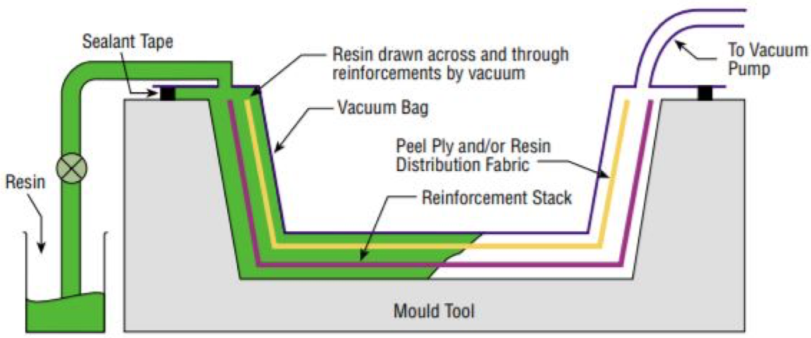

Figure 2.15: *Vacuum assisted resin transfer moulding (VARTM) production process (Gurit, 2018).*

2.3.2 Long Term Effects

FRP is a fairly new construction material in civil engineering structures, meaning that the knowledge about long term behaviour is rather limited (Karbhari et al., 2003). Nevertheless, based on the current knowledge, the long term effects can be estimated to a certain extent. However, it should be noted that the accelerated experiments are based on small specimens during short periods of time. The data from these experiments are extrapolated, which may lead to inaccurate assumptions and contradictions when trying to interpret the results. Further on, the FRPs ability to be tailored makes it difficult to adapt existing knowledge in practice, since the long term effects depend on the composition of the specific FRP (Karbhari et al., 2003). Here the tailorability, which is commonly considered as an advantage, becomes a disadvantage. Research is ongoing on the subject of long term effects.

Like other organic materials, FRPs are susceptible to moisture induced effects. The part of the FRP which is affected the most is the matrix (Heshmati, 2015). Studies have shown that the resin can absorb surrounding moisture which leads to changes in mechanical and chemical characteristics (Karbhari et al., 2003; Heshmati, 2015). The changes in characteristics can in extension lead to cracking, fibre/matrix debonding and loss of structural capacity or deterioration at the fibre level (Heshmati, 2015). Furthermore, the cracks enables more moisture to penetrate the material which in turn accelerates the deterioration. Depending on the length of exposure and how much water that is absorbed, the changes in the matrix might be irreversible. An increase of moisture content could reduce the *glass transition temperature*, T_g (the temperature where a material goes from a more hard and brittle state, to a more rubbery and viscous). The carbon fibres themselves are chemically stable and are therefore not affected by neither moisture, nor salts in seawater (Heshmati, 2015). According to Potyrala et al. (2011) the impact on FRP-materials from deicing salts, which is commonly used in Sweden during winter, is negligible. Temperature variations might lead to changes in the chemical composition of the matrix and thereby the binding to the fibres, which decreases strength. In practical implementation, it is important to consider the synergistic effects that might arise due to moisture absorption and temperature variations in the material (Karbhari et al., 2003).

The creep properties of a FRP is dominated by the composition of matrix and fibres, and the mechanical properties of the matrix (Karbhari et al., 2003). The contribution from fibres and interfacial mechanical properties are negligible. For CFRP, studies have shown little effect from creep degradation.

Chemical deterioration could dissolve the matrix structure and lead to loss of structural integrity (Karbhari et al., 2003). Chemicals can, besides from affecting the matrix, also have an impact on the fibre itself leading to degradation and loss of structural integrity. Karbhari et al. (2003) also states that CFRP is affected by photodegradation when exposed to Ultra Violet (UV) radiation from the sun. Photodegradation can also lead to loss of structural integrity of the material. The effects of UV-radiation can be somewhat mitigated by using a protection method with UV-coating or gel-coating (Bengtsson and Magnusson, 2016). UV stabilizing additives might also be added to the matrix.

2.3.3 Carbon Fibre Reinforced Polymers

The tensile strength of CFRP depends on both the quality of the fibres and their orientation and it is therefore considered to be an anisotropic material (Schober et al., 2015). The anisotropic properties makes the material versatile since it can be tailored to fit the specific needs, with high strength in desired directions. Illustration of a plain weave made up of carbon fibres can be seen in Figure 2.16.

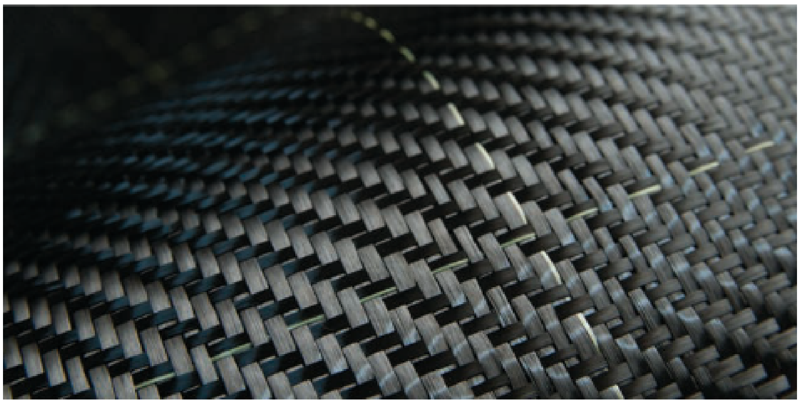

Figure 2.16: *Plain carbon fibre weave (Gurit, 2018).*

When it comes to the carbon fibre itself, the material properties are highly dependent on the temperature during manufacturing (Hollaway and Teng, 2008). For higher temperatures, the crystallinity increases (i.e. degree of structural order which in turn increases the hardness). This means that the fibres' modulus of elasticity increases with higher temperatures (especially when more than 2000°C). At the same time, the tensile strength reaches its maximum at about 1600°C. According to Hollaway and Teng (2008), the fibres can be categorized in the following way:

- Standard/low modulus (E $\approx$ 200GPa)
- High strength (E $\approx$ 220 GPA and $f_t \approx$ 3GPa)
- High modulus (E $\approx$ 220 - 300 GPa)
- Ultra-high modulus (E $>$ 450 GPa)

2.4 CFRP Reinforced Glulam

Since both CFRP and timber posses anisotropic properties, they have favourable prerequisites for being an efficient material when combined. On the other hand, it is still uncertain how these materials interact and therefore it is necessary to further study the aspects of this composite.

2.4.1 Reinforcing Techniques

There are numerous ways to reinforce a glulam beam with CFRP to increase the flexural capacity. The most common methods are externally bonded reinforcement (EBR), wrapping with CFRP sheets and near-surface mounted reinforcement (NSM) and internally bonded reinforcement (IBR). All these methods can be seen in Figure 2.17. Also, Figure 2.17 illustrates the reinforcement method suggested in this thesis, internally bonded reinforcement. Usually, the beam is reinforced on the tension side to increase the tensile capacity (Allann, 2006). A positive effect of strengthening the beam on the tensile side, is that compression failure will take place first. The compression failure is a plastic phenomenon, which gives the beam having a more ductile behaviour.

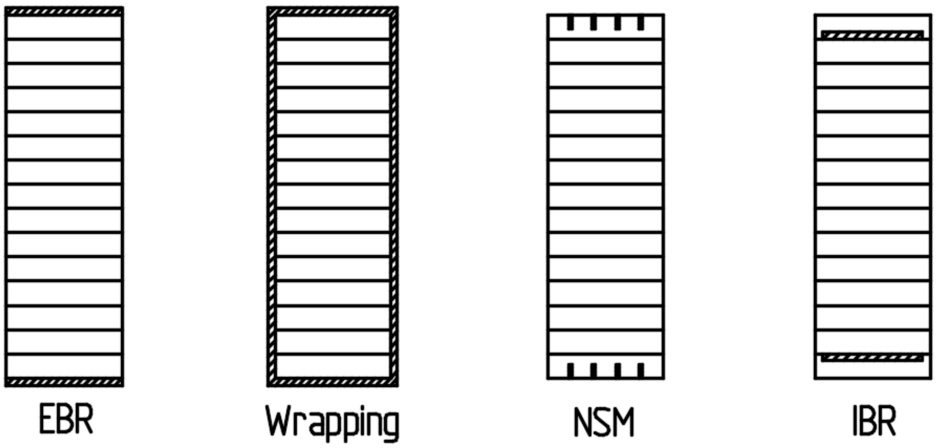

Figure 2.17: *Illustration of the three different reinforcing techniques previously used (EBR, wrapping and NSM). To the right is the suggested reinforcing method in this thesis, IBR.*

Wrapping and EBR are techniques that are often considered when reinforcing an already existing structure. According to Johnsson et al. (2006), the wrapping technique is mainly applicable for restoring the beam due to partial deterioration or cracking. The EBR technique is used to achieve an increase of flexural strength in-situ.

The NSM reinforcement method has been investigated in many studies. An advantage with the method is that it restrain smaller areas of the timber, reducing the risks of splitting due to moisture movements (Johnsson et al., 2006). In addition, NSM is recommended when having reinforcement in the compressive zone, since an externally applied CFRP lamina has a larger risk of buckling (Schober et al., 2015).

2.4.2 Adhesives and Surface Preparation Considerations

An important aspect of achieving satisfying composite action is the bonding of the CFRP to the timber, which is made by using specific adhesives. There are some alternatives available on the market, with additional research ongoing. They are epoxies, polyurethanes, polyesters, phenolics and aminoplastics (Broughton and Hutchinson, 2003). For application at site, epoxy based adhesives have generally been used (Schober et al., 2015). However, many of these epoxies have mainly been developed to be used with other materials, meaning that there is no chemical bonding to the timber and the mechanical anchorage cannot always be guaranteed.

As a substrate, timber is good for adhesion (Hollaway and Teng, 2008). Hardwoods are in general worse than softwoods, due to a higher presence of extractives (tannins and oils) and a higher density. However, necessary surface preparations have to be made before applying the adhesive. The timber surface degrades over time due to oxidation. Therefore, it is important to clean the surface properly and remove all dust before applying the adhesive. The moisture content at bonding also affects the adhesion. Wheeler and Hutchinson (1998) investigated how the bonding properties changed due to the moisture content in the timber. When using polyurethane, the shear strength in the adhesive was reduced for moisture contents between 18 and 22%, compared to 10% moisture content. This behaviour is explained by the chemical reaction between the polyurethane and water from high moisture levels, producing a foam that impairs the bond properties. Wheeler and Hutchinson (1998) also reported that polyurethane is sensitive to moisture changes in the wood. After some cycles, the shear strength of the bond experienced a significant reduction and cohesive failure followed. Furthermore, the same tests were also conducted using epoxy adhesives. In the tests, a more consistent shear strength could be observed, both when comparing moisture content at bonding, and cyclic moisture changes.

2.4.3 Mechanical Properties

The mechanical properties are improved compared to a regular unreinforced glulam beam. More specific, an increased stiffness is achieved for the composite cross section. Regarding the bond properties of CFRP-to-timber interfaces, there are many parameters that affect the capacity of the interface (Juvandes and Barbosa, 2012). These are shear and tensile strength of the surface lamella of timber, cohesive strength in the adhesive and interlaminar strength of the CFRP.

When conducting single shear tests of FRP-to-timber joints, a study showed that all softwood joints failed predominantly in the timber, whilst for the test with hardwood timber, failure took place in the interface (Schober et al., 2015). This could be explained by the adhesion qualities described in 2.4.2.

Glulam has, despite consisting of flammable material, a good fire resistance compared to concrete or steel (Fröbel and Crocetti, 2016). When a timber beam is ignited, the surface will start to char, creating a protective layer for the interior members, see Figure 2.18. This protective layer slows down the penetration of the fire and the structural capacity can be maintained for a longer period of time. The adhesive used, as well as the corresponding melting point at which it loses the adhesive power, can however affect the fire resistance. The loss of adhesive power can occur for the adhesive between the timber lamellas and the CFRP lamina as well. Embedding the CFRP lamina, can due to the charring of the outer lamella of the glulam beam, further protect the CFRP from fire damage and thereby sustain structural capacity. Fröbel and Crocetti (2016) also state that connectors such as bolts or dowels are important to consider when evaluating the fire safety. They can act as conductors as they increase the heat flow into the core or the CFRP lamina, why it is extra important to protect these.

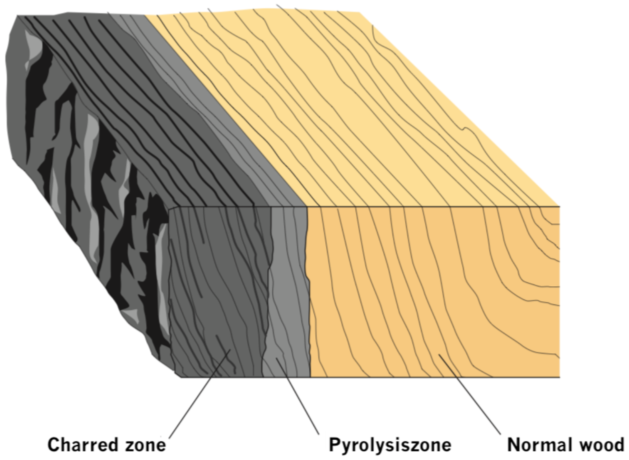

Figure 2.18: *Fire progression in a regular glulam beam (Johansson, 2016).*

There has been some experimental research conducted on how CFRP resond to fire. When FRPs are exposed to high temperature, they undergo a chemical transition phase called pyrolysis (Yang, 2017). The pyrolysis changes the chemical composition of the FRP, enabling it to react with oxygen, creating a self-supporting combustion. Furthermore, the process also reduce the structural capacity of the material. However, the fire resistance is highly dependent on the amount of fibres, and the resin used for the matrix (Zhang et al., 2017). The adaptable properties makes it difficult to predict the fire resistance of a specific CFRP material, but when ordering from suppliers, they are usually tested before production. An additional problem could be the development of toxic gases when the FRP is combusted (Karbhari et al., 2003). Other measures to increase the fire resistance are to mix flame retardant additives into the matrix, or to add an insulating coating (Yang, 2017; Hollaway and Teng, 2008). This could provide the CFRP with fire resistance exceeding that of many other common building materials (Composite UK, 2017).

Studies suggest that loss of structural capacity for FRP-reinforced glulam beams due to fatigue loading is small, close to negligible (Davids et al., 2005). However, the available data and performed experiments on this subject are lacking. This is also true regarding the fatigue behaviour of solely CFRP, lack of data makes it difficult to interpret the behaviour, whereby the combination of glulam and CFRP is difficult to estimate (Karbhari et al., 2003). Even though the fatigue life of the structure often can be neglected, it is important to consider connections, bonded or mechanical, which could induce fatigue damage or stress concentrations (Potyrala et al., 2011).

2.4.4 Production Methods

To evaluate the feasibility of the proposed IBR configuration, the way of producing glulam beams with CFRP has to be considered. E. Martinson (Martinsons Trä, personal communication, March 11 2019) described the glulam production process and how it would be possible to include the reinforcement.

The first alternative would be to glue the CFRP lamina onto a glulam beam and then add an extra sacrificial lamella outside the CFRP lamina. This would be done manually after the inner glulam beam has been produced. E. Martinson (Martinsons Trä, personal communication, March 11 2019) states that this process would be quite expensive and labour intensive. In this case, the CFRP lamina has the same width as the beam, like the EBR-configuration in Figure 2.17.

Another alternative is to create a slot in the sacrificial lamella, after which the CFRP lamina is prepared and glued on to the exterior lamella, see Figure 2.19. A regular glulam beam is produced, and then after hardening, the exterior lamellas (including the CFRP) are glued onto the beam. The exterior lamella is kept in place with screws while the adhesive is hardening. This method requires more preparatory work, but it can be performed simultaneously as the production of the inner beam, making it a faster method. Embedding the reinforcement also further protects the CFRP from outside wear such as moisture and UV-radiation. The drawback with this method is that the width of the CFRP lamina decreases, and thereby some of the stiffness is lost.

Figure 2.19: *Illustration of the how the sacrificial lamella can be constructed. Cross section of the sacrificial lamella.*

Either way, the small scale production of these methods is labour intensive and expensive. If the concepts proves itself to be feasible, the process could be automatised and time and cost can be decreased.

2.5 Dynamic Behaviour of Timber Pedestrian Bridges

Something which is often limiting for timber pedestrian and bicycling bridges is the behaviour in Serviceability Limit State (SLS), predominately dynamic behaviour (E. Martinson, Martinsons Trä, personal communication, February 14 2019).

From a pedestrian's foot, three force components can be derived. There are the distinct ones acting downwards (vertical) and forwards (longitudinal), but there is also a force in sideways (lateral) direction since the pedestrians centre of mass is shifting with each step. The force components are illustrated in Figure 2.20.

Figure 2.20: *Illustration of the force components created from a pedestrian whilst walking.*

Furthermore, as pedestrians are walking on a swaying structure, they adapt and counteract the movements of the structure to maintain balance. These constant adaptation might induce new loads and change the behaviour, or further amplify the already existing vibration of the bridge (Sétra, 2006). It could create a potentially dangerous effect called lock-in, where the frequency of the pedestrians and the bridge are the same. Since the experienced movements of the bridge make pedestrians compensate to keep balance, the crowd load is synchronized and the movements are further excited and the problem amplifies, theoretically towards infinite deflections. To avoid lock-in, the structure should be designed so that the lowest and most energetic structural frequency of the bridge is higher than the excitation frequency (Mårtensson, 2016). For timber pedestrian bridges constructed with stress laminated deck, the effect of the transversal forces caused by pedestrians is rather small due to the high stiffness in that direction (G. Nedev and M. Bäckström, Sweco, personal Communication, February 20 2019).

Vibrations that are induced by pedestrians are often considered to be a load that varies over time regarding amplitude and intensity, generally with a rather low frequency. For heavy structures with a sufficient amount of stiffness, pedestrian loads are not considered to be a problem. In lighter structures, pedestrian loads can have a large impact and lead to large vibrations and discomfort for the user (Sétra, 2006). In practice, a bridge is subjected to simultaneous actions by many pedestrians at the same time, since every person has its own characteristic footprint depending on weight, frequency, speed or footwear (Sétra, 2006; Mårtensson, 2016). Thereby the load induced on the bridge is also different. An additional complication is that on an actual structure, the phase shift between individual pedestrians from when they enter until they leave the bridge needs to be considered.

In theory, when a member is put into motion, it moves forever. In reality however, there is always some damping built into the structure in terms of friction (Mårtensson, 2016). An example of how the deformations decay over time for different damping coefficients (zeta) can be seen in Figure 2.21.

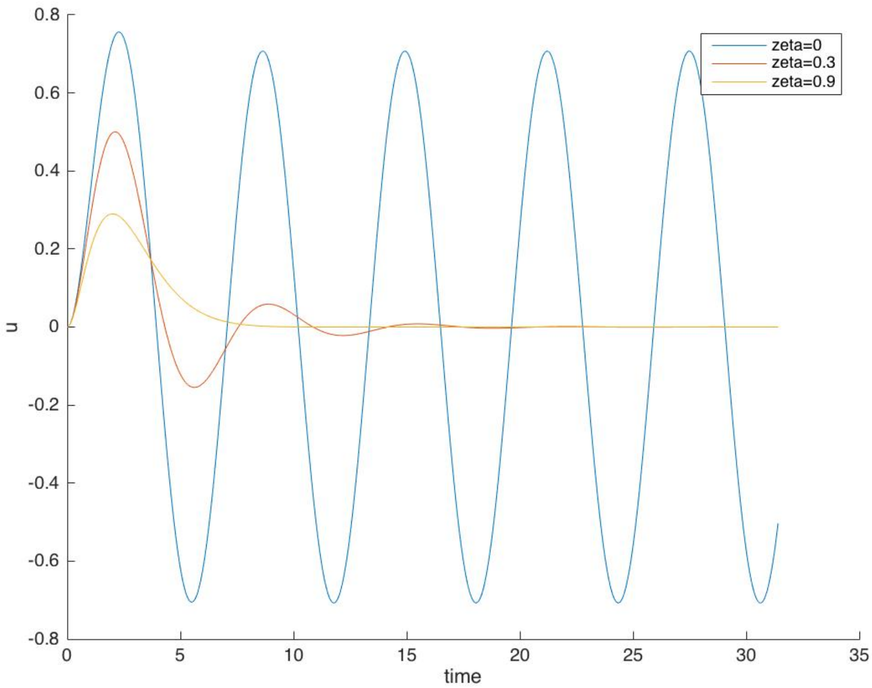

Figure 2.21: *Illustration of different damping coefficients, zeta=0 is the theoretical free vibrating case, 0.3 and 0.9 respectively indicates increased damping and thereby faster decay.*

Since bicyclists have a continuous contact with the ground when crossing the bridge at a nearly constant speed, they do not cause the same amplitude of vibrations as pedestrians do, and can therefore be neglected when evaluating the dynamic performance (Heinemeyer, 2009). Furthermore, runners do not need to be considered since the time it takes to cross the bridge is relatively short and does thereby not leave time for any resonance to settle (Sétra, 2006). However, larger running events must be considered with caution. Figure 2.22 shows an example of how the impulses for walking and running differs.

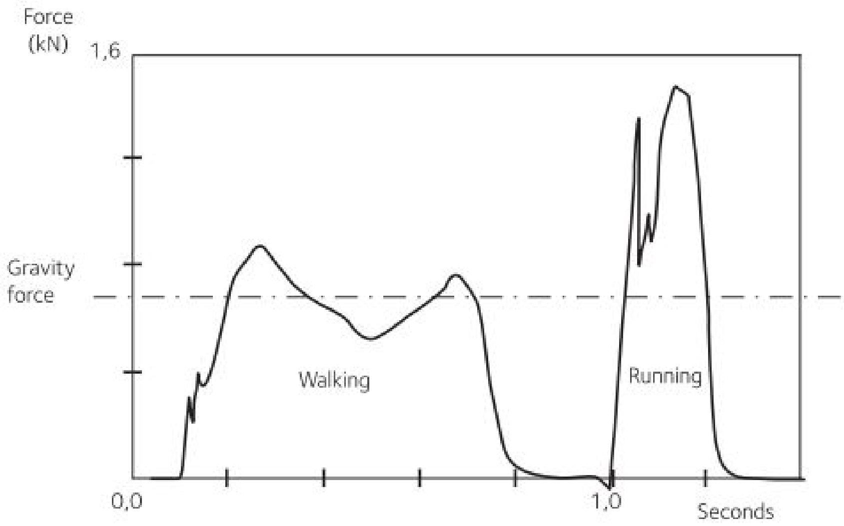

Figure 2.22: *Example of the footfall forces from different actions (Mårtensson, 2016). In reality it differs depending in the characteristic of the person and the bridge deck.*

If sufficient stiffness cannot be achieved in the production, it is possible to fit the bridge with dampers or try to change the structural frequency of the bridge. The problem with changing the natural frequency is that it can either be done by increasing the stiffness or decreasing the mass (Fitzpatrick and Smith, 2001; Heinemeyer, 2009). That might be complicated since increasing the stiffness often involves increasing the overall mass of the structure and vice versa. Fitting with dampers is a more straightforward solution, but it is also often more expensive (Fitzpatrick and Smith, 2001). Dynamic problems may also arise through excitation by wind, which could lead to collapse of the structure. Resonance occurs when one of the structural frequencies coincide with the frequency of the wind (Heinemeyer, 2009). However, this is not considered to be a problem for low bridges with short spans (Trafikverket, 2016).

2.6 Applications of Glulam beams

A regular straight beam is not commonly used for infrastructural purposes. However, for buildings and structures with smaller spans where the deflections are limited, it is more common. Figure 2.23 shows a beam-column system that is used in a timber multi-storey house. The loads in the beams are mainly transferred through bending and shear.

Figure 2.23: *Illustration of straight beams used in a residential building (Lidelöw, 2016).*

A variant of the straight beam is the T-beam. The T-beam consists of two joined pieces of glulam. One standing part comprising the web, and one flange on top, see Figure 2.24. The load is mainly transferred through bending and shear.

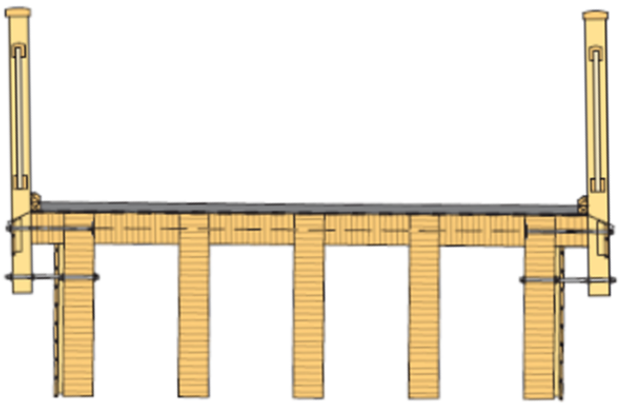

Figure 2.24: *Illustration of a typical T-beam pedestrian bridge (Fröbel and Crocetti, 2016).*

For infrastructural purposes, the chosen beam is most often pre-cambered. Pre-cambering means adding a positive deflection to counteract the deflection from the self-weight of the bridge. This is to reach the often limiting demand for allowed deflections and sustain visual appearance for the user. A pre-cambered beam then becomes slightly arched, as can be seen in Figure 2.25. With a pre-cambered beam, it is possible to sustain larger loads and longer spans.

Figure 2.25: *Älvsbackabron, a bridge design with pre-cambered beams and cables. Located in Skellefteå, Sweden.*

Placing a series of beams in the longitudinal direction of the bridge and then tighten them together via a tension rod perpendicular to the beams, produces a stress laminated deck bridge. The bridge basically becomes a linear multiplication of a straight beam. For the interaction between the beams to be sufficient, the tension rods must be adequately tensioned. The bridge can be prefabricated in a protected environment and then transported with trucks and fully assembled on site, see Figure 2.26. The loads are transferred in the same way as for the beams which composes the stress laminated deck.

Figure 2.26: *A prefabricated stress laminated deck bridge, seen from the side, in the factory ready for transportation.*

The tension rods, which keep the individual beams together, are inserted and tensioned on site. The rod configuration can be seen in Figure 2.27.

Figure 2.27: *Constructive configuration of where to the tension rods can be inserted.*

3

Literature Study

A summary of existing research and knowledge within the field of CFRP reinforcement of timber structures.

3.1 Existing Research

Ever since the first attempts of strengthening timber structures in the early 60s, research in forms of modelling and experiments have continuously been performed to increase the knowledge about the composite behaviour. In general, the focus has been on how to reinforce and rehabilitate already existing structures, often with the configurations Externally Bonded Reinforcement (EBR) or Near Surface Mounted reinforcement (NSM), see Figure 3.1. To be able to analyse and critically investigate the results of the suggested method, it is important to consider previous knowledge and research.

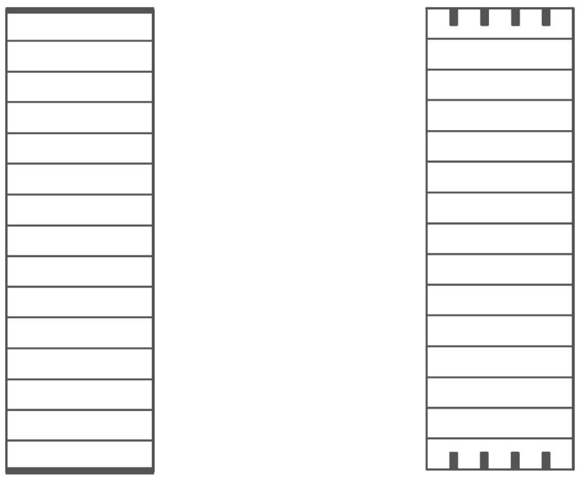

Figure 3.1: *Illustration of EBR (left) and NSM (right) configurations.*

3.2 Existing Experiments

Barragán and Jacob (2007) carried out a series of test to investigate how the performance of a carbon reinforced glulam beam varied due to placement of the reinforcement. In the experiments, attempts were made with reinforcement only in the tensile zone, as well as both in compression and tensile zone. Calculations showed that the optimal configuration for increasing the bending capacity was to place 75% of the reinforcement in the tensile zone and 25% in the compression zone. This was something which the tests confirmed, where the highest increase in bending capacity was found for a test beam with 66.7% reinforcement in tensile zone and 33.3% in compression zone. However, if increased stiffness is the main priority, the reinforcement configuration should be chosen to 50% in both zones, where the experiments showed an increase of more than 100% in stiffness. For a configuration with reinforcement only in the tensile zone, the bending capacity increased with 57% and the stiffness with 81%.

Barragán and Jacob (2007) also stated that care should be taken when including CFRP in the compression zone, as the unidirectional fibres might buckle and lose all their strength. It is advantageous if the designer can detect this in an early design phase, and eventually choose another material for compression reinforcement.

Glišović et al. (2016) also performed a four-point bending test to study the behaviour of a glulam beam with EBR configuration. The results showed an average increase in bending capacity of 54.3% and in stiffness of 18.1%, with a reinforcement amount of 0.46% of the cross sectional area.

Romani and Blass (2001) conducted experiments where an extra sacrificial timber lamella was used in most configurations, because of fire safety and aesthetic reasons. In most cases, the sacrificial timber lamella first failed in tension, after which the load could be increased with 30%. The authors state that a different reinforcement configuration could generate a more ductile failure, which Barragán and Jacob (2007) also confirmed.

Raftery and Harte (2013) developed a model that accounts for the non-linearities that occur in a CFRP reinforced glulam beam with low-graded timber. Experiments were compared with a FE-model and a strong correlation was shown. The two reinforcing schemes that were studied by Raftery and Harte (2013) were EBR and a variation of IBR.

3.3 Studies Related to Thermal Expansion of CFRP

When compared to other common civil engineering materials, the Coefficient for Thermal Expansion (CTE) for CFRP is both negative (contraction) and relatively small (Ahmed et al., 2012). However, in a composite application, it is important to account for since shear stresses might arise due to different CTE values of the composite materials.

Calvet et al. (2015) conducted a study where the bond between CFRP bars and concrete was studied. The thermal coefficient for the CFRP was estimated to -2.25 $[10^{-6} \cdot K^{-1}]$. Other studies have measured different CTE values; Joven et al. (2012) estimated it to be -0.79 whilst Ahmed et al. (2012) found it to be -0.76 in their tests.

The variation in results depends on the property of the CFRP. For example, a decrease in fibre volume could give a positive value of the CTE (Ahmed et al., 2012). Additionally, the fibre direction has a large influence on the CTE. Even though the CTE values may differ, the studies give an indication about the expected behaviour.

4

Problem definition

To investigate the effects of reinforcing a glulam beam with CFRP, it is important to have a well-defined problem with clear limitations. To make the application realistic, the model is based on planned crossings over the center canal in Gothenburg, Sweden.

4.1 Definition of Geometry

The model consisted of a simply supported glulam beam with a free span of 20 meters. The beam is composed of inner lamellas à 45 millimeter and outer lamellas à 15 millimeter. Embedded between the outer lamellas, thin laminas of CFRP were placed, see Figure 4.1.

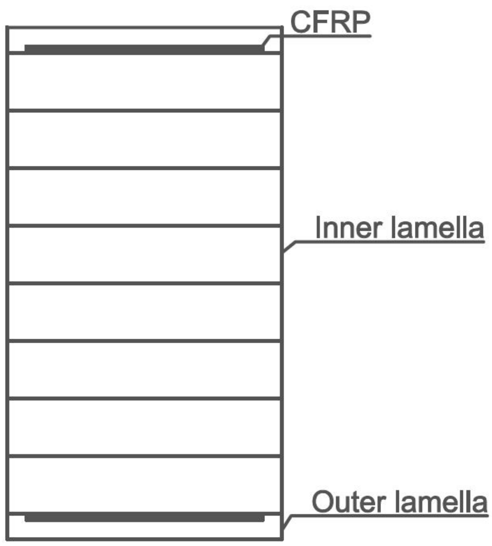

Figure 4.1: *The illustration shows how the CFRP is embedded in the glulam beam.*

The studied cross section, exemplified here with a height of 625 millimeter, can be seen in Figure 4.2. To achieve maximum stiffness of the beam, and thereby mitigate the problem of dynamic behaviour and deflections, the reinforcement was equally distributed on compression and tension side of the cross section. In this example, the beam was reinforced with one CFRP lamina á 5 millimeter in tension and compression respectively.

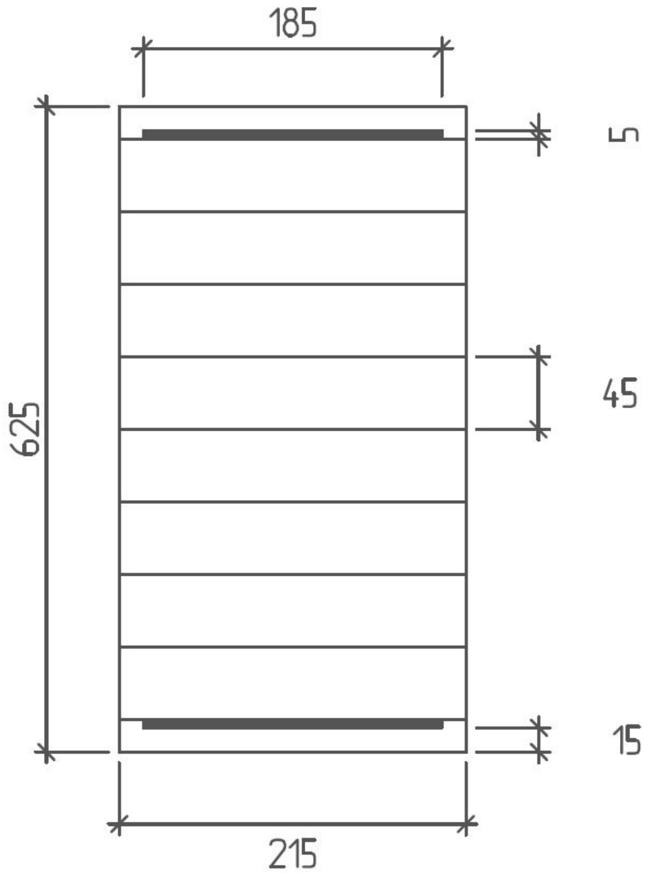

Figure 4.2: *Illustration of the cross section used. Note that the dimensions are only an example and may differ for different configurations in the analyses.*

The supports were analysed analytically to be 100 millimeters wide, sufficient to avoid failure due to compression failure perpendicular to the grain. A longitudinal view of the modelled beam can be seen in Figure 4.3.

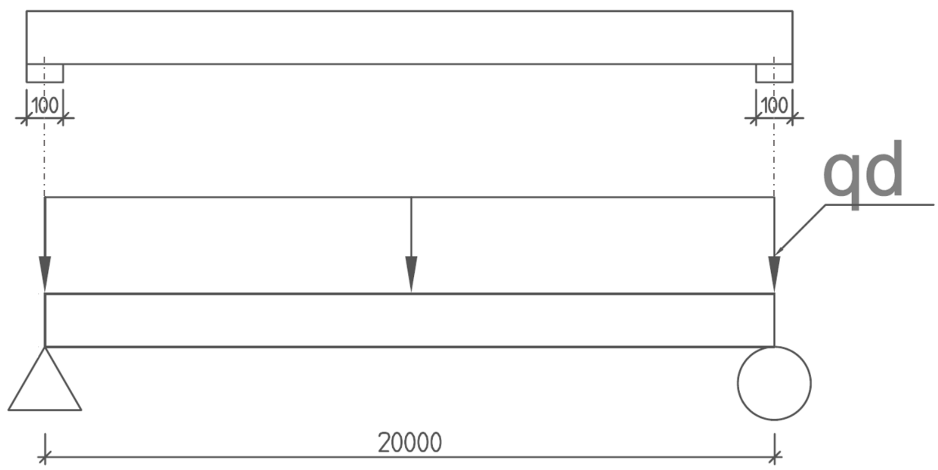

Figure 4.3: *Illustration of the support conditions.*

According to E. Martinson (Martinsons, personal communication, March 11 2019), the most commonly used glulam class for pedestrian bridges is GL28c. This strength class has therefore been implemented throughout the entire calculations in this thesis. The characteristic values are based on Swedish standard (Borgström, 2016) and can be found in Table 4.1. The coefficient for temperature expansion is provided by Eurocode (SIS, 2014a).

Table 4.1: *Characteristic strengths for glulam beams (Borgström, 2016).*

Glulam strength GL28c		
Tension parallel to grain (f_{tk})	[MPa]	19.5
Compression parallel to grain (f_{ck})	[MPa]	24
Bending parallel to grain (f_{mk})	[MPa]	28
Shear (f_{vk})	[MPa]	3.5
Rolling shear (f_{rk})	[MPa]	1.2
Young's modulus parallel to grain (E_{mean})	[GPa]	12.5
Young's modulus parallel to grain ($E_{0.05}$)	[GPa]	10.4
Density mean (ρ)	$[kg/m^3]$	420
Temperature expansion coefficient	$[10^{-6} \cdot K^{-1}]$	5.0

According to Eurocode, certain aspects need to be considered such as safety factors for the material, load duration and long term effects such as creep to obtain the design strength. The factors used are presented in Table 4.2. The factor considering the size of the beam, k_h, is varying with the height of the beam.

Table 4.2: *Safety and reduction factors for glulam (Borgström, 2016; SIS, 2009).*

Eurocode safety and reduction factors	
Service Class	3
γ_{glulam}	1.25
k_h	1.0-1.1
k_{cr}	0.67
k_{def}	2
k_{mod}	0.8
ψ_{red}	0.4
γ_{cfrp}	1

Strength characteristics for CFRP materials are more difficult to obtain since the polymer composition varies among different manufacturers and standards for the material do not exist. Therefore, the material parameter values were mostly based on recommendations from supervisors, weighted with values from manufacturers. The coefficient of thermal expansion was assumed to be -1.0, as the value may differ with variations in CFRP compositions, see Section 3.3. In Table 4.3, the material properties used are presented.

Table 4.3: *Characteristic strengths for CFRP lamina (Gurit, 2018).*

CFRP properties		
Tensile parallel to grain ($f_{t.cfrp}$)	[MPa]	2800
Compression parallel to grain ($f_{c.cfrp}$)	[MPa]	1400
Young's modulus low	[GPa]	205
Young's modulus mid	[GPa]	300
Young's modulus high	[GPa]	375
Young's modulus ultra-high	[GPa]	450
Density mean	$[kg/m^3]$	1600
Temperature expansion coefficient	$[10^{-6} \cdot K^{-1}]$	-1.0

The loads acting on the beam are self-weight and variable load from both pedestrians and service vehicles. According to Sétra (2006) and Heinemeyer (2009), traffic classes 2 and 3 were used to evaluate the dynamic performance of the bridge. The values used for both static and dynamic analyses are specified in Table 4.4.

Table 4.4: *Loads used for both static and dynamic analyses (SIS, 2007; Sétra, 2006).*

Loads		
Self-weight (g)	$[kN/m]$	Derived from density and cross sectional area
Pedestrian load (q)	$[kN/m^2]$	5
Service vehicle axle 1	$[kN]$	80
Service vehicle axle 2	$[kN]$	40
Pedestrian weight	$[kN]$	0.7
Traffic class 2	$[kN/m^2]$	0.14
Traffic class 3	$[kN/m^2]$	0.35

These loads were then combined with corresponding partial safety factors for the calculation of ULS and SLS load cases, see Table 4.4. The ULS combination is used when calculating shear and moment capacities. For deflection controls, it is only the deflection caused by the variable load that is governing (Trafikverket, 2016). For the fundamental structural frequencies, the self-weight is the only considered load in the dynamic assessment. When calculating the frequencies due to pedestrian loading, traffic classes according to Table 4.4 is used.

Table 4.5: *Load combinations used for ULS and SLS according to Eurocode SIS (2005)*

Load Combinations	
Ultimate Limit State (ULS)	1.2•g+1.5•q
Serviceability Limit State (SLS), deflection	ψ_{red}•q
Serviceability Limit State (SLS), natural frequency	1.0•g

4.2 Model assumptions

Since composite elements can be highly complex, relevant assumptions were necessary to make a good assessment. Schober et al. (2015) suggest an approach were the following assumptions are made:

- The CFRP has a linear behaviour in both compression and tension.
- The timber has a linear behaviour in tension.
- The timber has a nonlinear behaviour in compression.
- The timber and CFRP fully interact.
- Plane sections remain plane in bending.

Timber is generally weaker in tension than in compression. Having the CFRP equally distributed on the compression and tension side, means that the timber predominantly fails in tension, before it fails in compression. Therefore, the assumption about timber having a nonlinear behaviour in compression was not included in the model. The nonlinear behaviour would only be relevant if the beam had more reinforcement on the tension side than on the compression side.

The existing information about partial safety factors and Eurocode implementation for CFRP is scarce. The material safety factors were based on the suggestions in the *Prospect for new guidance in the design of FRP* (Ascione et al., 2016). In this case, the production of the CFRP was assumed to be in a controlled and certified environment. Most often, long term effects are quite small compared to timber, and therefore they were neglected in these calculations. Instead, all partial factors for long term effects in the analytic calculations were based on timber.

For the analytic calculation, the timber at the same level as the CFRP was excluded in the analysis due to minor influence, see Figure 4.4.

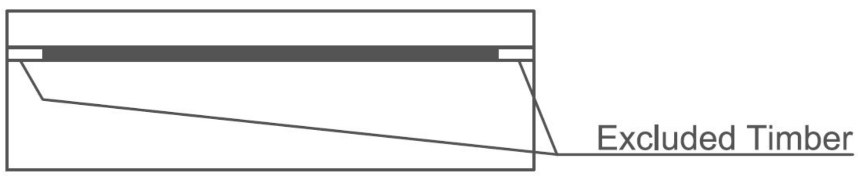

Figure 4.4: *Illustration of the timber pieces excluded in the calculation model for analytic analysis.*

5

Analytic Calculations

The calculations are based on recommendations from Swedish Wood including Design of timber structures (Borgström, 2016). Furthermore, Structural Timber Design to Eurocode 5 (Porteous and Kermani, 2007) and Eurocode 5 (SIS, 2014b) have been used. For glulam beams reinforced with CFRP, calculation standards and recommendations are sparse. Therefore, calculations are mainly based on previous research and composite linear elastic cross section analysis. The analytic calculations was also used to verify the results obtained in the FE-analysis.

5.1 Eurocode Considerations

According to Eurocode and the national annex in Sweden, a structure should be designed with regards to certain requirements in Ultimate Limit State (ULS) and Serviceability Limit State (SLS) (Kliger, 2016). ULS concerns the demands related to structural safety, collapse or other structural failures. After reaching ULS, the structure can no longer fulfill its structural purpose. The controls that were performed analytically in ULS are stated in Equation 5.1.

$$\frac{M_{Ed}}{M_{Rd}} \leq 1, \qquad \frac{V_{Ed}}{V_{Rd}} \leq 1 \tag{5.1}$$

In contrast to ULS, SLS requirements might not lead to a direct failure or collapse of the structure. However, it is important to fulfill the demands with regards to comfort for the user and general appearance of the bridge (Mårtensson, 2016). Therefore, deflections should be kept within allowed limits. Excessive deflection might in fact not damage the structure but it gives the user a feeling of insecurity (Mårtensson, 2016). The SLS checks that were performed for the analytic calculations were considering deflections and vibrations. SIS (2009) suggest a limit for deflections, according to Equation 5.2.

$$\delta_{max} \leq \frac{L}{400} \tag{5.2}$$

As mentioned in Section 2.5, dynamic conditions are many times decisive for design of timber structures. According to Heinemeyer (2009), the critical range for structural frequencies in vertical direction is:

$$1.25Hz < f_i \leq 4.6Hz \tag{5.3}$$

According to SIS (2005), the first frequency should be over *5 Hz* to avoid the acceleration checks completely. If a structural frequency of a structure is within the range described by Equation 5.3, the acceleration generated by a pedestrian footstep might be decisive. As described in Section 2.5, accelerations are highly subjective and different standards suggest different limits. According to SIS (2014b), the acceleration should not exceed $0.7m/s^2$, while Sétra (2006) states that the mean comfort level for users is in the range of $0.5 - 1.0m/s^2$. Due to this ambiguity, the maximum allowed acceleration was chosen to $0.75m/s^2$, stated in Equation 5.4.

$$a < 0.75m/s^2 \tag{5.4}$$

5.2 Linear Elastic Model for the Composite Cross Section

The limiting strains in the cross section are governed by the strength of the outer lamella in the glulam. The strain limits can be expressed according to Equation 5.5 for compression, and according to Equation 5.6 for tensile.

$$\varepsilon_{c.el.gl} = \frac{f_{t.0.k}}{E_{timber}} \tag{5.5}$$

$$\varepsilon_{t.el.gl} = \frac{f_{c.0.k}}{E_{timber}} \tag{5.6}$$

Since timber is a highly linear elastic material before failure, the strain distribution over the cross section can be assumed to be linear in ULS. With the limits described in the Equations 5.5 and 5.6, the capacity for the cross section in Figure 5.1 can be calculated by assuming that the ultimate tensile strain is reached.

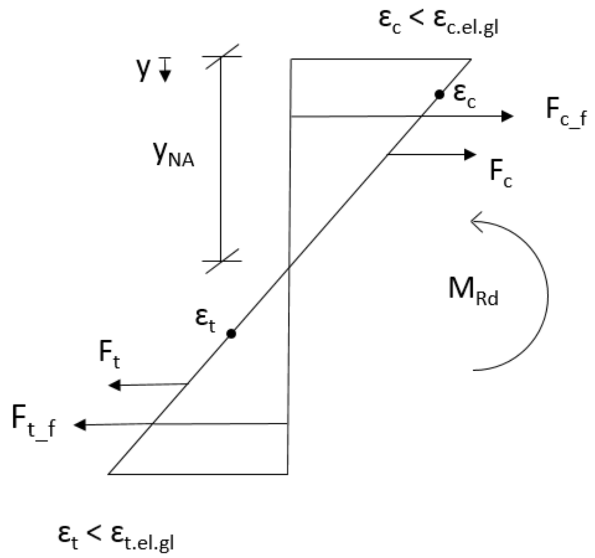

Figure 5.1: *Strain compatibility in case of linear elastic analysis.*

From Figure 5.1, the force equilibrium equation can be derived according to Equation 5.7.

$$F_t + F_{frp.tension} = F_c + F_{frp.compression} \tag{5.7}$$

To calculate the forces in a composite cross section, a factor α is used to transform the stiffness properties of CFRP into equivalent timber. This is done by increasing the CFRP width with a factor α, as can be seen in Figure 5.2. The factor is calculated by using the modulus of elasticity for the two materials, as can be seen in Equation 5.8.

$$\alpha = \frac{E_{CFRP}}{E_{timber}} \tag{5.8}$$

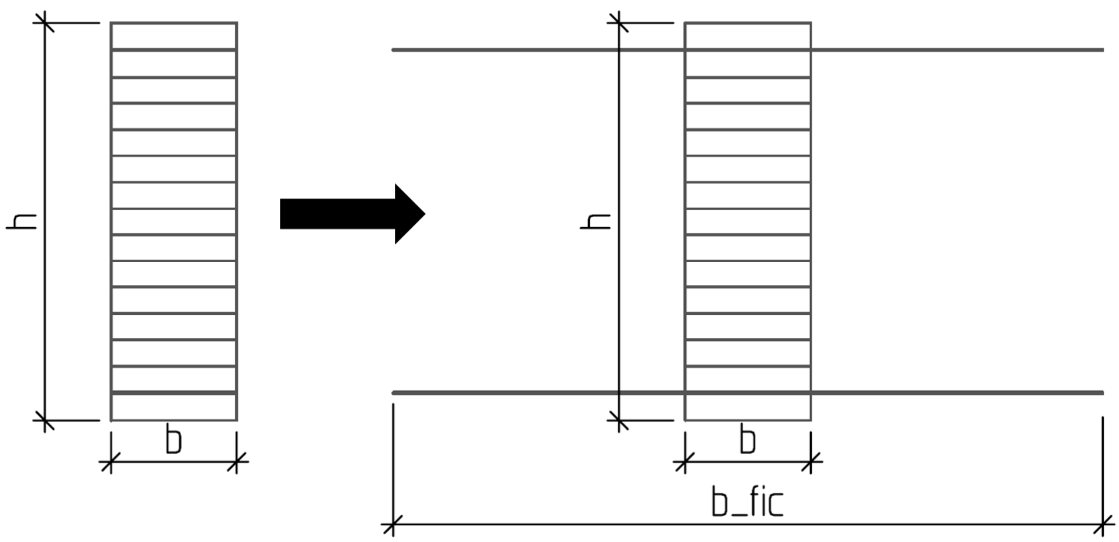

Figure 5.2: *By using the factor α, the composite cross section can be transformed into an equivalent timber section, where the fictitious width of the CFRP (b_{fic}) is calculated using α.*

With the value for α known, the bending stiffness can be calculated by using the young's modulus for timber together with the second moment of area for the transformed cross section. Since the strains in the cross section constitute a set of similar triangles, the strains can be calculated at any height when the position of the neutral axis is known, see Equation 5.9 and 5.10.

$$\varepsilon_t(y) = \varepsilon_t(0) \cdot \frac{y_{NA} - y}{y_{NA}} \tag{5.9}$$

$$\varepsilon_c(y) = \varepsilon_t(h) \cdot \frac{y - y_{NA}}{h - y_{NA}} \tag{5.10}$$

With the strains known, the moment capacity can be calculated by assuming a linear response and then use force equilibrium.

5.3 Calculation of Load Effects and Capacity

With the problem and assumptions explicitly defined, the design effect and resistance can be calculated accordingly. To achieve sufficient structural capacity, the static and the dynamic case must both be fulfilled.

5.3.1 Linear Analysis of the Static Case

In statics, the requirements in Equation 5.1 and 5.2 must be fulfilled. To ensure enough capacity in ULS, the load effects M_{Ed} and V_{Ed} should be calculated and compared with the design capacities M_{Rd} and V_{Rd}. The design capacities are calculated based on the characteristic values together with partial safety factors and reduction factors described in Table 4.2, see Equation 5.11 for example.

$$f_{md} = \frac{f_{mk}}{\gamma_{glulam}} \tag{5.11}$$

The moment capacity, M_{Rd}, is then calculated by multiplying the sectional forces with their respective lever arm from an arbitrary point in the cross section, see Figure 5.1. It is then compared to the calculated flexural load effect, given by Equation 5.12. Note that the ULS load case, see Table 4.5, is used.

$$M_{Ed} = \frac{(1.2 \cdot g + 1.5 \cdot q) \cdot L^2}{8} \tag{5.12}$$

The shear load effect is calculated according to Equation 5.13.

$$V_{Ed} = \frac{(1.2 \cdot g + 1.5 \cdot q) \cdot L}{2} \tag{5.13}$$

For a composite cross section, the shear effect is transformed into applied shear stress, according to Equation 5.14. This should be less or equal to the shear stress capacity, τ_{Rd}.

$$\tau_{Ed} = \frac{S \cdot V_{Ed}}{I_{composite} \cdot b} \tag{5.14}$$

The deflection of a composite cross section is calculated according to Equation 5.15, and then compared to the SLS requirements. According to SIS (2005), a factor ψ_{red} is used to reduce the effect of the traffic load.

$$\delta = \frac{5 \cdot (q \cdot \psi_{red}) \cdot L^4}{384 \cdot (EI)_{composite}} \tag{5.15}$$

Being a composite material, it is likely that shear stresses will develop in the interlaminar area between the timber and CFRP. Therefore, failure in the timber in the vicinity of the adhesive layer must be checked. Since the adhesive layer is assumed to have full interaction and sufficient load carrying capacity, failure will not occur in the adhesive layer. However, these controls are highly complex and are therefore done in the numerical analysis, see Chapter 6.

5.3.2 Linear Analysis of the Dynamic Case

As mentioned in Section 2.5, dynamic conditions put high demands on timber structures. The most critical demand is the structural frequency of the bridge. The first and second vertical structural frequencies are calculated according to Equation 5.16 and 5.17.

$$f_i = \frac{1}{2 \cdot \pi} \cdot \frac{9.869}{L^2} \cdot \sqrt{\frac{E_{mean} \cdot I_{tot}}{m_g}} \tag{5.16}$$

$$f_i = \frac{1}{2 \cdot \pi} \cdot \frac{39.478}{L^2} \cdot \sqrt{\frac{E_{mean} \cdot I_{tot}}{m_g}} \tag{5.17}$$

Since the free span of the bridge is less than 50 meters, wind loads were considered to be negligible in the dynamic calculations (Trafikverket, 2016). Furthermore, no checks were performed for lateral movements due to the high amount of stiffness in the lateral direction of the bridge. The traffic classes used for the dynamic calculations are presented in Table 5.1. Traffic class 5 corresponds to exceptionally dense traffic where it is hard to move and unpleasant to reside on the bridge. Traffic class 1 corresponds to very weak traffic, often disregarded for the benefit of traffic class 2.

Table 5.1: *Pedestrian load for different traffic classes (Heinemeyer, 2009).*

Pedestrian loads	
Traffic class	Density of pedestrians $[P/m^2]$
TC2	0.2
TC3	0.5
TC4	1.0
TC5	1.5

To calculate the structural frequencies, a load of 700 N was used, corresponding to the weight of a pedestrian (Heinemeyer, 2009). This was then multiplied with the traffic density suggested by the traffic classes in Table 5.1. For calculations of maximum acceleration in vertical direction, the vertical component 280 N is used instead (Heinemeyer, 2009). Since the traffic density rarely exceeds the one corresponding to traffic class 3, traffic classes 4 and 5 were disregarded in the calculations.

Similar to the the acceleration requirements described in Section 5.1, there are some ambiguity regarding the damping ratio for timber in dynamic models. The damping ratio is mostly dependent on the material itself, but also on the used connectors. According to Heinemeyer (2009) the damping ratio should be chosen to 1.5% while Sétra (2006) suggest a value of 3%. The most unfavourable case of 1.5% was chosen for the model.

5.4 Evaluated Beam Configurations

To evaluate the concept of fibre reinforced glulam elements, different configurations were evaluated to investigate for which the reinforcement concept would proven itself most useful. The configurations were chosen based on suggestions and interests from Sweco and the collaborator Martinson Trä. This section presents the configurations and why they were chosen. The cross sections were all configured in the same way, with a beam height of 625 millimeters with 5 millimeters thick CFRP laminas in compression and tension respectively, exemplified in Figure 4.2.

The first evaluated configuration was a simply supported reinforced straight beam, illustrated in Figure 5.3. This configuration served as a base for the other configurations, meaning that the results could be compared with results from other configurations to study how alterations change stresses and deflection. The complete calculations can be found in Appendix A.

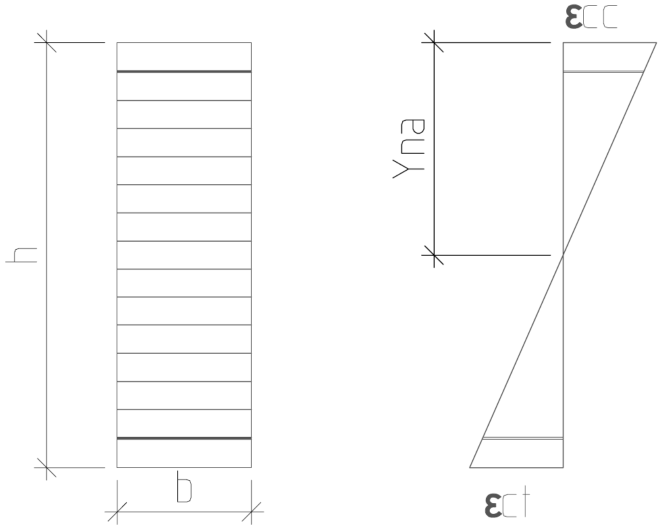

Figure 5.3: *Illustration of the calculation model used.*

Since the IBR method is a new concept, it is important to compare it with other reinforcement techniques to investigate how they differentiate. Therefore, a straight beam with NSM reinforcement was studied, see Figure 5.4. The beams were configured in the same way and the reinforcement ratio of the cross section was adjusted to be the same in both cases. The complete calculations can be found in Appendix D.

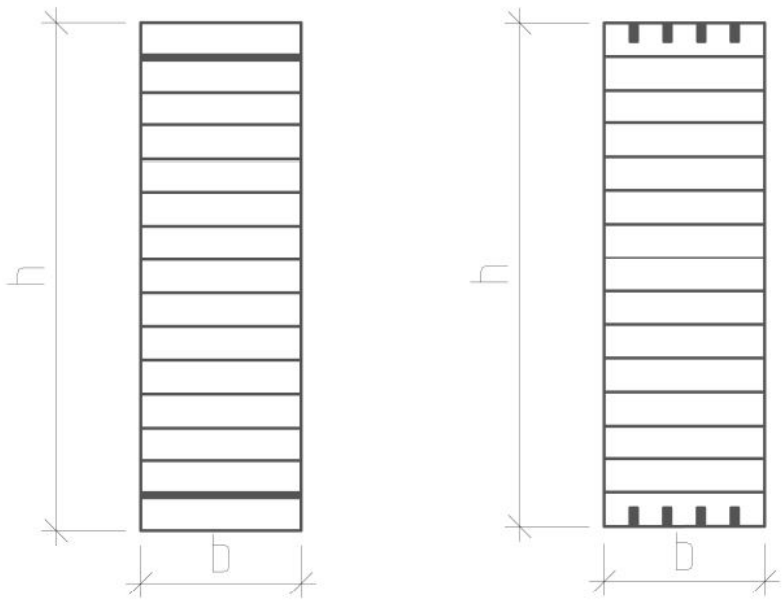

Figure 5.4: *Illustration of the two different calculation models used for the comparison, IBR (left) and NSM (right).*

The calculations for a T-beam are similar to those of a straight beam, with the addition of a wider upper flange. The width of the upper flange should be reduced by finding an effective with of the beam, which is the width that contributes to the actual structural capacity. To ensure enough stiffness, the reinforcement area should be the same in both the compression and tension zone. A sketch of the cross section is presented in Figure 5.5. Since the upper flange is wider than the web, more CFRP was needed in the bottom of the beam to achieve equilibrium of the cross section. The complete calculations can be found in Appendix B.

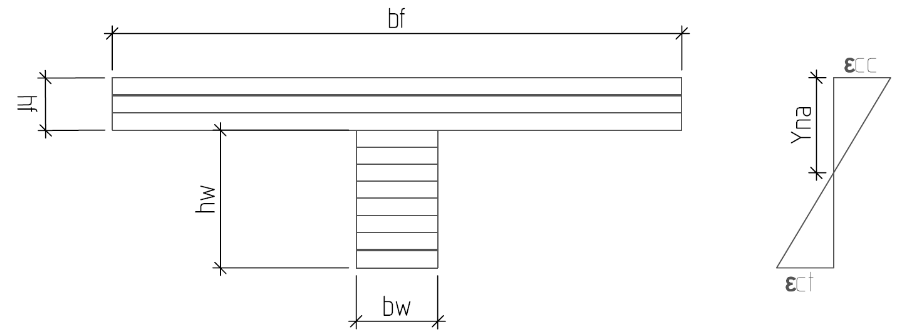

Figure 5.5: *Cross section of the T-beam together with the strain distribution across the cross section.*

5.5 Stress-Laminated Deck as a Bridge Concept

As mentioned in Section 2.6, a stress-laminated deck is a linear multiplication of a single straight beam. However, additional loads such as service vehicles, weight of railings, pre-stressing bars and walkway covers increases the stress on the bridge, see Figure 5.6. This corresponds in theory to an actual preliminary sizing of a timber bridge and strengthens the reinforcement configuration as a proof of concept. The complete calculations can be found in Appendix C.

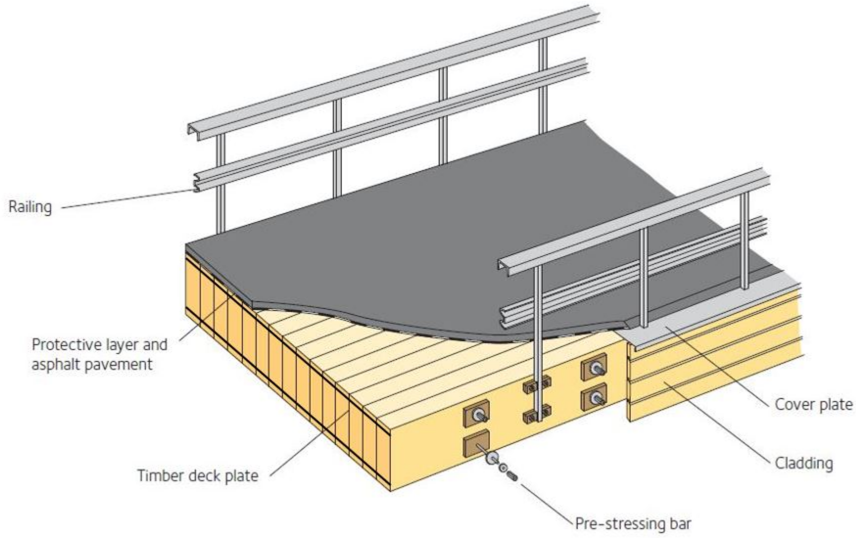

Figure 5.6: *Illustration of a complete stress laminated deck bridge, the black horizontal lines corresponds to the added CFRP laminas (Pousette, 2016).*

There are two possible failure modes where the needed prestressing force is too small (Ekholm et al., 2012). Either the transverse bending moment is larger than the prestressing force and gaps are created between the glulam beams. The other failure mode is vertical interlamellar slip. Both failure modes are illustrated in Figure 5.7. The failure occurs when the transverse shear forces are larger than the friction forces between the glulam beams.

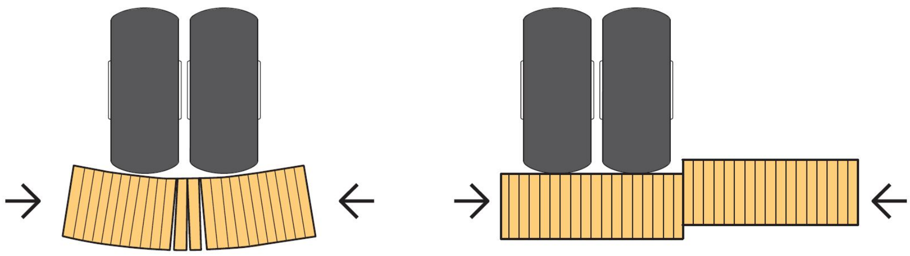

Figure 5.7: *Illustration of possible failure modes between the beams in a stress laminated deck (Pousette, 2016). Transverse bending (left) and vertical interlaminar slip (right).*

The needed pre-stressing force is determined according to Equation 5.18 and 5.19 (Ekholm et al., 2012).

$$F_{ps} \geq \frac{6 \cdot M_T}{h_{tot}} \tag{5.18}$$

$$F_{ps} \geq \frac{3 \cdot V_T}{2 \cdot \mu_{timber}} \tag{5.19}$$

An illustration of how the prestressing bar works in a stress-laminated deck can be seen in Figure 5.8. It is assumed that sufficient tension force is reached and thereby no further checks of failure between the beams are needed.

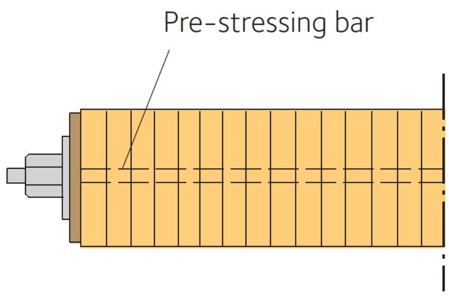

Figure 5.8: *Illustration of stress-laminated deck with prestressing bar (Pousette, 2016).*

5.6 Investigation of Parameter Choice Effects

A parametric study was performed to investigate which parameters that would have the largest effect on the concept. The study serves to show how changes in young's-modulus, density and choice of damping coefficient influence the result. Further on, an investigation of the possible span lengths is performed. The investigated spans range from 5 to 30 meters, in order to observe what failure modes that are governing for a shorter and longer beams. This also makes it possible to obtain a theoretical upper limit of feasible span lengths, and observe a lower limit where the CFRP is superfluous.

5.7 Optimisation of Beam Configurations

An attempt to optimise the reinforcement scheme was made to ensure that the CFRP and timber is combined in the most efficient way. The available height is often, as previously mentioned, a limiting demand at the site. Also, it is of interest to minimise the amount of CFRP due to the high cost and environmental impact.

The optimisation was performed with four different optimisation objectives. The first objective was to have a minimum amount of reinforcement. The minimum amount of reinforcement corresponds to adding a 2.5 millimeter CFRP lamina, one of the standard dimensions according to S&P (Personal communication, S&P Reinforcement, March 29 2019). For the three remaining optimisations, there was no consideration taken regarding available standard dimensions. In the second, third and fourth objective, the goal was to reduce the height with approximately 25, 40 and 50% respectively. All while still maintaining sufficient structural capacity of the cross section and satisfying the SLS requirements. The first and third optimisation objectives were used for the investigation of parameter choice effects.

The optimisations are done iteratively by either increasing the CFRP height with 0.1 millimeter every iteration, or by increasing the timber height with one lamella, corresponding to an increase of 45 millimeter. Based on the parametric study results, the CFRP young's modulus was chosen to 300 GPa. It was identified that 300 GPa would give the largest difference in height, see Section 9.1.2.

6
Finite Element Analysis

Finite Element Analysis (FEA) is a computerized numerical method used to solve engineering and mathematical physics. The method is used to obtain an approximate solution to a real engineering application where the analytic solution generally is too complicated to solve. The method uses boundary conditions and limitations of domain provided by material data, support conditions or loading cases to solve the differential equations. Thereby, it is important to be certain of the input to the model, to be able to analyse and critically interpret the output.

The specific software used in this thesis is Brigade/Plus 6.2 from Scanscot Technology. It is a software based on the platform of Abaqus/CAE developed specifically for bridge-engineering purposes (Scanscot Technology AB, 2019).

The FEA was used to evaluate the concept of a pre-cambered CFRP reinforced glulam beam. Especially the stresses between the timber and CFRP parts were studied in order to evaluate the risk for local shear failure. An additional straight model was created to verify the FE-model and assumption, using the results of the analytic calculations.

Self-weight, variable load and temperature variations were the considered loads in the analysis. For the temperature, it was assumed that the initial temperature was 20°C and that it is either decreased or increased to -20°C or 40°C respectively.

For the analysis, the beam was chosen to consist of 12 timber lamellas à 45 millimeters. Together with a CFRP thickness of 5 millimeters and outer lamellas, the total height was 580 millimeters.

6.1 FE-modelling of Fibre Reinforced Timber

Since the CFRP is embedded in the exterior timber lamella and has a smaller width than the width of the cross section, see Figure 2.19, three dimensional solid elements were used. Otherwise it would not be possible to observe some of the effects. Also, if other studies were to be performed based on this thesis, a 3D-model gives a possibility to evaluate stresses due to lateral loads.

Both the timber and CFRP were modelled as linear-elastic materials. However, while the CFRP was chosen to be isotropic, the timber was modelled with engineering constants, meaning that the young's modulus and the shear modulus were varying with the direction of the material. The values used for material properties are presented in Table 6.1. Also, temperature expansion coefficients were included to see how the model responds to temperature variations.

Table 6.1: *Characteristic strengths for reinforced glulam elements (Borgström, 2016; Gurit, 2018; SIS, 2014b).*

Material Properties FE-model			
		Glulam (GL28c)	CFRP
Density	$[kg/m^3]$	420	1600
E_L	$[GPa]$	12.6	-
E_R	$[GPa]$	0.7	-
E_T	$[GPa]$	0.37	-
G_{LR}	$[GPa]$	0.72	-
G_{LT}	$[GPa]$	0.35	-
G_{RT}	$[GPa]$	0.03	-
ν_{LR}	$[-]$	0.03	-
ν_{LT}	$[-]$	0.04	-
ν_{RT}	$[-]$	0.35	-
E_{CFRP}	$[GPa]$	-	300
ν_{CFRP}	$[-]$	-	0.3

The interface between the CFRP and timber was modelled with fully constrained ties, since full interaction was assumed. Having full interaction, makes it impossible to study any bond-slip behaviour. However, shear stresses can still be monitored to see if they could cause a shear failure in the vicinity of the interface. In Figure 6.1, the constraints are shown. Note that it is only the horizontal edge of the CFRP that is tied to the timber. In reality, the vertical CFRP edge would be glued to the outer lamella. Likewise, the outer lamella would also be tied to the inner lamellas. This will have a negligible effect on the structural behaviour, which is why it was disregarded in the model.

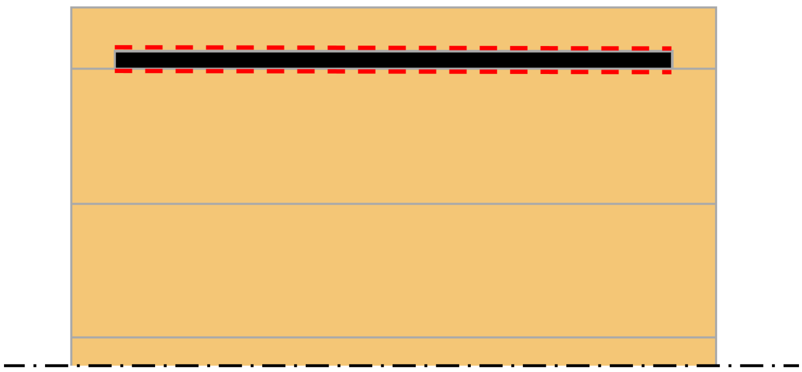

Figure 6.1: *The dashed red line illustrate where the materials have been tied together in the FE-model.*

The assumption about full interaction is reasonable. Many studies have shown that failure usually occurs in the timber fibres close the the CFRP lamina, and that the adhesive, in most cases epoxy, has sufficient strength (Schober et al., 2015; Trimble et al., 2010; Valipour and Crews, 2011). Also, data regarding bond-slip properties of CFRP-to-timber connections is difficult to obtain theoretically. If the bond-slip relation is needed, full scale tests with the specific configuration would have to be performed.

Being a simply supported beam, adequate boundary conditions need to be applied. On the left side, the beam is locked for movement in x,y and z-directions. On the right side, the beam is locked for movement in y and z. To achieve a realistic response at the boundaries, a very stiff beam element (young's modulus of 1 000 000 GPa) was included at the supports. The beam element was then locked in x-, y- and z-direction on the left side, and y- and z-direction on the right side. The beam elements let the beam rotate at the support in a correct way. If they would not be included, unreasonable large stresses would occur by the supports, influencing the shear stress between the timber and bottom CFRP lamina. An illustration of the boundary conditions can be seen in Figure 6.2 and further specified in Figure 6.3.

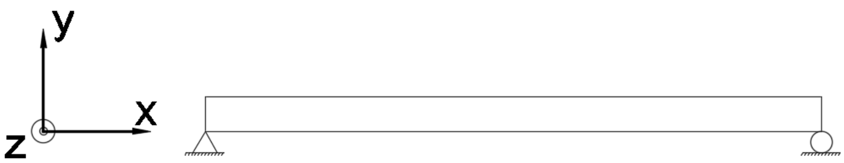

Figure 6.2: *Illustration of the beam's boundary conditions and its coordinate system.*

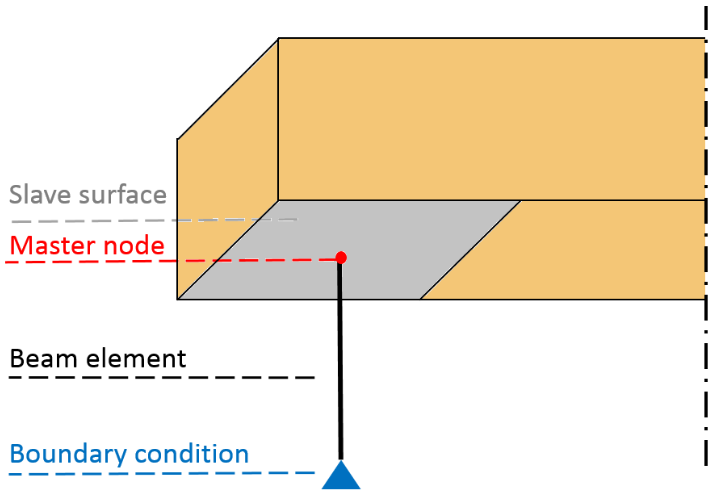

Figure 6.3: *Illustration of the boundary conditions and how they are applied in the FE-model. Here exemplified with the left support. The right support is modelled in the same way.*

6.1.1 Load Combinations in the FE-analysis

To evaluate the performance of the beam, it is important to study the most critical load case. By using different partial factors and combining them with the self-weight, variable load and temperature variations, many different load cases arise.

However, the considered cases in this thesis are relatively few. Therefore, the most unfavourable load cases can be considered, presented in Table 6.2. During the simulations, it was found that heating of the beam is unfavourable in all cases, which is why cooling was excluded.

Table 6.2: *The table describes the combinations of loads and safety factors that were used for the finite element analysis.*

Load combinations			
	Type of load and the safety factor used		
Type of analysis:	Self-weight	Traffic	Temperature Difference
Shear stresses in the timber	1.2	1.5	$1.5 * 0.7$
Deflection	0	0.4	0
Frequency	0	0	0
Tension perpendicular to grain	1.2	1.5	$1.5 * 0.7$

6.2 Mesh Convergence Study

A mesh is the subdivision of the model into finer parts which are evaluated piecewise by the FE-software. A fine mesh sets high demands on computational power and analysis time, but it will also yield a more refined and stable result. It is therefore of interest to optimise the mesh-size. To verify that the created mesh was fine enough to obtain valid results a mesh convergence study was performed based on the deflection of the beam, see Figure 6.4 and 6.5. From this an optimal mesh is selected both regarding satisfying stability of the results, but also optimal processing time for the analysis. The mesh convergence study was performed for both the static and the dynamic analysis, based on the straight beam model.

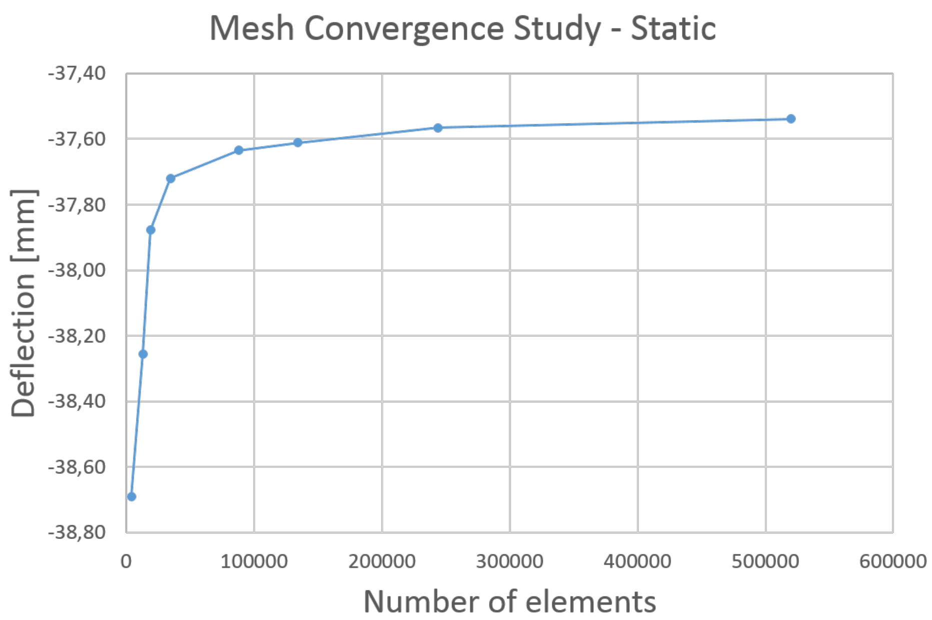

Figure 6.4: *Mesh convergence study based on the static straight model.*

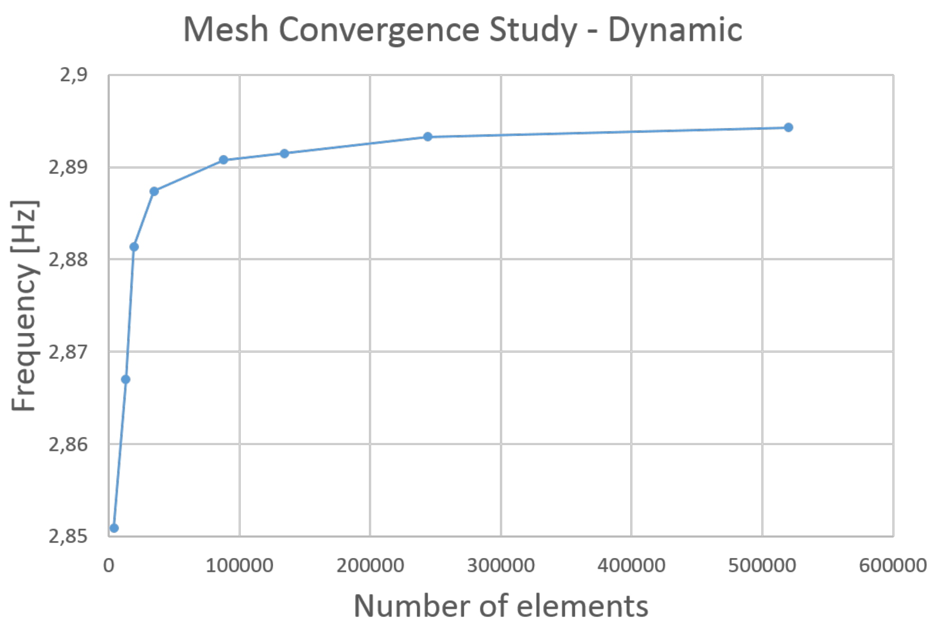

Figure 6.5: *Mesh convergence study based on the dynamic straight model.*

Based on the mesh-convergence study, presented in Figure 6.4 and 6.5, a mesh size of 40 millimeters was chosen. A refined mesh was used for the areas closest to the supports to better obtain the local effects and reliability in the results, as it is there the shear stresses in the interfacial layer will be largest. With a mesh-size of 20 millimeter in the support regions, the total amount of elements for the entire beam was 201 480. The elements used in the model were linear hexahedral elements of the type C3D8R. The mesh used in the model is shown in Figure 6.6. The same mesh was used for the pre-cambered model, as the differences were deemed to be negligible.

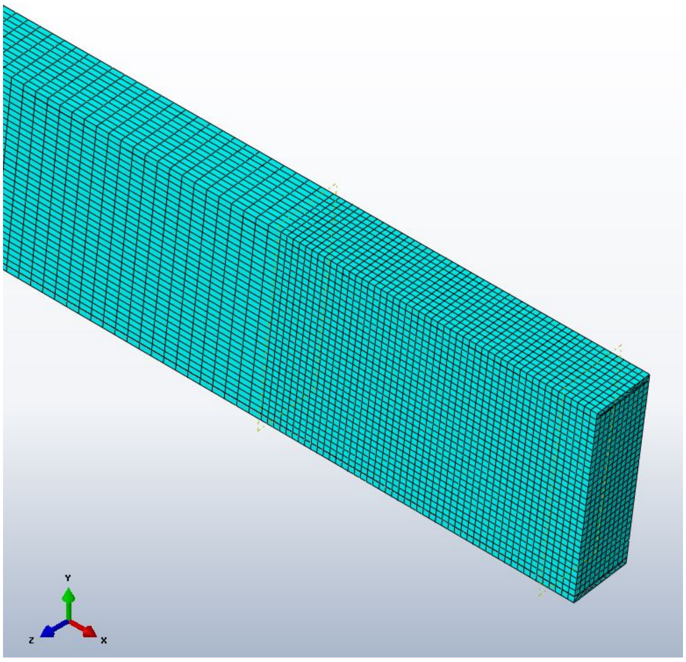

Figure 6.6: *A cut-out which illustrates the mesh used in the FE-model.*

6.3 Investigation of Shear Stresses Between Timber and CFRP

To further evaluate the concept with embedded CFRP reinforcement, it was of interest to study stresses that are difficult to consider in analytic calculations. When a CFRP reinforced beam is loaded in bending, the shear stresses between timber and CFRP need to be studied. In most literature, see Section 2.4, the failure takes place in the timber, rather than in the adhesive or the CFRP. Therefore, the shear stresses in the timber close to the CFRP should be assessed and compared to the shear capacity of timber. The shear forces between timber and CFRP should be the largest by the supports, which is why the mesh was refined in this area.

Furthermore, the shear stresses might increase when pre-cambering a beam. Therefore, beams with different amounts of pre-cambering were also evaluated. For a pre-cambered beam, one of the critical zones is the apex zone, see Figure 6.7. In this zone tension perpendicular to the grain occurs, which might lead to failure of the beam. Therefore, these stresses were also evaluated.

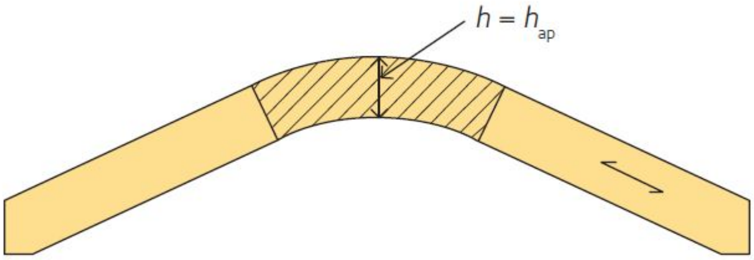

Figure 6.7: *Illustration of the apex zone (shaded area) in a pre-cambered beam (Crocetti, 2016).*

From the analytic calculations, the pre-camber to counteract the deflection from self-weight was estimated to be 25 millimeters. This amount was used for comparison with a straight beam, after which the pre-camber was increased.

The analytic calculations showed that the concept also could be used for a beam with a span of 30 meters. To control the viability of the longer spans, the shear stresses were also monitored in this case. The ratio of pre-camber contra span length was the same as for the beam with a 20 meters span, meaning a pre-camber of 37.5 millimeters was used. The number of timber lamellas and the thickness of CFRP was chosen based on the analytic results, resulting in 18 lamellas à 45 millimeters and 3 millimeter CFRP on both tension and compression sides. The total height of the beam is then 816 millimeters.

7

Economic comparison

The purpose of the economic comparison was to investigate the competitiveness of the reinforcement configuration and to evaluate if it is a viable implementation option with current material prices. Only other lightweight alternatives were considered, for example glulam or steel. The comparison is divided into three parts. Firstly, prices for the different materials are gathered. Afterwards, the necessary dimensions to manage the demands set by Eurocode are calculated. The dimensions for the glulam and CFRP reinforced glulam are calculated analytically. The dimensions for a corresponding steel pedestrian bridge was provided by Sweco. The prices are multiplied with the dimensions and then divided with the total square surface of the bridge. This is to obtain the functional unit of the comparison, which is $[SEK/m^2]$. The height is in this case irrelevant. The material costs vary depending on manufacturer and time, which is why an upper and a lower value have been calculated.

7.1 Economic Trends for Materials

Studying the price trend presented in Figure 7.1, it can be observed that the cost for carbon fibre is decreasing and that the forecast predicts further decrease in the near future (Rao et al., 2018). To acquire more specific data regarding price trends, the price development for a specific CFRP composition over time is needed. However, since prices for raw material are decreasing every year and the production is becoming more efficient, CFRP will most likely be more economically competitive in the future (Rao et al., 2018).

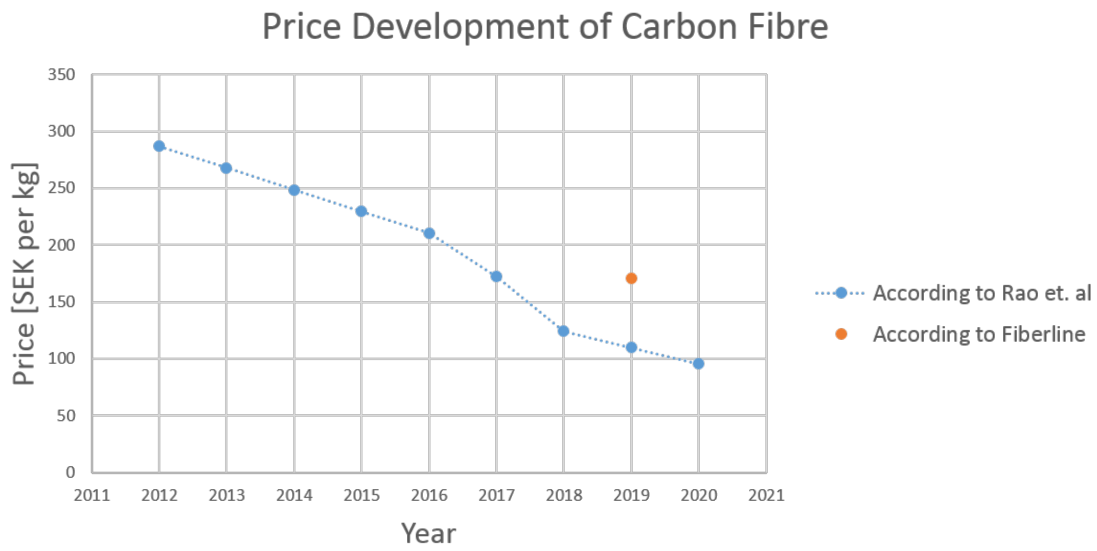

Figure 7.1: *Price trends and forecast for carbon fibre (Rao et al., 2018; Fiberline, 2016). The price was recalculated using the dollar and euro rates the 7th of May 2019, 9.56 SEK/USD and 10.7 SEK/EUR respectively.*

Rao et al. (2018) also indicate that there is an increasing demand worldwide, especially in non-aerospace applications, putting pressure on the industry to streamline the production to meet the demand. Streamlining the production methods also increases the repetitiveness which would result in a more homogeneous quality of the products. Even though the price of the raw material is decreasing, the largest cost influence for producing CFRP is the choice of manufacturing method, see Section 2.3.1 (Rao et al., 2018). Depending on the labour intensity and how much equipment that is needed, the cost of a product can vary significantly. Small scale production is more expensive and the price decreases rapidly with increasing scale.

For glulam products, E. Martinson (Personal communication, Martinsons Trä, April 25 2019) stated that data showing how the price has changed with respect to time is hard to obtain. However, the product has been in use for more than 100 years, and better techniques to automatise and streamline the production have already been implemented to a great extent. Therefore, it was assumed that it will be kept at a constant level in the future. According to E.Martinson (Personal communication, Martinsons Trä, March 27 2019) the current price from glulam products is 6000 SEK/m^3.

Steel is a material that has been used for a long time as well. Depending on supply and demand, certain fluctuations from year to year occurs. In recent years, the price has been relatively stable, which is why the price is assumed to be kept on a constant level for the purpose of this thesis. The current price for a HEB450 beam is approximately 25 SEK/kg, obtained from Stena Stål AB (2019). However, this was the standard price for a beam and to account for variations in price over time the upper value in the comparison has been increased with 10 SEK/kg.

7.2 Economic Comparison with Glulam and Steel

To evaluate the economic feasibility of the suggested reinforcement method, it was compared to two other lightweight materials. The CFRP reinforced glulam bridge was compared to an unreinforced glulam bridge and a steel bridge. The bridges in the comparison have similar loading and geotechnical conditions. The free span is 20 meters and the width of the bridge is 3 meters. The compared costs are only for the material in the superstructure, since the cost of the substructure, railings, etc. is independent of the material. This is reasonable since the governing load for pedestrian bridges is the variable load, which is equal for all cases regardless of material. The economic comparison serves as an investigation whether a CFRP reinforced glulam bridge is a competitor for sites where the structural height is limiting the possible concepts. The bridges in the comparison all have different heights, depending on what is needed to fulfill the demands for a pedestrian bridge.

The glulam bridge alternative is a regular stress laminated deck bridge, with steel tension rods and an asphalt cover. The structural height of the beams are 840 millimeters. The reinforced glulam bridge that was used in the comparison was the result of the preliminary sizing of the stress laminated deck, meaning that the height of the beams is 711 millimeters.

The steel bridge alternative is a composite structure, consisting of steel and timber. The primary girders consist of HEB450 beams and cross beams act as secondary girders. On top of the steel beams, a deck of Azobe D70 is placed. Azobe is a timber material that is commonly used for pedestrian bridge decks (Kärnsund Wood Link AB, 2019). The structural height of the beams is 450 millimeters, together with a deck of approximately 120 millimeters, resulting in a total height of 570 millimeters.

7.3 Investigation of Price Effects

The anisotropic and adaptable properties make it difficult to estimate the price of different products. Therefore, this investigation was performed to see both how much the price affects the results, but also to consider different proces of the manufacturers. The study shows in a qualitative way where the break even point is, i.e how much the CFRP price has to decrease before it is equivalent with the price of the reduced timber. The price comparison is performed using CFRP with a young's modulus of 300 GPa.

8

Risk Analysis

Risks need to be considered when constructing a bridge. It is especially important for bridges with heavy traffic or if boats pass beneath.

For a heavily reinforced cross section, loss of the CFRP strength means a significant decrease in structural capacity and instant collapse or progressive failure over time. For a beam with minimum reinforcement, the opposite behaviour is expected due to the smaller dependency on the CFRP for structural capacity. Thereby, the calculations in the risk analysis are based on the results of the third objective optimisation, corresponding to a reduction in height with approximately 40%.

8.1 Traffic Collision

The bridge is assumed to be constructed for pedestrian and bicycling traffic, but also for an additional service vehicle. Therefore, the existing redundancy is sufficient in case a car accidentally drives up onto the bridge. However, there is also a risk that a car would ram into the railings or land supports. This could be prevented by adding crash barriers at both ends of the bridge. Since detailing is not considered in this thesis, no calculations are performed for these cases.

8.2 Boat Collision

For bridges that stretch over a waterway, there is a risk for boat collisions. A boat can collide with either end or intermediate supports, or the bottom of the superstructure. No checks are performed regarding collision with supports. However an analytic check of collision with the bottom of the bridge, resulting in loss of the bottom timber lamella and CFRP-lamina is performed to observe the behaviour and redundancy of the system. The utilisation ratios are presented in Table 8.1.

Table 8.1: *Utilisation ratios for decreased load carrying capacity due to collision with boat.*

Utilisation ratios for decreased load carrying capacity		
Moment Capacity	[%]	32.1
Shear Capacity	[%]	21.5
Deflection	[%]	153
Frequency	[Hz]	3.57

8.3 Fire

In case of fire on the bridge, the exterior timber lamella will act as an initial protection towards the flames. Simultaneously as the exterior lamella is sacrificed, the overall temperature of the beam increases. At a certain point, the glass transition temperature of the CFRP matrix is reached and the the structural capacity of the CFRP is decreased. The same happens when the maximum operating temperature of the adhesive layer is reached and the bonding to the CFRP lamina is lost. Therefore, in the case of fire, a structural capacity accounting for only the interior timber lamellas, is calculated. It is assumed that the interior timber part is kept protected for some time. The utilisation ratios are presented in Table 8.2.

Table 8.2: *Utilisation ratios for decreased load carrying capacity due to fire.*

Utilisation ratios for decreased load carrying capacity		
Moment Capacity	[%]	55.7
Shear Capacity	[%]	22.8
Deflection	[%]	292
Frequency	[Hz]	2.69

8.4 Adhesive Failure

Another possible risk with this construction method, which is by itself a risk for unreinforced glulam as well, is failure in the adhesive layer. Assuming that the adhesive fails between the CFRP lamina and the timber lamellas, the load capacity will decrease in the same way as described in Table 8.2. A failure of the adhesives between the timber lamellas is unlikely since the production process is already highly controlled and automatised. The risk of adhesive failure would be covered by material safety factors in the sizing of a glulam beam.

9

Results

In this chapter the results from the analytic, numerical and economic analyses are presented, following the same order as treated in the thesis.

9.1 Analytic Results

The analytic results are divided into two categories. In the first subsection, the results from different configurations together with the results from the stress laminated deck is presented. In the next subsection, the evaluation of different parameters is presented.

9.1.1 Results for Different Geometrical Configurations

The result from the analytic calculation of the straight beam is presented in Table 9.1.

Table 9.1: *Moment capacity, deflection and frequency for the straight beam.*

Straight beam			
	M_{Rd} [kNm]	δ [mm]	f_1 [Hz]
Unreinforced glulam beam	242.8	51.6	3.8
1 lamina low modulus CFRP	592.4	31.5	4.7
1 lamina mid modulus CFRP	687.3	26.7	5.2
1 lamina high modulus CFRP	762.2	23.8	5.5
1 lamina ultrahigh modulus CFRP	837.1	21.5	5.7

The result of the analytic calculation for the T-beam is presented in Table 9.2.

Table 9.2: *Moment capacity, deflection and frequency of the T-beam.*

T-beam			
	M_{Rd} [kNm]	δ [mm]	f_1 [Hz]
Unreinforced glulam T-beam	283.6	171	3.6
1 lamina low modulus CFRP	1956	84.8	4.3
1 lamina mid modulus CFRP	2628	69.0	4.8
1 lamina high modulus CFRP	3171	59.7	5.1
1 lamina ultrahigh modulus CFRP	3721	52.4	5.5

The result of the analytic calculation for the stress laminated deck is presented in Table 9.3.

Table 9.3: *Moment capacity, deflection and frequency of the stress laminated deck.*

Stress laminated deck			
	M_{Rd} [kNm]	δ [mm]	f_1 [Hz]
Unreinforced glulam plate	3388.9	51.6	3.1
1 lamina low modulus CFRP	8264.3	31.5	3.9
1 lamina mid modulus CFRP	9587.7	26.7	4.2
1 lamina high modulus CFRP	10633	23.9	4.5
1 lamina ultrahigh modulus CFRP	11677	21.5	4.7

The results of the comparison between IBR and NSM configurations are presented in Table 9.4. For the comparison, a CFRP with a young's modulus of 300 GPa was used.

Table 9.4: *Comparison between IBR and NSM configurations. The moment capacity, deflection and frequency are presented.*

IBR/NSM comparison			
	M_{Rd} [kNm]	δ [mm]	f_1 [Hz]
IBR configuration	488	39.3	4.32
NSM configuration	483	40.1	4.29

The results of the preliminary sizing for a stress laminated deck bridge are presented in Table 9.5. The actual reduction of the height became 15.36%. The CFRP amount presented is needed in both the compression and tensile zone.

Table 9.5: *Results of the preliminary sizing of a stress laminated deck bridge. Amount of reinforcement is kept to a minimum aim.*

Preliminary sizing of stress laminated deck	
h_{glulam} [mm]	705
h_{CFRP} [mm]	3.00
h_{tot} [mm]	711
M [%]	22.8
τ [%]	18.8
δ [%]	46.0
f_1 [Hz]	4.38
A_{cfrp} [%]	0.73

9.1.2 Results of the Parametric Study

The result of the parametric study regarding sensitivity of varying E-modulus is shown in Figure 9.1.

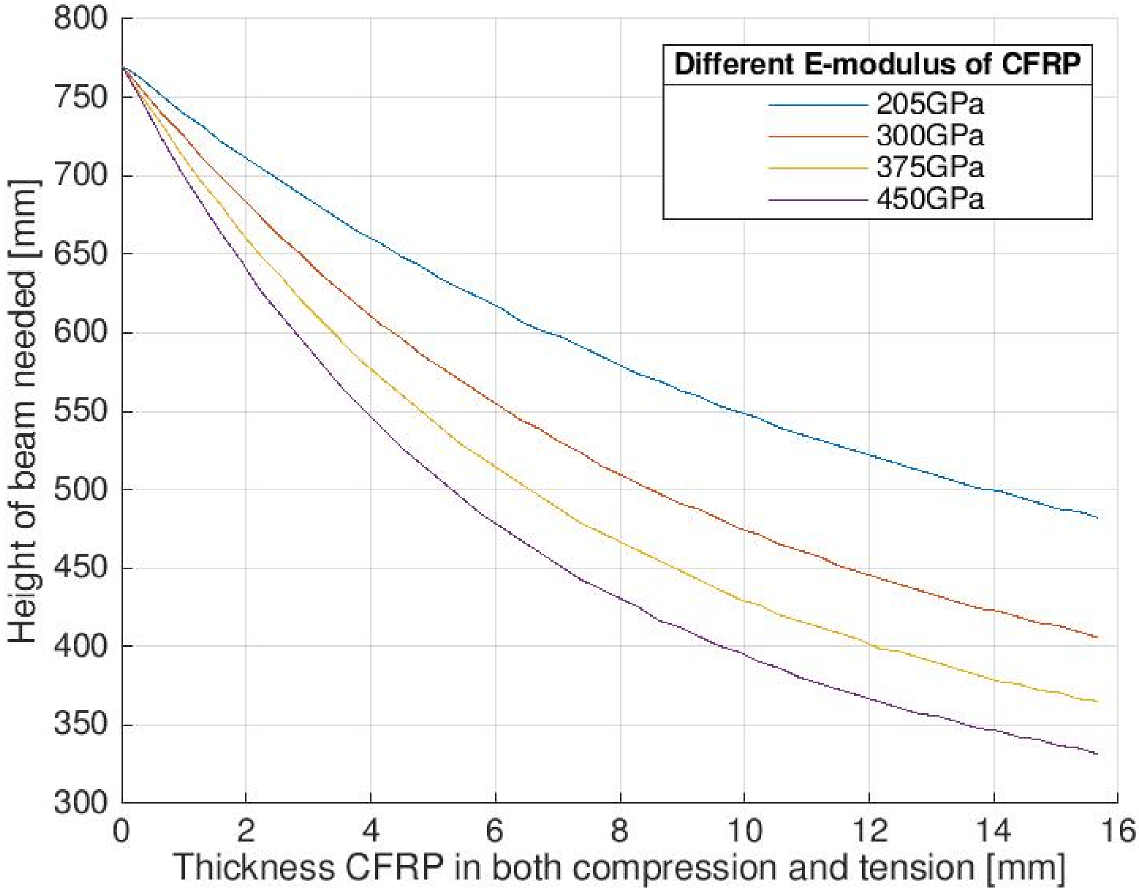

Figure 9.1: *Parametric study of the influence of different young's-modulus for the height of the beam.*

Based on the results of the first objective optimisation, the parametric study showed that changes in glulam density of +/- 200 kg/m^3 had little or no effect on the CFRP amount. The same effect was observed when altering the damping ratio. Both cases resulted in approximately +/- 0.1 millimeter of CFRP.

For the configuration reaching the third optimisation objective, the results varied more. The parametric study showed that a change in glulam density of +/- 200 kg/m^3 resulted in approximately +/- 0.5 millimeter of CFRP. Altering the damping coefficient resulted in +/- 0.3 millimeter of CFRP. The extremity is found when the lowest density is combined with the highest damping coefficient, which would yield a possible reduction of the CFRP with 0.7 millimeter.

The result of the parametric study regarding sensitivity of varying span length is shown in Figure 9.2. The "jump" in the graph for the span length of 30 meters, corresponds to a change in governing demand between deflection and acceleration.

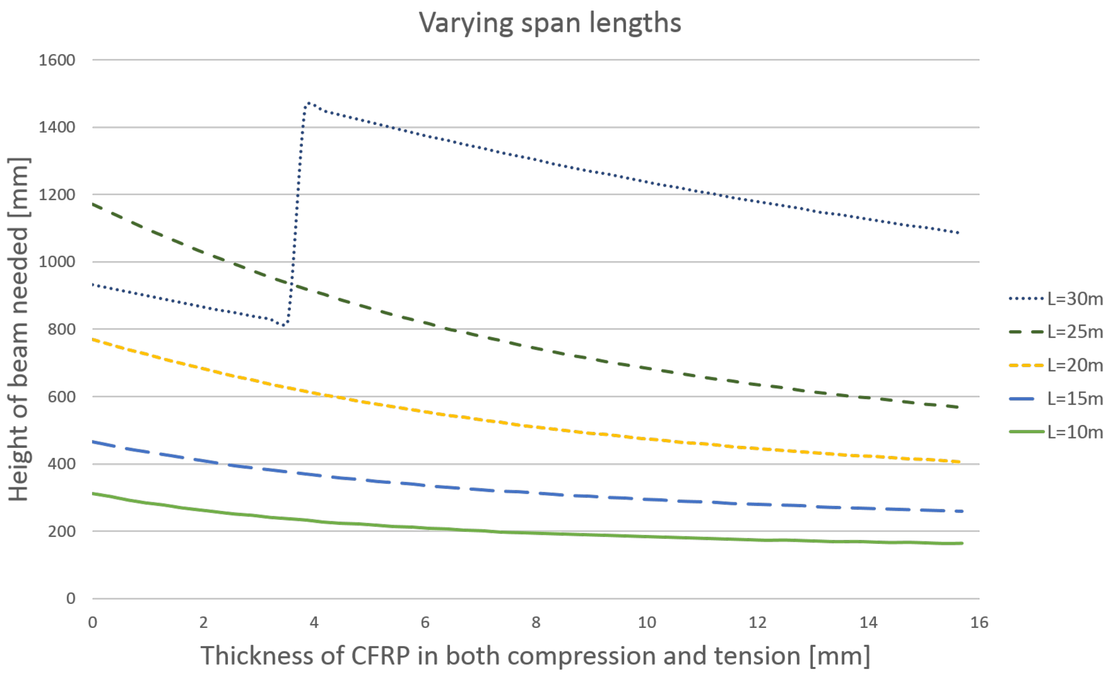

Figure 9.2: *Parametric study of the influence of different span length for the height of the beam.*

9.1.3 Results of Optimised Configurations

The beam was optimised considering four different objectives which are presented below. As a comparison, the heights for an unreinforced glulam beam and the utilisation ratois are presented in Table 9.6. The CFRP amount presented is needed in both the compression and tensile zone.

Table 9.6: *Results for an unreinforced beam.*

Unreinforced beam		
h_{glulam}	[mm]	795
M	[%]	19.7
τ	[%]	15.0
δ	[%]	47.8
f_1	[Hz]	4.92

The results of the first optimisation objective are presented in Table 9.7. The actual reduction of the height became 16.4%.

Table 9.7: *Results of the first optimisation to fulfill the structural demands, aiming at minimum reinforcement.*

Optimisation of straight beam, first objective		
h_{glulam}	[mm]	660
h_{CFRP}	[mm]	2.50
h_{tot}	[mm]	665
M	[%]	19.9
τ	[%]	15.5
δ	[%]	58.3
f_1	[Hz]	4.82
A_{cfrp}	[%]	0.67

The results of the second optimisation objective are presented in Table 9.7. The actual reduction of the height became 27.0%.

Table 9.8: *Results of the second optimisation to fulfill the structural demands.*

Optimisation of straight beam, second objective		
h_{glulam}	[mm]	570
h_{CFRP}	[mm]	5.00
h_{tot}	[mm]	580
M	[%]	19.2
τ	[%]	16.4
δ	[%]	64.8
f_1	[Hz]	4.85
A_{cfrp}	[%]	1.48

The results of the third optimisation objective are presented in Table 9.7. The actual reduction of the height became 42.5%.

Table 9.9: *Results of the third optimisation to fulfill the structural demands.*

Optimisation of straight beam, third objective		
h_{glulam}	[mm]	435
h_{CFRP}	[mm]	11.0
h_{tot}	[mm]	457
M	[%]	17.0
τ	[%]	18.3
δ	[%]	75.0
f_1	[Hz]	4.91
A_{cfrp}	[%]	4.14

The results of the third optimisation objective are presented in Table 9.7. The actual reduction of the height became 52.0%.

Table 9.10: *Results of the fourth optimisation to fulfill the structural demands.*

Optimisation of straight beam, fourth objective		
h_{glulam}	[mm]	345
h_{CFRP}	[mm]	18.5
h_{tot}	[mm]	382
M	[%]	14.7
τ	[%]	21.3
δ	[%]	80.4
f_1	[Hz]	4.95
A_{cfrp}	[%]	8.33

9.2 Results of the Finite Element Analysis

Two fundamental FE-analyses were executed in Brigade/Plus, one for the static case and one for the dynamic. The results are presented in this section. Further on, the results of the pre-camber effect investigation are presented.

9.2.1 Verification of the FE-model

The FE-model for the straight beam was compared with the analytic analysis, to verify the accuracy of the model. The calculated deflection is the instantaneous deflection, meaning that long-term effects were not considered. The results of all three models are presented in Table 9.11. The comparison between the pre-cambered and the two straight models are not as consistent, but gives an indication of the pre-cambered how the results between the two FE-models might differ. The amount of pre-camber was set to 25 millimeters.

Table 9.11: *Comparison of the results from the analytic calculations of the straight beam and both FE-analyses.*

Comparison Between FE and Analytic Results				
		Analytic Calculations	FE Straight	FE Pre-cambered
f_1	$[Hz]$	4.85	4.75	4.75
f_2	$[Hz]$	19.4	19.0	19.0
Deflection	$[mm]$	10.8	11.0	11.0

The first two vertical structural frequencies for the straight beam can be seen in Figure 9.3. The deflection for the straight beam is shown in Figure 9.4. The pre-cambered beam showed the same behaviour.

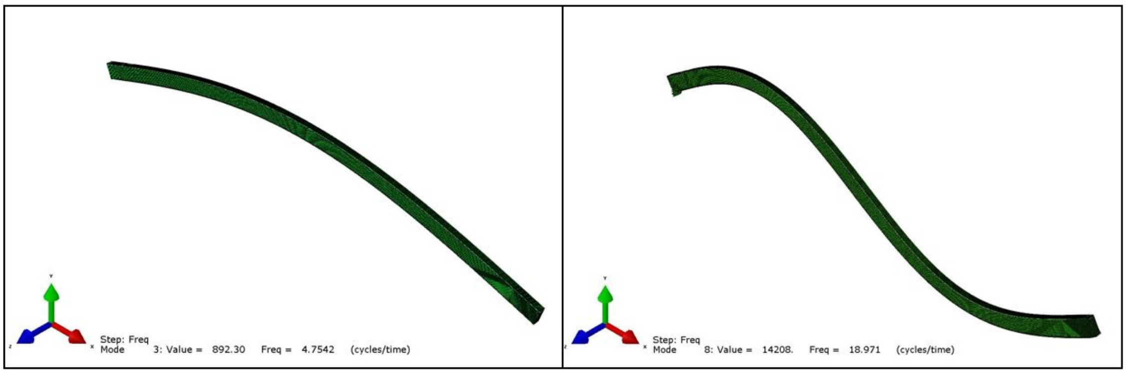

Figure 9.3: *The two first vertical structural frequencies for a straight beam calculated by Brigade. Left is the first vertical frequency, the right is the second.*

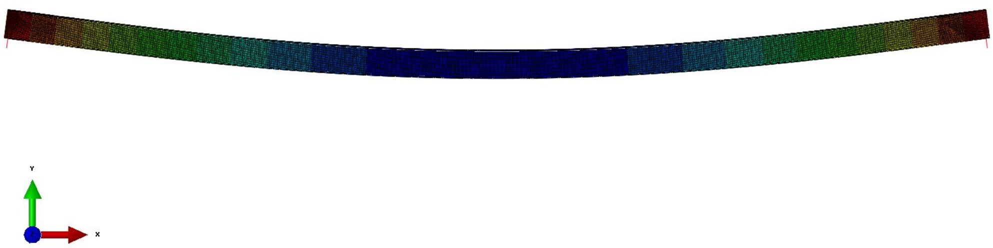

Figure 9.4: *The deflection of the straight beam subjected to self-weight. The scale is magnified (scale factor = 50) to highlight the effects.*

9.2.2 Comparison Between the Straight and Pre-cambered Beam

The shear stress was evaluated at five different levels of the cross section, see Figure 9.5. The largest shear stresses were always taking place at the bottom-top level.

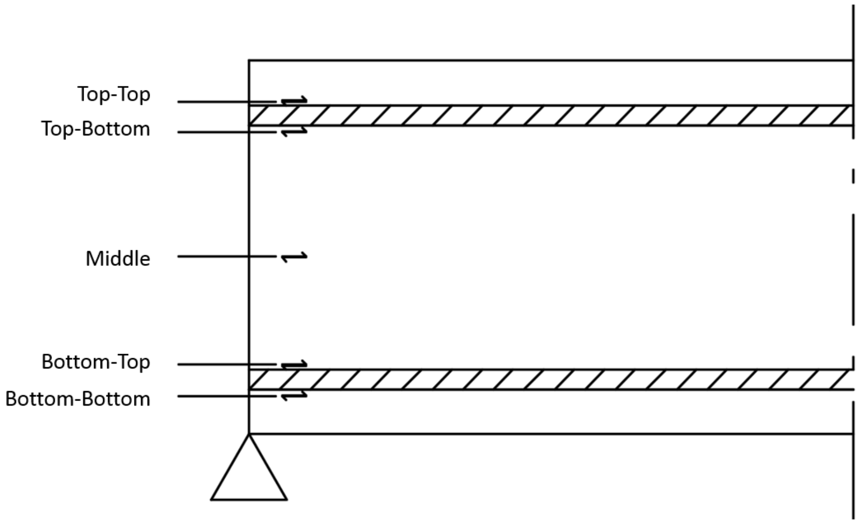

Figure 9.5: *The locations where the shear stresses were monitored. The bottom-top cut was the most critical in all analyses.*

The results from the straight beam can be seen in Figure 9.6. The maximum shear stress is found in the bottom-top cut. Also, the shear stresses in the middle cut was 0.24 MPa, corresponding well to the analytic results.

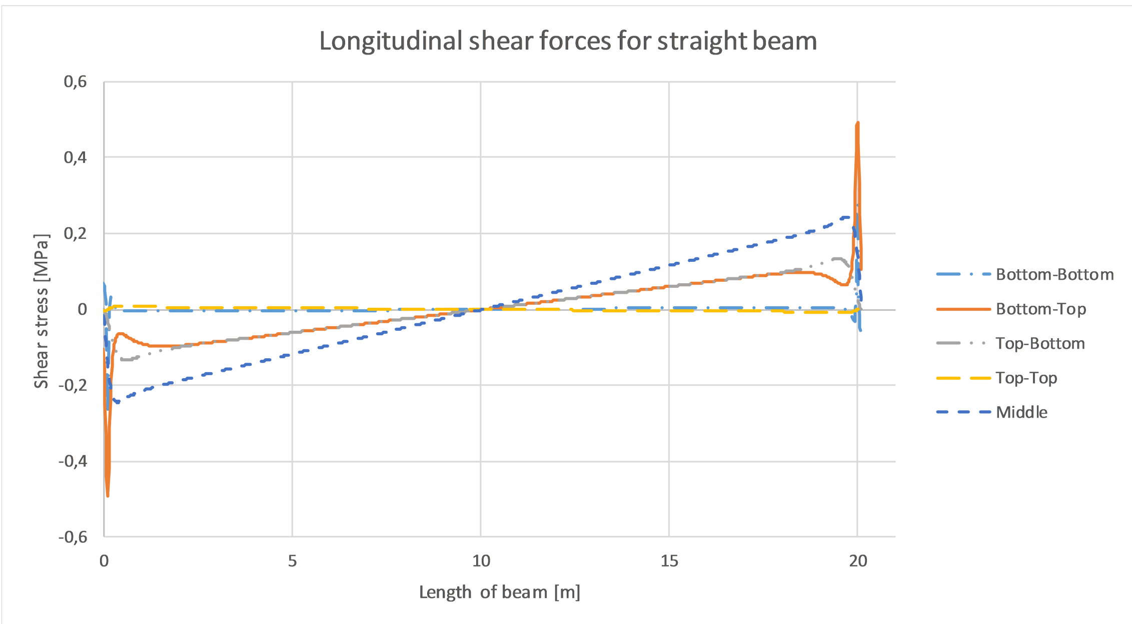

Figure 9.6: *Shear stresses at different levels of the straight beam. The Bottom-Top cut has the highest shear stress with 0.747 MPa.*

The same analysis was performed for the pre-cambered beam. The results are presented in Figure 9.7.

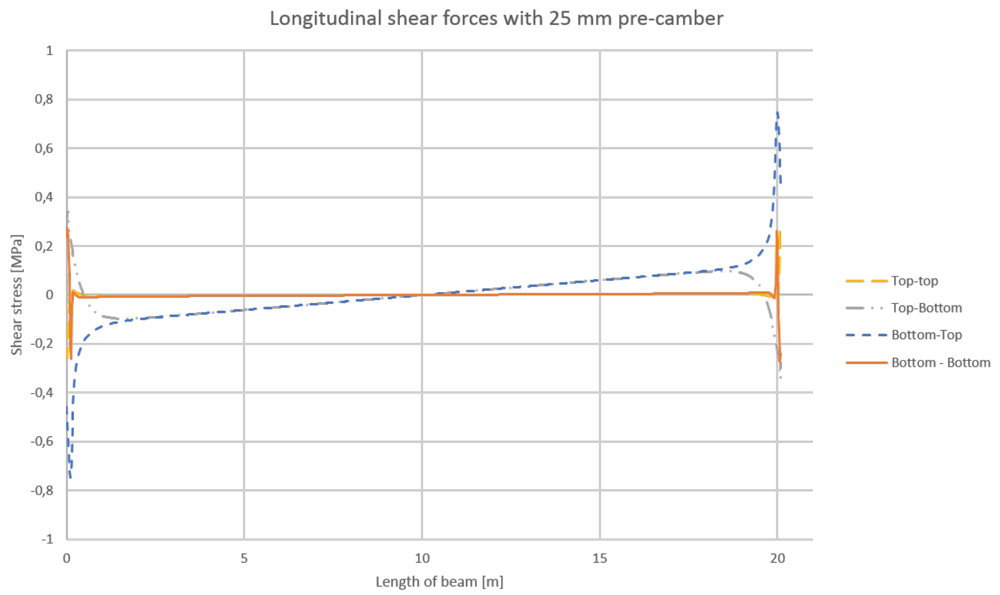

Figure 9.7: *Shear stresses at different levels of the pre-cambered beam. The Bottom-Top cut has the highest shear stress with 0.748 MPa.*

9.2.3 Results of the Pre-camber Effects Investigation

Since the bottom-top cut was the most critical in all evaluated cases, Figure 9.8 shows the shear stresses at this level for different amounts of pre-camber. The figure only shows the first 0.2 meters of the beam, where the stress was found to be the largest. The shear stress was measured to approximately 0.74 MPa for all amounts of pre-camber, with a small difference in magnitude.

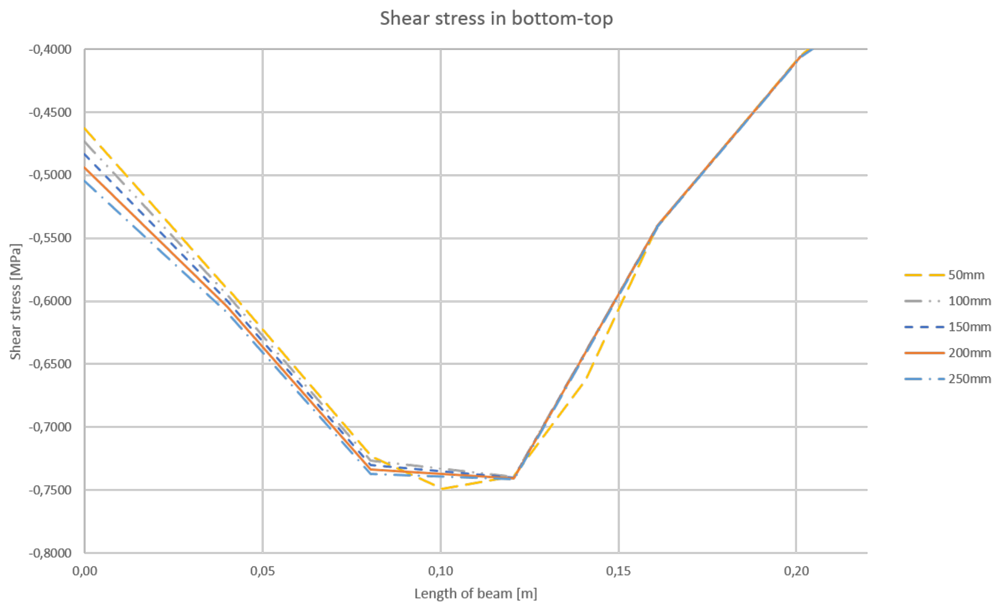

Figure 9.8: *Shear stresses in the bottom-top cut for the first 0.2 meters of the beam. The highest shear stress for all cases is approximately 0.74 MPa.*

The stress perpendicular to grain was also studied in the middle of the span. The result is presented in Figure 6.3

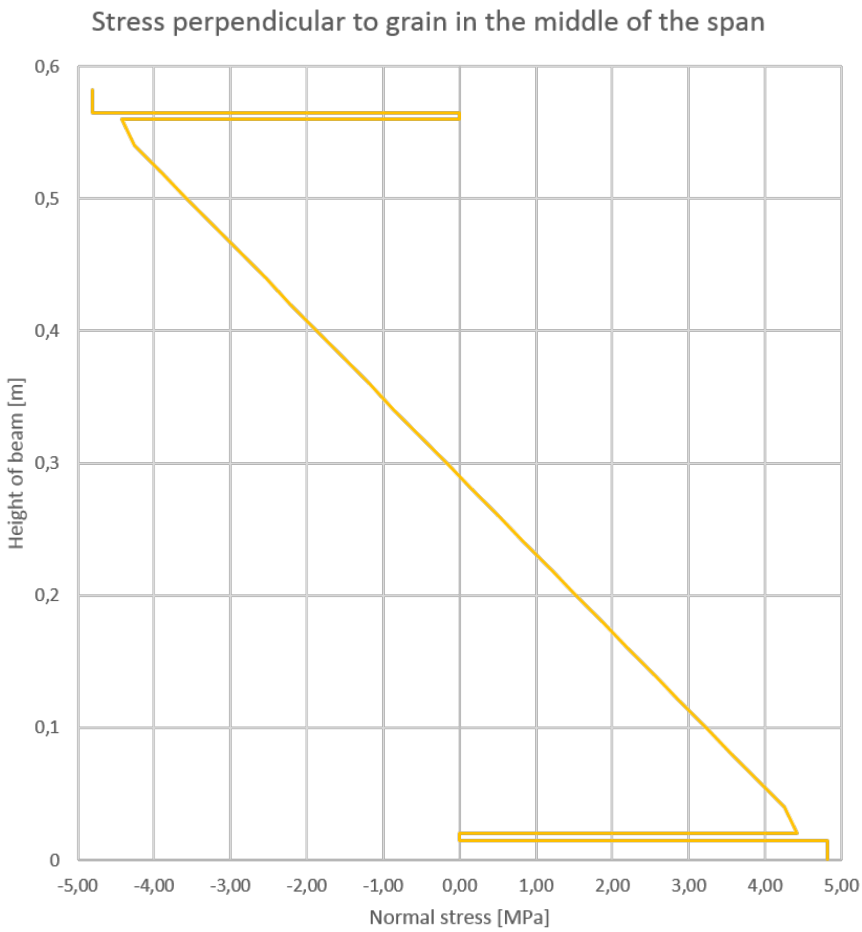

Figure 9.9: *Stress perpendicular to the grain in the middle of the span. The tensile stress is above 4 MPa in the bottom of the beam.*

The results for a beam with a 30 meter long span can be seen in Figure 9.10. For better visibility, the same result for the first meter is shown in Figure 9.11. The CFRP thickness is 3 millimeters, in both compression and tension, and the number of timber lamellas is 18. The maximum stress was in the bottom-top cut, having an amplitude of 0.97 MPa.

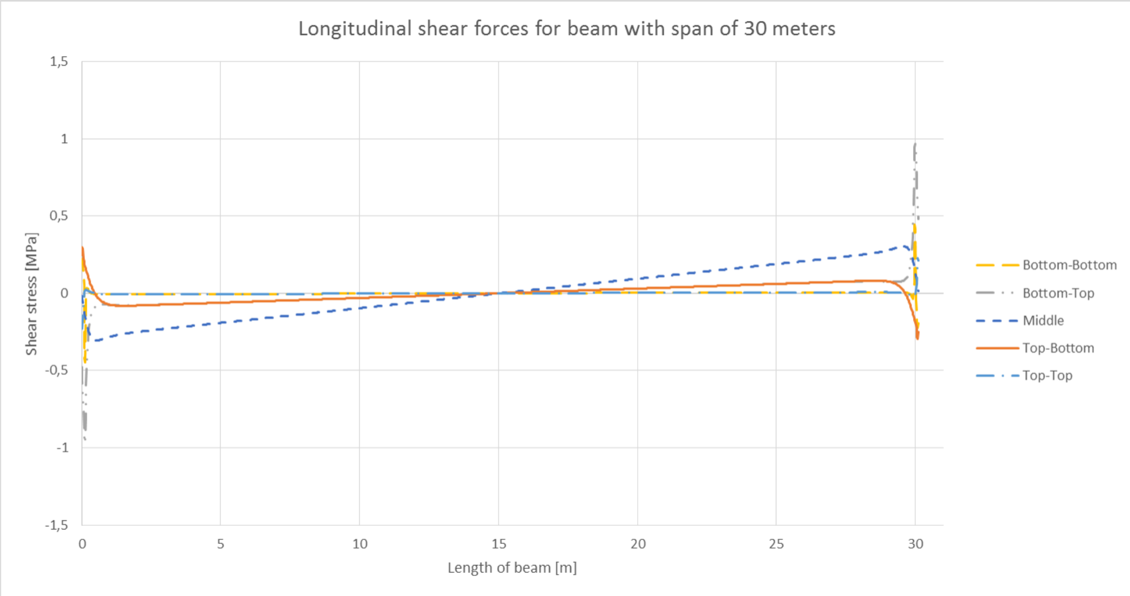

Figure 9.10: *Shear stresses for beam with 30 meters span. The maximum shear stress is 0.968 MPa.*

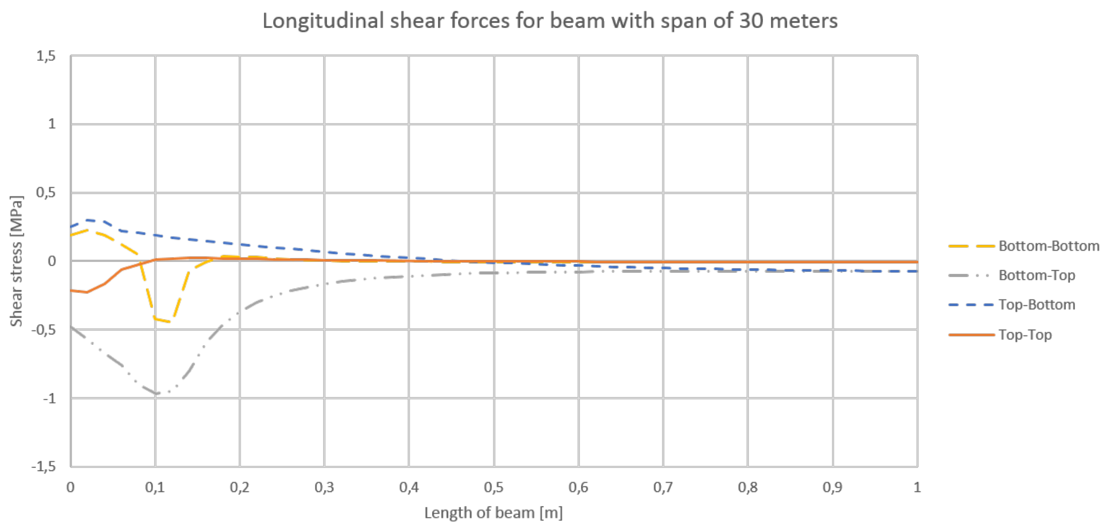

Figure 9.11: *30 meter beam.*

9.3 Results of the Economic Comparison

In Figure 9.12, the material costs for three different bridge types are shown. Upper and lower values have been used to indicate the possible deviation of the material costs.

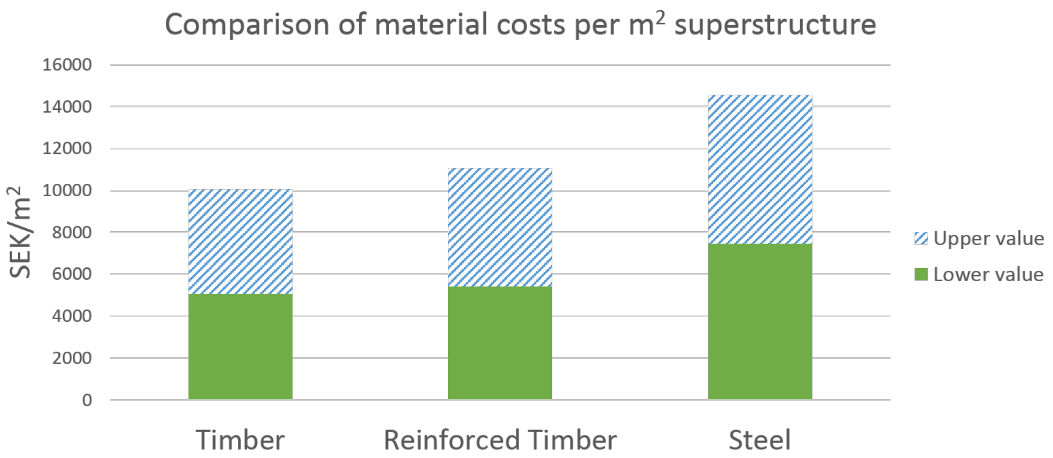

Figure 9.12: *The variations of the material cost, compared for the three alternatives together. Timber prices from Martinsons Trä, CFRP prices from Fiberline and Rao et al., Steel prices from Stena Stål and Azobe deck prices from Kärnsund Wood Link AB.*

The result of the investigation regarding sensitivity of varying prices of CFRP is shown in Figure 9.13.

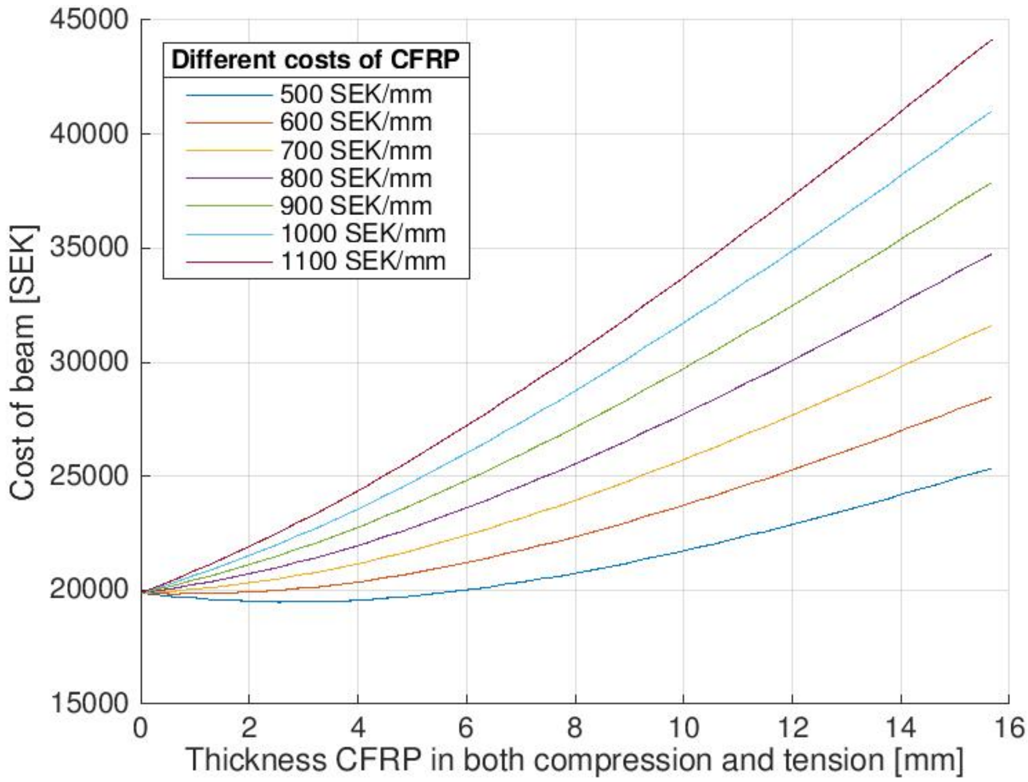

Figure 9.13: *Price for a CFRP reinforced timber beam with different CFRP-prices. The prices are for a complete beam with a span of 20 meters and a CFRP with young's-modulus of 300GPa.*

10

Discussion

The results presented in Chapter 9 are discussed in the following chapter. The discussion is divided into the three main parts of the thesis: analytic analyses, FE-analyses and the economic investigation. Finally, a more general discussion is conducted, to treat overall aspects of the concept.

10.1 Analytic model

The analytic model does not consider compression failure, since it was assumed that tension failure occurs first. This assumption can be made since the amount of reinforcement is equal on both tension and compression side, meaning that the neutral axis will be in the center of the cross section and tension and compression strains will have the same amplitude. Since timber is weaker in tension, it will predominately experience tension failure before compression failure parallel to the grain.

The critical demands for lightweight pedestrian bridges are often deflection and acceleration. The deflection is calculated completely according to Eurocode and no assumptions were made for the calculation, leaving no room to question the result. Regarding the limit for allowed accelerations, a choice of 0.75 m/s^2 was made, considering the variations in different design standards. Using the upper limit of 1 m/s^2, or the lower limit of 0.5 m/s^2, would certainly affect the the result. However, since the majority of the studied configurations had structural frequencies outside the range stated in Equation 5.3, the acceleration limit would have a small effect on the final configuration.

After the initial analysis of the T-beam configuration, no further optimisation was performed. The optimisation of the T-beam would be cumbersome to perform analytically, as the neutral axis may shift between the flange and the web depending on their respective heights and reinforcement amount. In the end, the benefits would be negligible due to the high cost of carbon fibre in relation to the small reduction in height. Further on, E. Martinson (Martinsons Trä, personal communication, February 14 2019) states that the T-beam is not commonly used for pedestrian bridges nowadays, due to an unfavourable use of material and relatively high structure.

It would be possible to further reduce the height of the beams presented in Table 9.7 to 9.10, by reducing or completely removing the exterior sacrificial lamella. However, this would influence the producibility of the beam. In extension, the benefits of the sacrificial lamella in terms of fire resistance, and protection against moisture and UV-radiation would be lost. One possibility that was not investigated in this thesis is to replace the outer lamella by a thinner OSB, particle board or plywood, to further reduce the height. However, the change in self-weight, together with the change of stiffness due to shorter lever arms, might influence the dynamic behaviour of the beam.

The parametric study regarding density and damping of Glued Laminated Timber (Glulam) were based on the first and third optimised beams, i.e. aiming to have a minimum amount of reinforcement and a height reduction of 40% respectively. These were thought to be the most interesting beam configurations as the changes in behaviour between first to second objective, and third to fourth respectively, did not differ substantially. When comparing the results from the parametric study, presented in Section 9.1.2, it can be seen that the influence from altering the young's modulus is larger compared to changing the glulam density or the damping coefficient. Nevertheless, the damping coefficient and glulam density should be chosen with care.

When investigating the varying span length, presented in Figure 9.2, a jump in the graph can be seen for a span length of 30 meters. The jump is due to a change in governing criterion from deflection to acceleration at a certain amount of added CFRP. Increasing the amount of CFRP and thereby changing the governing demand is actually unfavourable and increases the height of the beam. The same change in governing demand can be observed when changing the length of the span. The jumps occur frequently when changing the span length, however not as visible in the graphs as for the case with a 30 meter span. For span lengths below 20 meters, the deflection demand is governing with approximately 95% in utilisation. When the span length increases to 20 meters, the governing criterion changes to acceleration which is shown by the deflection utilisation ratios. The utilisation decreases from around 65% for a 20 meter span to around 25% for a 30 meter span, with a CFRP amount below 4%, where the acceleration criterion is governing. Considering the graph in Figure 9.2, this explains why the needed height for a 25 meter span is larger than the needed height for a 30 meter span. The governing criteria for a 25 meter beam is frequency. The governing criteria for a 30 meter beam is, for a CFRP thickness less than 4 millimeters, deflection.

The gradients of the graph in Figure 9.2 indicate that the CFRP is better utilised for longer spans, since the height is reduced more with a small amount of CFRP. The better efficiency is due to the height of the beam in longer spans, where the lever arms of the CFRP are higher and hence have a larger influence on the second moment of area. Investigating the extreme points in the graph with 16 millimeter of embedded CFRP, for a 10 meter span, the height is reduced by approximately 50%, corresponding to 150 millimeters timber. For a beam with a span of 20 meters, the same ratio of reduction is achieved, but instead reducing more than 300 millimeter timber. For a longer span of 30 meters, it is impossible to draw the same conclusions since the governing criterion is changing with the increase of reinforcement, and actually increasing the height. However, it can be seen that 3.5 millimeter CFRP can reduce the height with more than 100 millimeters which, together with the gradient discussed above, indicate that CFRP is more efficiently used for the longer spans, see Figure 9.2.

The focus of this thesis was to reduce the needed structural height, without compromising the structural capacity. Instead of decreasing the height of the beam, the reinforcement can be used to increase the possible span length. Reaching a theoretical span of 40 meters, might mean that an intermediate support can be removed, reducing time and cost as well as decreasing the environmental impact. However, increasing the span above 30 meters, imposes on the regulations for transportation on roads and special permits would be required.

10.1.1 Disregarded Reinforcing Configurations

The CFRP is best utilised in certain types of configurations. According to existing studies and experiments, these are configurations where loads are mainly carried in bending. Therefore, the thesis has focused on these types of beams and not shown the configurations where this reinforcement scheme is not deemed effective. Amongst the disregarded reinforcement configurations are arch beams and truss bridges. Arches are already an optimised shape to utilise the material and maximise the load carrying capacity. Contrary to the other configurations, an arch carries the load via compression action. A truss is built up by a network of rods and struts, which mainly carry the load via compression and tension. The change of main load carrying system removes this possible configuration as well. For an arch or a truss, other stresses might arise and expose the CFRP to normal forces instead of flexural. The new stresses might also alter the governing failure mode, which is why these configurations are not covered in the analytic analyses.

The comparison in Table 9.4 shows rather small differences between NSM and IBR. The results indicate a slight advantage for the IBR configuration. The IBR configurations has a small amount of capacity in the excluded timber surrounding the CFRP lamina (Figure 4.4), which is not utilised. Another discrepancy arises since the IBR beam is approximately 10 millimeter higher than the NSM beam, when the reinforcement is embedded. The flexural capacity is not a problem for either configurations, the governing demands are rather deflection and frequency. Finally, this indicates that there are no significant advantages to arrange the reinforcement in a vertical position. The disadvantage in the production stage, and the fact that the laminas are more exposed to wear makes IBR a more competitive configuration.

10.2 Finite Element Model

The frequencies and deflections presented in Table 9.11 coincide well with the results obtained from the analytic calculations. The negligible differences that occur between the straight beam and the pre-cambered beam are probably a consequence of having some loads transferred through normal components due to the slight arch of the pre-camber. This strengthens both the correctness of the analytic model but also the viability of the reinforcement method. Potential differences in the analytic calculation and the FE-analyses are probably due to the anisotropic properties of timber that are included in the FE-model, but not to the same extent in the analytic calculations. Studying Figure 9.4, it can be seen that the deflection behaviour is as expected for a simply supported straight beam. In principal, a pre-cambered beam will deflect in the same way. The significant difference is that a pre-cambered beam will end up in an nearly horizontal position when only subjected to its self-weight.

The shear stresses in the straight beam were also evaluated. By the supports, in the middle of the cross section, the shear stress was 0.24 MPa. This value corresponded well to the analytic results, again confirming the correctness of the FE-model. The small difference in the result can be due to the temperature variations that were included in the FE-model, but not in the analytic calculations. Apart from the shear stress in the middle of the cross section, the shear stress close to the CFRP needed to be checked. The analysis showed that the highest shear stress was found on the upper side of the bottom CFRP lamina, with a magnitude of 0.74 MPa. The stress was also large beneath the top CFRP lamina having a value of 0.34 MPa. The shear stresses in the outer lamellas were smaller, which is reasonable since shear stresses are normally larger closer to the middle of the beam.

The results from having a pre-camber of 25 mm are found in Figure 9.7. It was expected that the shear stresses would be higher for the pre-cambered case. Although the results showed an increase in stress, the increase was relatively small, meaning that there is no harm in pre-cambering a CFRP reinforced beam. However, in some cases there might be a spatial reason to pre-camber the beam even more. Therefore, concepts with a pre-camber up to 250 mm were evaluated.

The gradual increase of pre-camber and the gradual change in load effects can be seen in Figure 9.8. It showed that there are almost no differences in shear stress when adding a pre-camber. For every 50 millimeters, there is a small increase of approximately 0.0005 MPa in shear stress. Also note that the stress for 50 millimeter pre-camber, at x=0.1 meter, is larger than the others. This can be explained by the meshing in the FE-model, where the model for 50 mm pre-camber had a node at x=0.1 meter. The other models have one node at 0.08 meters and 0.12 meter, explaining why the 50 millimeter pre-camber had a slightly larger stress.

Since no bond slip test has been performed, or delamination of CFRP laminas were of interest, full interaction has been assumed for the entire model. As mentioned in Section 6.1 this is reasonable since failure most often occurs in the timber, rather than in the adhesive.

The tension stress perpendicular to the grain was estimated to 4 MPa, which would cause tension failure perpendicular to the grain. However, this is an unreasonable large stress and therefore further calculations were performed analytically to verify the results. The analytic calculations showed a stress corresponding 0.006 MPa, in the apex zone for a plain timber beam. Naturally, the results may vary when having a beam with CFRP reinforced timber. However, when considering the results of the hand calculations, together with the fact that the pre-camber amount is 25 millimeters on a 20 meter long beam, the stress should not be very large due to the relatively small curvature of the beam. Therefore, the evaluated stress perpendicular to the grain in the FE-model is unreasonable. However, since the deflection and frequencies, together with the shear stress in the middle of the beam have a good correlation with the hand calculations, the results for the shear stress in the CFRP-timber interface is still believed to be accurate.

One possibility of the exaggerated tensile stresses given by the FE-model could be the orientation assignment of the material. In the model, a cylindrical coordinate system was used in the pre-camber case to make a realistic model. When using a cartesian coordinate system, the tensile stress perpendicular to grain is more similar to the hand calculated result, although there is a worse correlation between the other evaluated parameters: deflection and structural frequency.

10.3 Economic Comparison

The scope of the economic comparison is wide since prices for CFRP vary significantly depending on composition and different manufacturers. Unfortunately, data was scarce and the lack of active producers in Europe was problematic. Therefore, it needs to be emphasized that most data was retrieved from the supervisors of the thesis. The same difficulty was experienced when trying to obtain prices for timber and steel pedestrian bridges. A pedestrian bridge made of concrete was not considered in the economic comparison, since they are not considered economically viable with current prices, in addition to the on-site preparatory work. Further on, the environmental impact from a concrete structure is larger.

The economic comparison presented in Figure 9.12 only considers the investment cost for the materials included in the bridges' superstructure. Still, it indicates that the price of CFRP needs to decrease for the concept to hit a break even point. It also shows that the reinforced timber bridge is less expensive compared to a steel bridge. In this case, the graph is somewhat misleading, since the steel bridge has a lower height than the reinforced beam. A comparison with height as a functional unit means that the amount of CFRP would increase, further increasing the price of the bridge. However, the concept still gives a possibility of constructing a timber bridge where it was not possible without reinforcement. When the surrounding context and environmental benefit is more important than cost efficiency, timber strengthened with CFRP is a good alternative. The cost of producing a CFRP reinforced timber bridge is in the vicinity of 5-10% more expensive. This might come to change in the future, with decreasing price of CFRP and increased streamlining of the production process. For a steel structure, part of the cost is carried by welding and preparatory work before assembly, which means that regardless of the material choice, production costs and work on site must be considered in the price comparison.

As mentioned earlier, the price of CFRP largely influences the total price of the beam. This is something that is visualized in Figure 9.13. Figure 9.13 also shows that as more CFRP is added, a larger portion of the beam's total cost is CFRP. The desired break even point allows less CFRP when the price increases. As an example, for a price of 500 SEK/mm the break even point is around 6 millimeters, corresponding to a height reduction of approximately 30%. To reach a point where the price of the added CFRP is the same as the price of the reduced timber, assuming minimum reinforcement of 2.5mm, the price needs to decrease towards 650 SEK/mm. As indicated by the industry, see Figure 7.1, the prices are decreasing, which ensures that the reinforcement method will become more competitive in the future. The prices presented in Figure 7.1 are recalculated into a price per millimeter height of CFRP, which is used for the economic comparison. The exchange rate differs from day to day, and the value of SEK as well, making it difficult to interpret the values over time. However, the comparison acts as an indication towards where the industry is heading. According to Fiberline (2016), the price is 1094 SEK/mm, which is used as the upper value in the comparison. According to Rao et al. (2018) the price is 704 SEK/mm, which is used as the lower value in the comparison.

The CFRP has the largest influence on the height reduction when first introduced in the timber beam, which can be seen by the decreasing gradient in Figure 9.2. The decreasing gradient also indicates that the most beneficial reinforcement configuration, from an economic point of view, is for a small thickness of CFRP, rouhgly below 3 millimeters. Figure 9.13 also confirms that CFRP is best, from an economic perspective, for small amounts of the material.

A reduction in height results in weight reduction. A lighter structure puts lower demands on the substructure, and the need for large or advanced foundations decreases. This presents an opportunity to replace an existing superstructure where it has deteriorated or lost structural capacity, without extensive work on the substructure. Compared to replacing the entire bridge, this would potentially save money and time as well as having less environmental impact.

Similar to plain timber or EWPs, the CFRP reinforced timber is suitable to prefabricate in a factory with a controlled environment. Prefabrication is often less expensive compared to construction work on-site. It also ensures a higher quality and an easier assembly, resulting in a faster construction time.

10.4 General discussion

Apart from discussing the results from the analyses performed in this thesis, it is also important to highlight some more general aspects. Even though the concept is viable in theory, there are some practical aspects that need to be treated, such as production methods and sustainability.

The reinforcement concept has not been attempted in practise. Even though the production method has been discussed in theory, there might be some difficulties when actually executing it. It is important to reassure that there is sufficient adhesion between the exterior lamellas (containing CFRP) and the beam. When the CFRP laminas have a thickness of a few millimeters, it might be problematic to create a recess accurate enough to fit the CFRP. If the recess were to be uneven, the surface of the exterior lamella will also be uneven after applying the CFRP, leading to poor adhesion when gluing the exterior lamella to the beam.

From the risk analysis it was found that, whilst suffering from increased deformation and change in behaviour, an immediate collapse after an accident is not expected. However, actions should be taken to repair the structure. The strengthening methods suggested in Chapter 3 might be of interest.

Also, the possibilities to recycle a CFRP reinforced glulam beams has to be considered. By embedding the CFRP in the timber, it might be a difficult process to reuse the material, once the CFRP has been glued to the timber.

11

Concluding Remarks

The analytic analysis showed that Carbon Fibre Reinforced Polymers (CFRP) is a relevant alternative in reducing the height of Glued Laminated Timber (Glulam) beams. It was also shown that the governing demand criterion changes with the span length. For short spans, the deflection criterion is governing. When increasing the span, it changes to acceleration, and then back again to deflection if increasing eve more. The governing criterion can also be changed with the amount of CFRP, as can be seen in the case of a 30 meter long beam. Meaning that there is an theoretical upper limit for the amount of CFRP viable for that span. In conclusion, to maximise the utilisation of the CFRP, the beam should span 20 to 30 meters.

According to the literature study, a commonly used reinforcement configuration is the NSM. Through analytic analysis, it was shown that the IBR configuration, proposed in this thesis, is slightly more efficient. In conclusion, it can be stated that the IBR configuration utilises the extra stiffness of the added CFRP in a better way.

The FE-analysis showed that having CFRP laminas embedded in a glulam beam does not result in local shear failure in the timber close to the CFRP. The FE-analysis also showed that pre-cambering the beam has a small affect on these local effects. The same was shown for a increasing the amount of pre-camber to the maximum allowed inclination of the bridge deck.

Based on the economic comparison, it was shown that CFRP reinforced timber could serve as a realistic alternative for future pedestrian bridges. It was also concluded that reinforced beams could be used to construct a new lighter superstructure, where the existing superstructure or substructure lost sufficient structural capacity. Thereby saving money, time and environment since there is no need to replace the entire bridge. A lighter bridge is also easier and faster to install, having less impact on surrounding traffic. The impact on surrounding traffic is an important aspect to consider in a larger city like Gothenburg, which may have many larger infrastructure projects ongoing, already obstructing the traffic flow.

In conclusion, the suggested reinforcement configuration is a feasible way of increasing the area of application for structural glulam beams.

12 Future Research Possibilities

As this is a vast subject to cover, there were some further issues that arose throughout the thesis work. Performing these studies is of importance, to implement the method in reality.

- Experimental validation of the suggested reinforcement/production method. This could also serve as a development platform to further optimise the method.
- The long term behaviour of the reinforcement interface needs to be studied, including varying coefficients for shrinkage, creep, moisture and temperature movements.
- Fatigue investigation of the composite cross section.
- Anchoring and joining of CFRP reinforcement laminas for continuous longer beams.
- Investigate the possibility to use Carbon Fibre Reinforced Polymers (CFRP) tensioning rods instead of steel rods in a stress-laminated timber deck bridge.
- Investigate a more environmentally friendly adhesive.
- An extensive LCC-analysis to determine the competitiveness of CFRP reinforced timber compared to other materials.
- Investigate the feasibility of implementing the reinforcement method in timber bridges subjected to traffic loads.
- Investigate how the CFRP reinforced beam can be recycled, is it possible to reuse the materials?

To provide the thesis with extra credibility it would have been interesting to examine further suppliers and manufacturers of Glulam and CFRP.

Bibliography

Ahmed, A., Tavakol, B., Das, R., Joven, R., Roozbehjavan, P., and Minaie, B. (2012). Study of thermal expansion in carbon fiber-reinforced polymer composites. *SAMPE International Symposium Proceedings*.

Allann, A. (2006). Fibres for Strengthening of Timber Structures. *(Research report, Luleå University of Technology, Department of Civil and Environmental Engineering)*.

Angst-Nicollier, V. (2012). Moisture inuced stresses in Glulam. *(Doctoral dissertation, Norwegian University of Science and Technology)*.

Ascione, L., Caron, J.-F., Godonou, P., van Ijselmuijden, K., Knippers, J., Mottram, J., Oppe, M., Gantriis Sorensen, M., Taby, J., and Tromp, L. (2016). *PROSPECT FOR NEW GUIDANCE IN THE DESIGN OF FRP Support to the implementation, harmonization and further development of the Eurocodes*.

Barragán, O. L. G. and Jacob, J. (2007). Flexural strengthening of glued laminated timber beams with steel and carbon fiber reinforced polymers. *(Master's thesis, Chalmers University of Technology, Department of Civil and Environmental Engineering)*.

Bengtsson, D. and Magnusson, T. (2016). Durability of construction solutions with fiber-reinforced polymers (FRP) in pedestrian bridges.

Borgström, E. (2016). *Design of timber structures, Rules and formulas according to Eurocode 5. Volume 2*. Swedish Wood, Stockholm.

Broughton, J. G. and Hutchinson, A. R. (2003). Review of relevant materials and their requirements for timber repair and restoration, LICONS.

Brundin, J. and Fröbel, J. (2016). *Handelssortering av sågade trävaror i Europa enligt SS-EN 1611-1*. Swedish Wood, Stockholm.

Calvet, V., Valcuende, M., Benlloch, J., and Cánoves, J. (2015). Influence of moderate temperatures on the bond between carbon fibre reinforced polymer bars (CFRP) and concrete. *Construction and Building Materials*, 94:589–604.

Composite UK (2017). Fire Performance. *(Technical Sheet regarding fire safety of FRP)*.

Crocetti, R. (2016). *Design of timber structures, Structural aspects of timber construction. Volume 1. Chapter 3 - Design of Structural Timber Elements in ULS*. Swedish Wood, Stockholm.

Davids, W. G., Richie, M., and Gamache, C. (2005). Fatigue of glulam beams with fiber-reinforced polymer tension reinforcing. *Forest Products Journal*, 55(1):93.

Ekholm, K., Crocetti, R., and Kliger, R. (2012). Stress-Laminated Timber Decks Subjected to Eccentric Loads in the Ultimate Limit State. *Journal of Bridge Engineering*, 18(5):409–416.

Eurenius, K. (2017). Till sist: Grönt ljus för cykelbro i rosenlund.

Fiberline (2016). Fiberline Carbon Strips Product Sheet.

Fitzpatrick, T. and Smith, R. R. (2001). Stabilising the London Millenium Bridge. *Ingenia*, pages 18–22.

Frankhauser, Jr., W. and O'Connor, J. (2015). Advances in fiber-reinforced polymer (frp) composites in transportation infrastructure. *(Technical report)*.

Fröbel, J. and Crocetti, R. (2016). *Limträhandbok del 1.* Swedish Wood, Stockholm.

Gentile, C. J. (2000). Flexural strengthening of timber bridge beams using FRP. *(Master's thesis, University of Manitoba, Department of Civil and Geological Engineering)*.

Glišović, I., Stevanovic, B., Todorovic, M., and Stevanovic, T. (2016). Glulam beams externally reinforced with cfrp plates. 61:141–154.

Gurit (2018). Guide to Composites.

Heinemeyer, C. (2009). Design of Lightweight Footbridges for Human Induced Vibrations Sétra. *JRC Scientific and Technical Reports*, 3:55–60.

Heshmati, M. (2015). Hygrotherman Durabolit of Adhesively Bonded FRP/Steel Joints. *(Thesis for the Degree of Licentiate, Chalmers University of Technology, Department of Civil and Environmental Engineering)*.

Hollaway, L. C. and Teng, J. (2008). *Strengthening and rehabilitation of civil infrastructures using fibre-reinforced polymer (FRP) composites.* Woodhead Publishing Limited, Cambridge, England.

Johansson, M. (2016). *Design of timber structures, Structural aspects of timber construction. Volume 1. Chapter 2 - Structural Properties of Sawn Timber and Engineered Wood Products.* Swedish Wood, Stockholm.

Johnsson, H., Blanksvärd, T., and Carolin, A. (2006). Glulam members strengthened by carbon fibre reinforcement. *Materials and Structures*, 40:47–56.

Joven, R., Das, R., Ahmed, A., Roozbehjavan, P., and Minaie, B. (2012). Thermal properties of carbon fiber epoxy composites with different fabric weaves. *SAMPE International Symposium Proceedings*, (June):14.

Juvandes, L. F. P. and Barbosa, R. M. T. (2012). Bond analysis of timber structures strengthened with FRP systems. *Strain*.

Karbhari, V. M., Chin, J. W., Hunston, D., Benmokrane, B., Juska, T., Morgan, R., Lesko, J. J., Sorathia, U., and Reynaud, D. (2003). Durability Gap Analysis for Fiber-Reinforced Polymer Composites in Civil Infrastructure. *Journal of Composites for Construction*.

Kliger, R. (2016). *Design of timber structures, Structural aspects of timber construction. Volume 1. Chapter 1 - Introduction to Design and Design Process.* Swedish Wood, Stockholm.

Kärnsund Wood Link AB (2019). Azobe Produktblad.

Lidelöw, H. (2016). *Structural Systems for Infrastructure. Volume 1. Chapter 8 - Timber building systems for housing.* Swedish Wood, Stockholm.

Mårtensson, A. (2016). *Design of timber structures, Structural aspects of timber construction. Volume 1. Chapter 7 - Design for Serviceability.* Swedish Wood, Stockholm.

Nedev, G. (2019). FRP Konstruktioner. Lunchföreläsning FRP Konstruktioner, Sweco 2019-01-16.

Porteous, J. and Kermani, A. (2007). *Structural Timber Design to Eurocode 5.* Blackwell Publishing.

Potyrala, P. B., Ramón, J., and Rius, C. (2011). PROJECTE O TESINA D ' ESPECIALITAT Títol Use of Fibre Reinforced Polymer Composites in Bridge Construction . State of the Art in Hybrid and All-Composite. *Polymer Composites.*

Pousette, A. (2001). Cable Stayed Timber Bridges. *(Trätek, Stockholm).*

Pousette, A. (2016). *Structural Systems for Infrastructure. Volume 1. Chapter 9 - Design for Serviceability.* Swedish Wood, Stockholm.

Raftery, G. M. and Harte, A. M. (2013). Nonlinear numerical modelling of FRP reinforced glued laminated timber. *Composites Part B: Engineering*, 52:40–50.

Rao, S. N., G A, S. T., P, R. K., and Kumar V V, R. G. (2018). Carbon Composites Are Becoming Competitive and Cost Effective. *Infosys Navigate your next*, pages 2–3.

Romani, M. and Blass, H. J. (2001). DESIGN MODEL FOR FRP REINFORCED GLULAM BEAMS. *Earth and Planetary Science Letters.*

Scanscot Technology AB (2019). Brigade/Plus Scanscot Technology.

Schober, K.-U., Harte, A. M., Kliger, R., Jockver, R., Xu, Q., and Chen, J.-F. (2015). Frp reinforcement of timber structures. *(Elsevier)*, 97:106–118.

Sétra (2006). Footbridges - Assesment of vibrational behaviour of footbridges under pedestrian loading.

SIS (2005). *Eurocode: Basis of structural design.*

SIS (2007). Eurokod 1 : Laster på bärverk – Del 2 : Trafiklast på broar. *Euro code SS-EN 1991-2.*

SIS (2009). *SS-EN_1995-2:2004, Eurocode 5: Design of timber structures - Part 2: Bridges.*

SIS (2013). *Svensk Standard SS-EN 14080:2013.*

SIS (2014a). *Eurocode 1: Actions on structures - Part 1-5: General actions - Thermal actions.*

SIS (2014b). *Eurocode 5: Design of timber structures - Part 1-1: General - Common rules and rules for buildings.*

Stena Stål AB (2019). Stena Stål pris- och sortimentlista.

Trafikverket (2016). Krav Brobyggande. pages 0–351.

Trimble, B., Wilson, D., Davalos, J., Qiao, P., Johnson, W., and Masters, J. (2010). Fiber-Reinforced Composite and Wood Bonded Interfaces: Part 1. Durability and Shear Strength. *Journal of Composites Technology and Research*, 22(4).

Valipour, H. R. and Crews, K. (2011). Efficient finite element modelling of timber beams strengthened with bonded fibre reinforced polymers. *Construction and Building Materials*, 25(8):3291–3300.

Wheeler, A. S. and Hutchinson, A. R. (1998). Resin repairs to timber structures. *International Journal of Adhesion and Adhesives*, 18(1):1–13.

Yang, F. (2017). *Novel Fire Retardant Polymers and Composite Materials, chapter 10.* Elsevier.

Zhang, J., Delichatsios, M. A., Fateh, T., Suzanne, M., and Ukleja, S. (2017). Characterization of flammability and fire resistance of carbon fibre reinforced thermoset and thermoplastic composite materials. *Journal of Loss Prevention in the Process Industries*, 50:275–282.

A
Mathcad Straight Beam

Calculation of cross-sectional capacity of CFRP reinforced straight beam

Material properties

Service class 3, according to Swedish standards

Characterisic values Timber(GL28c, DoTS Volume 2 Table 3.4)

$f_{mk} := 28\ MPa$

$f_{ck} := 24\ MPa$

$f_{c.90.k} := 2.5\ MPa$

$f_{tk} := 19.5\ MPa$

$f_{vk} := 3.5\ MPa$

$f_{rk} := 1.2\ MPa$

$\rho_w := 420\ \frac{kg}{m^3}$ Mean density

$E_w := 10.4\ GPa$

$E_{mean} := 12.5\ GPa$

$\varepsilon_{c.el.gl} := \frac{f_{ck}}{E_w} = 2.308\ 10^{-3}$

$\varepsilon_{t.el.gl} := \frac{f_{tk}}{E_w} = 1.875\ 10^{-3}$

CFRP properties (S&P C laminat, product sheet)

$f_{t.cfrp} := 2800\ MPa$ Tensile strength

$f_{c.cfrp} := 1400\ MPa$ Compressive strength
Assumption of half

$\rho_{cfrp} := 1600\ \frac{kg}{m^3}$ Density

$\gamma_{cfrp} := 1.0$ assuming certified manufacturer

$E_{cfrp} := 300\ GPa$

low = 205
mid = 300
high = 375
ultrahigh = 450

$\alpha := \frac{E_{cfrp}}{E_{mean}} = 24$

CFRP Properties (Fiberline, Product Sheet)

$f_{t.cfrp.fiberline} := 1640\ MPa$ Tensile strength

$f_{c.cfrp.fiberline} := 890\ MPa$ Compressive strength

$f_{m.cfrp.fiberline} := 900\ MPa$ Flexural strength

$f_{tt.cfrp.fiberline} := 18\ MPa$ Tensile transverse strength

$f_{ils.cfrp.fiberline} := 52\ MPa$ Inter laminar shear strength

$\rho_{cfrp.fiberline} := 1550\ \frac{kg}{m^3}$ Density

Beam geometry

Carbon fibre geometry

$b_{cfrp} := 185\ mm$

$h_{cfrp} := 5\ mm$

$A_{i.cfrp} := b_{cfrp} \cdot h_{cfrp} = 925\ mm^2$

$n_c := 1$ Number of laminations (compressive)

$n_t := 1$ Number of laminations (tensile)

Timber geometry

The exterior timber part surrounding the CFRP-laminas on the sides (15 mm x h_cfrp) is exluded as it is assumed to have little effect on the overall behaviour.

$h_{lamella} := 45\ mm$ Thickness of lamellas

$h_{last.lamella} := 15\ mm$ Thickness of last sacrificial lamella

$n_{laminations} := 15$ Number of timber laminations (including outer lamellas)

$L := 20\ m$ Span of the beam

$h_{plain} := \left(n_{laminations} - 2\right) \cdot h_{lamella} + 2 \cdot h_{last.lamella} = 615\ mm$

$h_{reinforced} := \left(n_{laminations} - 2\right) \cdot h_{lamella} + 2 \cdot h_{last.lamella} + h_{cfrp} \cdot \left(n_c + n_t\right) = 625\ mm$

$b := 215\ mm$

$A_{timber} := b \cdot h_{plain} = \left(1.322 \cdot 10^5\right)\ mm^2$

$A_{reinforced} := b \cdot h_{reinforced} = \left(1.344 \cdot 10^5\right)\ mm^2$

lever arms CFRP

$y_c := h_{last.lamella} + \frac{h_{cfrp}}{2} \cdot n_c = 17.5\ mm$

$y_t := h_{reinforced} - \left(h_{last.lamella} + \frac{h_{cfrp}}{2} \cdot n_t\right) = 607.5\ mm$

$A_{t.cfrp} := n_t \cdot A_{i.cfrp} = 925\ mm^2$ Area reinforcement on compression side

$A_{c.cfrp} := n_c \cdot A_{i.cfrp} = 925\ mm^2$ Area reinforcement on tension side

$A_{cfrp} := A_{t.cfrp} + A_{c.cfrp} = \left(1.85 \cdot 10^3\right)\ mm^2$ Total reinforcement area

$$\frac{A_{cfrp}}{A_{reinforced}} = 1.377\%$$

Ratio reinforcement in cross section

Design Values Timber, values from DoTS volume 2

$k_{cr} := 0.67$

Reduction of shear capacity due to solar radiation and percipitation

$\gamma_{glulam} := 1.25$

Partial factor for material properties in glulam

$k_{def} := 2$

Factor considering long term effects, service class 3

$$k_h := \begin{array}{l} \text{if } h_{plain} < 600\ mm \\ \quad \left\| \min\left(\left(\frac{600\ mm}{h_{plain}}\right)^{0.1}, 1.1\right) \right. \\ \text{else if } h_{plain} \geq 600\ mm \\ \quad \| 1 \end{array} = 1$$

Size factor, DoTS section 3.3 Volume 2

$k_{mod.glulam} := 0.8$

Factor considering duration of load and service class 3

$k_{c.90} := 1$

Support condition factor, according to section 5.2 DoTS

$$f_{md} := \frac{k_h \cdot f_{mk} \cdot k_{mod.glulam}}{\gamma_{glulam}} = 17.92\ MPa$$

$$f_{cd} := \frac{f_{ck} \cdot k_{mod.glulam}}{\gamma_{glulam}} = 15.36\ MPa$$

$$f_{c.90.d} := \frac{k_{c.90} \cdot k_{mod.glulam} \cdot f_{c.90.k}}{\gamma_{glulam}} = 1.6\ MPa$$

$$f_{td} := \frac{f_{tk} \cdot k_{mod.glulam}}{\gamma_{glulam}} = 12.48\ MPa$$

$$f_{vd} := \frac{f_{vk} \cdot k_{mod.glulam}}{\gamma_{glulam}} = 2.24\ MPa$$

$$f_{rd} := \frac{f_{rk} \cdot k_{mod.glulam}}{\gamma_{glulam}} = 0.768\ MPa$$

$$E_{mean.fin} := \frac{E_{mean}}{1 + k_{def}} = 4.167\ GPa$$

Transformed area

$$A_{transformed} := A_{reinforced} + A_{cfrp} \cdot (\alpha - 1) = \left(1.769 \cdot 10^5\right)\ mm^2$$

Loads

$g := 9.82 \dfrac{m}{s^2}$ Gravitational constant

$g_k := \rho_w \cdot A_{timber} \cdot g + \rho_{cfrp} \cdot A_{cfrp} \cdot g = 0.574 \dfrac{kN}{m}$ Self-weight

$q_k := 5 \dfrac{kN}{m^2} \cdot b = 1.075 \dfrac{kN}{m}$ Distributed pedestrian load

$$M_{max} := \frac{(g_k + q_k) \cdot L^2}{8} = 82.471\ kN \cdot m$$

$q_{ULS} := 1.35 \cdot g_k + 1.5 \cdot q_k = 2.388 \dfrac{kN}{m}$ Load combination according to ULS

$$M_{Ed} := \frac{q_{ULS} \cdot L^2}{8} = 119.398\ kN \cdot m$$

Resistance of cross section (plain timber)

$W_{y.w} := \dfrac{b \cdot h_{plain}^2}{6} = 0.014\ m^3$ Assume that it is braced against lateral torsional buckling. kcrit=1

$$M_{Rd\_w} := W_{y.w} \cdot f_{md} = 242.871\ kN \cdot m$$

Plain timber deflection

$\psi_{red} := 0.4$ Reduction of traffic load, Eurocode 1

$\delta_{max} := \dfrac{L}{400} = 50\ mm$ Maximum allowed deflection, according to Trafikverket Krav Brobyggande

$\delta_{plain} := \dfrac{5 \cdot (\psi_{red} \cdot q_k) \cdot L^4}{384 \cdot E_{mean.fin} \cdot \dfrac{b \cdot h_{plain}^3}{12}} = 51.589\ mm$ The influence of shear deformation on deflection is assumed to be small on the final deflection. Eurocode 1

Calculation of neutral axis

$$y_{NA} := \frac{A_{t.cfrp} \cdot y_t \cdot (\alpha - 1) + A_{c.cfrp} \cdot y_c \cdot (\alpha - 1) + A_{reinforced} \cdot \dfrac{h_{reinforced}}{2}}{A_{transformed}} = 312.5\ mm$$

Stiffness of cross section

$$b_{fic.cfrp} := \alpha \cdot b_{cfrp} = 4.44\ m$$

$$I_{centre.of.gravity} := \begin{bmatrix} \dfrac{b \cdot h_{last.lamella}^{\;3}}{12} \\ \dfrac{b_{fic.cfrp} \cdot (h_{cfrp} \cdot n_c)^3}{12} \\ \dfrac{b \cdot (h_{reinforced} - 2 \cdot h_{last.lamella} - h_{cfrp} \cdot n_c - h_{cfrp} \cdot n_t)^3}{12} \\ \dfrac{b_{fic.cfrp} \cdot (h_{cfrp} \cdot n_t)^3}{12} \\ \dfrac{b \cdot h_{last.lamella}^{\;3}}{12} \end{bmatrix} = \begin{bmatrix} 6.047 \cdot 10^{-8} \\ 4.625 \cdot 10^{-8} \\ 0.004 \\ 4.625 \cdot 10^{-8} \\ 6.047 \cdot 10^{-8} \end{bmatrix} m^4$$

$$A := \begin{bmatrix} b \cdot h_{last.lamella} \\ b_{fic.cfrp} \cdot h_{cfrp} \cdot n_c \\ b \cdot (n_{laminations} - 2) \cdot h_{lamella} \\ b_{fic.cfrp} \cdot h_{cfrp} \cdot n_t \\ b \cdot h_{last.lamella} \end{bmatrix} = \begin{bmatrix} 0.003 \\ 0.022 \\ 0.126 \\ 0.022 \\ 0.003 \end{bmatrix} m^2$$

$$a := \begin{bmatrix} y_{NA} - \dfrac{h_{last.lamella}}{2} \\ y_{NA} - h_{last.lamella} - \dfrac{h_{cfrp}}{2} \cdot n_c \\ \mathrm{abs}\left(\dfrac{h_{reinforced}}{2} - y_{NA}\right) \\ h_{reinforced} - h_{last.lamella} - \dfrac{h_{cfrp}}{2} \cdot n_t - y_{NA} \\ h_{reinforced} - \dfrac{h_{last.lamella}}{2} - y_{NA} \end{bmatrix} = \begin{bmatrix} 305 \\ 295 \\ 0 \\ 295 \\ 305 \end{bmatrix} mm$$

$$I := I_{centre.of.gravity} + \overrightarrow{A \cdot a^2} = \begin{bmatrix} 0.3 \\ 1.932 \\ 3.587 \\ 1.932 \\ 0.3 \end{bmatrix} 10^{-3}\, m^4$$

$$I_{tot} := \sum I = 8.051\ 10^{-3}\, m^4$$

$$EI_{tot} := E_{mean} \cdot I_{tot} = 100.639\ MN \cdot m^2$$ Transformed CFRP to equivalent timber initial stage

$$E_d I_{tot} := E_{mean.fin} \cdot I_{tot} = 33.546\ MN \cdot m^2$$ Transformed CFRP to equivalent timber final stage

Resistance of cross section (CFRP reinforced)

$\varepsilon_t := \varepsilon_{t.el.gl} = 1.875\ 10^{-3}$ Assume tension failure

$\varepsilon_c := \dfrac{\varepsilon_t \cdot y_{NA}}{h_{reinforced} - y_{NA}} = 1.875\ 10^{-3}$ $\varepsilon_c < \varepsilon_{c.el.gl} = 1$ ok!

$$\varepsilon_{t.cfrp} := \varepsilon_t \cdot \frac{(y_t - y_{NA})}{h_{reinforced} - y_{NA}} = 1.77\ 10^{-3}$$

$$\varepsilon_{c.cfrp} := \varepsilon_c \cdot \frac{(y_{NA} - y_c)}{y_{NA}} = 1.77\ 10^{-3}$$

Strain compatability compression

$$\varepsilon_{c.edge} := \frac{(y_{NA} - h_{last.lamella}) \cdot \varepsilon_c}{y_{NA}} = 1.785\ 10^{-3}$$

$$\varepsilon_{c.edge.mean} := \frac{\varepsilon_{c.edge} + \varepsilon_c}{2} = 1.83\ 10^{-3}$$

$$\varepsilon_{c.mid} := \frac{\left(y_{NA} - y_c - \frac{h_{cfrp}}{2} \cdot n_c\right) \cdot \varepsilon_c}{y_{NA}} = 1.755\ 10^{-3}$$

$$\varepsilon_{c.mid.mean} := \frac{\varepsilon_{c.mid}}{2} = 8.775 \cdot 10^{-4}$$

Strain compatability tension

$$\varepsilon_{t.edge} := \frac{(h_{reinforced} - h_{last.lamella} - y_{NA}) \cdot \varepsilon_t}{h_{reinforced} - y_{NA}} = 1.785\ 10^{-3}$$

$$\varepsilon_{t.edge.mean} := \frac{\varepsilon_{t.edge} + \varepsilon_t}{2} = 1.83\ 10^{-3}$$

$$\varepsilon_{t.mid} := \varepsilon_t \cdot \frac{\left(y_t - y_{NA} - \frac{h_{cfrp}}{2} \cdot n_t\right)}{h_{reinforced} - y_{NA}} = 1.755\ 10^{-3}$$

$$\varepsilon_{t.mid.mean} := \frac{\varepsilon_{t.mid}}{2} = 8.775 \cdot 10^{-4}$$

Section forces

$$F_{c.edge} := \varepsilon_{c.edge.mean} \cdot E_w \cdot (h_{last.lamella}) \cdot b = 61.378\ kN$$

$$F_{c.mid} := \varepsilon_{c.mid.mean} \cdot E_w \cdot \left(y_{NA} - y_c - \frac{h_{cfrp}}{2} \cdot n_c\right) \cdot b = 573.911\ kN$$

$$F_{t.edge} := \varepsilon_{t.edge.mean} \cdot E_w \cdot \left(h_{last.lamella}\right) \cdot b = 61.378\ kN$$

$$F_{t.mid} := \varepsilon_{t.mid.mean} \cdot E_w \cdot \left(y_t - y_{NA} - \frac{h_{cfrp}}{2} \cdot n_t\right) \cdot b = 573.911\ kN$$

$$F_{t.cfrp} := \varepsilon_{t.cfrp} \cdot E_{cfrp} \cdot A_{t.cfrp} = 491.175\ kN$$

$$F_{c.cfrp} := \varepsilon_{c.cfrp} \cdot E_{cfrp} \cdot A_{c.cfrp} = 491.175\ kN$$

Check horizontal equilibrium

$F_{c.edge} + F_{c.mid} + F_{c.cfrp} = \left(1.126 \cdot 10^3\right)\ kN$ Compression

$F_{t.mid} + F_{t.edge} + F_{t.cfrp} = \left(1.126 \cdot 10^3\right)\ kN$ Tension

Moment capacity

Lever arms (distance from top)

$$z_1 := \frac{h_{last.lamella} \cdot \varepsilon_{c.edge} \cdot \frac{h_{last.lamella}}{2} + h_{last.lamella} \cdot \frac{\left(\varepsilon_c - \varepsilon_{c.edge}\right)}{2} \cdot \frac{h_{last.lamella}}{3}}{h_{last.lamella} \cdot \varepsilon_{c.edge} + h_{last.lamella} \cdot \frac{\left(\varepsilon_c - \varepsilon_{c.edge}\right)}{2}} = 7.439\ mm$$

$$z_3 := y_c + n_c \cdot \frac{h_{cfrp}}{2} + \frac{1}{3} \cdot \left(y_{NA} - \left(y_c + \frac{h_{cfrp}}{2} \cdot n_c\right)\right) = 117.5\ mm$$

$$z_4 := y_{NA} + \frac{2}{3} \left(y_t - y_{NA} - \frac{h_{cfrp}}{2} \cdot n_t\right) = 507.5\ mm$$

$$z_6 := y_t + n_t \cdot \frac{h_{cfrp}}{2} + \frac{h_{last.lamella} \cdot \varepsilon_{t.edge} \cdot \frac{h_{last.lamella}}{2} + h_{last.lamella} \cdot \frac{\left(\varepsilon_t - \varepsilon_{t.edge}\right)}{2} \cdot \frac{2 \cdot h_{last.lamella}}{3}}{h_{last.lamella} \cdot \varepsilon_{t.edge} + h_{last.lamella} \cdot \frac{\left(\varepsilon_t - \varepsilon_{t.edge}\right)}{2}} = 617.561\ mm$$

$$M_{Rd} := F_{c.edge} \cdot \left(z_6 - z_1\right) + F_{c.cfrp} \cdot \left(z_6 - y_c\right) + F_{c.mid} \cdot \left(z_6 - z_3\right) + F_{t.mid} \cdot \left(z_6 - z_4\right) + F_{t.cfrp} \cdot \left(z_6 - y_t\right) = 687.282\ kN \cdot m$$

Deflection of beam

$$\delta_{reinforced} := \frac{5 \cdot \psi_{red} \cdot q_k \cdot L^4}{384 \cdot E_d I_{tot}} = 26.704\ mm$$

Eurocode 1, table 5.1

Shear Capacity, section 6 DoTS volume 2

$$h_{te} := y_{NA} - h_{last.lamella} - h_{cfrp} \cdot n_c = 292.5\ mm$$

$$a_{te} := \frac{h_{te}}{2} = 146.25\ mm$$

$$S_{xx} := A(0) \cdot a(0) + A(1) \cdot a(1) + b \cdot h_{te} \cdot a_{te} = 16.73\ 10^{-3}\ m^3$$

$$V_{Ed} := (q_{ULS}) \cdot \frac{L}{2} = 23.88\ kN$$

$$\tau_{Ed} := \frac{S_{xx} \cdot V_{Ed}}{I_{tot} \cdot b} = 0.231\ MPa$$

$$\tau_{Rd} := k_{cr} \cdot f_{vd} = 1.501\ MPa$$

Check for shear failure of the outer most lamella

The area of the sheared of piece of timber and CFRP. Neglecting the small influence of the timber pieces surrounding the CFRP lamina

$$\Delta S_y := b_{cfrp} \cdot (h_{last.lamella} - h_{cfrp}) \cdot \left(y_{NA} - \frac{h_{last.lamella}}{2}\right) + b_{cfrp} \cdot h_{cfrp} \cdot \left(y_{NA} - h_{last.lamella} + \frac{h_{cfrp}}{2}\right) = (8.418 \cdot 10^5)\ mm^3$$

$$\tau_{Ed.glue} := \frac{V_{Ed} \cdot \Delta S_y}{I_{tot} \cdot b_{cfrp}} = 0.013\ MPa$$

Calculate necessary bearing length

$l_b := 100\ mm$ — Assume starting value

$\sigma_{c.90.d} := \dfrac{V_{Ed}}{b \cdot l_b} = 1.111\ MPa$ — According to Equation 4.22 STDtE5

```
if f_c.90.d > σ_c.90.d
    "OK"
else
    "Increase support length"
```
= "OK"

$f_{c.90.d} = 1.6\ MPa$

Stresses at different levels

$z_{top.lamella} := 0\ m$ Distance to top of cross-section

$z_{cfrp.u.top} := h_{last.lamella} = 0.015\ m$ Distance to top of upper CFRP

$z_{cfrp.u.bot} := h_{last.lamella} + n_c \cdot h_{cfrp} = 0.02\ m$ Distance to bottom of upper CFRP

$z_{cfrp.l.top} := h_{reinforced} - h_{last.lamella} - n_t \cdot h_{cfrp} = 605\ mm$ Distance to top of lower CFRP

$z_{cfrp.l.bot} := h_{reinforced} - h_{last.lamella} = 610\ mm$ Distance to bottom of lower CFRP

$z_{bot.lamella} := h_{reinforced} = 0.625\ m$ Distance to bottom of cross-section

$$z := \begin{bmatrix} \frac{h_{last.lamella}}{2} \\ h_{last.lamella} + \frac{n_c \cdot h_{cfrp}}{2} \\ h_{last.lamella} + n_c \cdot h_{cfrp} + \frac{(n_{laminations} - 2) \cdot h_{lamella}}{2} \\ h_{reinforced} - h_{last.lamella} - \frac{n_t \cdot h_{cfrp}}{2} \\ h_{reinforced} - \frac{h_{last.lamella}}{2} \end{bmatrix} = \begin{bmatrix} 0.008 \\ 0.018 \\ 0.313 \\ 0.608 \\ 0.618 \end{bmatrix} m$$

$$A := \begin{bmatrix} h_{last.lamella} \cdot b \\ h_{cfrp} \cdot b_{cfrp} \cdot n_c \\ (n_{laminations} - 2) \cdot h_{lamella} \cdot b \\ h_{cfrp} \cdot b_{cfrp} \cdot n_t \\ h_{last.lamella} \cdot b \end{bmatrix} = \begin{bmatrix} 0.003 \\ 9.25 \cdot 10^{-4} \\ 0.126 \\ 9.25 \cdot 10^{-4} \\ 0.003 \end{bmatrix} m^2$$

$$z_{na.i} := \frac{E_{mean} \cdot (A(0) \cdot z(0) + A(2) \cdot z(2) + A(4) \cdot z(4)) + E_{cfrp} \cdot (A(1) \cdot z(1) + A(3) \cdot z(3))}{E_{mean} \cdot (A(0) + A(2) + A(4)) + E_{cfrp} \cdot (A(1) + A(3))} = 312.5\ mm$$

$$z_{na.f} := \frac{E_{mean.fin} \cdot (A(0) \cdot z(0) + A(2) \cdot z(2) + A(4) \cdot z(4)) + E_{cfrp} \cdot (A(1) \cdot z(1) + A(3) \cdot z(3))}{E_{mean.fin} \cdot (A(0) + A(2) + A(4)) + E_{cfrp} \cdot (A(1) + A(3))} = 312.5\ mm$$

$$EI_{tot.i} := \sum E_{mean} \cdot I_{centre.of.gravity} + E_{mean} \cdot \left(A(0) \cdot (z_{na.i} - z(0))^2 + A(2) \cdot (z_{na.i} - z(2))^2 + A(4) \cdot (z_{na.i} - z(4))^2 \right) + E_{cfrp} \cdot \left(A(1) \cdot (z_{na.i} - z(1))^2 + A(3) \cdot (z_{na.i} - z(3))^2 \right) = 100.639\ MN \cdot m^2$$

$$EI_{tot.f} := \sum E_{mean.fin} \cdot I_{centre.of.gravity} + E_{mean.fin} \cdot \left(A(0) \cdot \left(z_{na.f} - z(0)\right)^2 + A(2) \cdot \left(z_{na.f} - z(2)\right)^2 + A(4) \cdot \left(z_{na.f} - z(4)\right)^2 \right) + E_{cfrp} \cdot \left(A(1) \cdot \left(z_{na.f} - z(1)\right)^2 + A(3) \cdot \left(z_{na.f} - z(3)\right)^2 \right) = 65.745\ MN \cdot m^2$$

ULS initial

$$\sigma_{top.ULS.i} := \frac{M_{Ed} \cdot E_{mean} \cdot \mathrm{abs}\left(z_{na.i} - z_{top.lamella}\right)}{EI_{tot.i}} = 4.634\ MPa$$

$$\sigma_{cfrp.u.top.ULS.i} := \frac{M_{Ed} \cdot E_{cfrp} \cdot \mathrm{abs}\left(z_{na.i} - z_{cfrp.u.top}\right)}{EI_{tot.i}} = 105.887\ MPa$$

$$\sigma_{cfrp.u.bot.ULS.i} := \frac{M_{Ed} \cdot E_{cfrp} \cdot \mathrm{abs}\left(z_{na.i} - z_{cfrp.u.bot}\right)}{EI_{tot.i}} = 104.107\ MPa$$

$$\sigma_{cfrp.l.top.ULS.i} := \frac{M_{Ed} \cdot E_{cfrp} \cdot \mathrm{abs}\left(z_{na.i} - z_{cfrp.l.top}\right)}{EI_{tot.i}} = 104.107\ MPa$$

$$\sigma_{cfrp.l.bot.ULS.i} := \frac{M_{Ed} \cdot E_{cfrp} \cdot \mathrm{abs}\left(z_{na.i} - z_{cfrp.l.bot}\right)}{EI_{tot.i}} = 105.887\ MPa$$

$$\sigma_{bot.ULS.i} := \frac{M_{Ed} \cdot E_{mean} \cdot \mathrm{abs}\left(z_{na.i} - z_{bot.lamella}\right)}{EI_{tot.i}} = 4.634\ MPa$$

ULS final

$$\sigma_{top.ULS.f} := \frac{M_{Ed} \cdot E_{mean.fin} \cdot \mathrm{abs}\left(z_{na.f} - z_{top.lamella}\right)}{EI_{tot.f}} = 2.365\ MPa$$

$$\sigma_{cfrp.u.top.ULS.f} := \frac{M_{Ed} \cdot E_{cfrp} \cdot \mathrm{abs}\left(z_{na.f} - z_{cfrp.u.top}\right)}{EI_{tot.f}} = 162.084\ MPa$$

$$\sigma_{cfrp.u.bot.ULS.f} := \frac{M_{Ed} \cdot E_{cfrp} \cdot \mathrm{abs}\left(z_{na.f} - z_{cfrp.u.bot}\right)}{EI_{tot.f}} = 159.36\ MPa$$

$$\sigma_{cfrp.l.top.ULS.f} := \frac{M_{Ed} \cdot E_{cfrp} \cdot \mathrm{abs}\left(z_{na.f} - z_{cfrp.l.top}\right)}{EI_{tot.f}} = 159.36\ MPa$$

$$\sigma_{cfrp.l.bot.ULS.f} := \frac{M_{Ed} \cdot E_{cfrp} \cdot \mathrm{abs}\left(z_{na.f} - z_{cfrp.l.bot}\right)}{EI_{tot.f}} = 162.084\ MPa$$

$$\sigma_{bot.ULS.f} := \frac{M_{Ed} \cdot E_{mean.fin} \cdot \mathrm{abs}\left(z_{na.f} - z_{bot.lamella}\right)}{EI_{tot.f}} = 2.365\ MPa$$

Utilization ratios stresses

$\frac{\sigma_{top.ULS.i}}{f_{cd}} = 30.172\%$

$\frac{\sigma_{top.ULS.f}}{f_{cd}} = 15.395\%$

$\frac{\sigma_{cfrp.u.top.ULS.i}}{f_{c.cfrp}} = 7.563\%$

$\frac{\sigma_{cfrp.u.top.ULS.f}}{f_{c.cfrp}} = 11.577\%$

$\frac{\sigma_{cfrp.u.bot.ULS.i}}{f_{c.cfrp}} = 7.436\%$

$\frac{\sigma_{cfrp.u.bot.ULS.f}}{f_{c.cfrp}} = 11.383\%$

$\frac{\sigma_{cfrp.l.top.ULS.i}}{f_{t.cfrp}} = 3.718\%$

$\frac{\sigma_{cfrp.l.top.ULS.f}}{f_{t.cfrp}} = 5.691\%$

$\frac{\sigma_{cfrp.l.bot.ULS.i}}{f_{t.cfrp}} = 3.782\%$

$\frac{\sigma_{cfrp.l.bot.ULS.f}}{f_{t.cfrp}} = 5.789\%$

$\frac{\sigma_{bot.ULS.i}}{f_{td}} = 37.135\%$

$\frac{\sigma_{bot.ULS.f}}{f_{td}} = 18.948\%$

Dynamic behaiour

$A_{deck} := b \cdot L = 4.3\ m^2$ Surface of the walkway

$P := 700\ N$ Body weight of a pedestrian

$m_g := \frac{g_k}{g} = 58.495\ \frac{kg}{m}$

$M_g := \frac{L \cdot m_g}{2} = 584.945\ kg$ Modal mass of the system

Traffic classes

$$TC := \begin{bmatrix} 0.2 \cdot \frac{1}{m^2} \\ 0.5 \cdot \frac{1}{m^2} \end{bmatrix} = \begin{bmatrix} 0.2 \\ 0.5 \end{bmatrix} \frac{1}{m^2}$$

Density of pedestrians according to traffic classes
Only calculating for traffic classes 2 and 3

$$d_{TC} := TC \cdot P = \begin{bmatrix} 0.14 \\ 0.35 \end{bmatrix} \frac{kN}{m^2}$$

$$m_{TC} := m_g + \frac{b \cdot d_{TC}}{g} = \begin{bmatrix} 61.56 \\ 66.157 \end{bmatrix} \frac{kg}{m}$$

$$f_{1.np} := \frac{1}{2 \cdot \pi} \cdot \frac{9.869}{L^2} \cdot \sqrt{\frac{EI_{tot}}{m_g}} = 5.151\ Hz$$

No pedestrian masses

$$f_{2.np} := \frac{1}{2 \cdot \pi} \cdot \frac{39.478}{L^2} \cdot \sqrt{\frac{EI_{tot}}{m_g}} = 20.603\ Hz$$

No pedestrian masses

$$f_{np} := \begin{bmatrix} f_{1.np} \\ f_{2.np} \end{bmatrix} = \begin{bmatrix} 5.151 \\ 20.603 \end{bmatrix} Hz$$

$$I := 0..1$$

According to Eurocode the eigenfrequency should be over 5 Hz, to avoid checks of accelerations.

```
if f_np(I) > 5 Hz
  ‖ "OK"
else
  ‖ "Check accelerations"
```

$$= \begin{bmatrix} \text{"OK"} \\ \text{"OK"} \end{bmatrix}$$

$$f_1 := \frac{1}{2 \cdot \pi} \cdot \frac{9.869}{L^2} \cdot \sqrt{\frac{EI_{tot}}{m_{TC}}} = \begin{bmatrix} 5.021 \\ 4.843 \end{bmatrix} Hz$$

With pedestrian masses

$$f_2 := \frac{1}{2 \cdot \pi} \cdot \frac{39.478}{L^2} \cdot \sqrt{\frac{EI_{tot}}{m_{TC}}} = \begin{bmatrix} 20.084 \\ 19.373 \end{bmatrix} Hz$$

With pedestrian masses

Determination of maximum acceleration

$$\xi_{damping.timber} := 0.015$$

1.5% according to JRC (most critical)
3% according to Setra

$$\xi_{crit} := \frac{1}{\sqrt{1 + \left(\frac{2 \cdot \pi}{\xi_{damping.timber}}\right)^2}} = 0.002387$$

$$n'_{TC1.3} := \frac{10.8 \cdot \sqrt{\xi_{damping.timber} \cdot A_{deck} \cdot TC(1)}}{A_{deck}} = 0.451\ \frac{1}{m^2}$$

Table 4-8: Parameters for load model of TC1 to TC5

P [N]		
Vertical	Longitudinal	Lateral
280	140	35
Reduction coefficient ψ		
Vertical and longitudinal 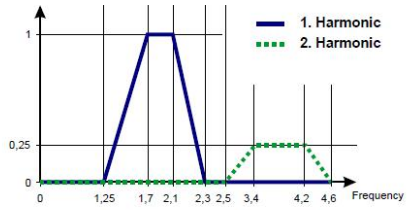		Lateral 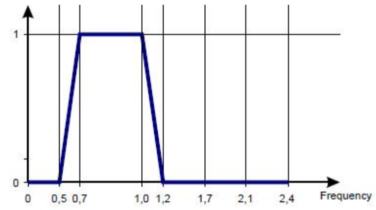
Equivalent number n' of pedestrians on the loaded surface S for load model of:		
TC1 to TC3 (density d < 1,0 P/m²): $n'=\frac{10{,}8\sqrt{\xi\times n}}{S}$ [m⁻²]		
TC4 and TC5 (density d ≥ 1,0 P/m²): $n'=\frac{1{,}85\sqrt{n}}{S}$ [m⁻²]		

Without pedestrian masses

$$\psi_{np_l} := \begin{cases} 0 & \text{if } f_{np}(l) \le 1.25\ Hz \\ \dfrac{f_{np}(l) - 1.25\ Hz}{0.45\ Hz} & \text{else if } 1.25\ Hz < f_{np}(l) \le 1.7\ Hz \\ 1 & \text{else if } 1.7\ Hz < f_{np}(l) \le 2.1\ Hz \\ 1 - \dfrac{f_{np}(l) - 2.1\ Hz}{0.2\ Hz} & \text{else if } 2.1\ Hz < f_{np}(l) \le 2.3\ Hz \\ 0 & \text{else if } 2.3\ Hz < f_{np}(l) \le 2.5\ Hz \\ \dfrac{f_{np}(l) - 2.5\ Hz}{4 \cdot 0.9\ Hz} & \text{else if } 2.5\ Hz < f_{np}(l) \le 3.4\ Hz \\ 0.25 & \text{else if } 3.4\ Hz < f_{np}(l) \le 4.2\ Hz \\ 0.25 - \dfrac{f_{np}(l) - 4.2\ Hz}{4 \cdot 0.4\ Hz} & \text{else if } 4.2\ Hz < f_{np}(l) \le 4.6\ Hz \\ 0 & \text{else if } f_{np}(l) > 4.6\ Hz \end{cases} = \begin{bmatrix} 0 \\ 0 \end{bmatrix}$$

$i := 0..1$

$$\psi_{1_i} := \begin{array}{l} \text{if } f_1(i) \le 1.25\ Hz \\ \quad \| \ 0 \\ \text{else if } 1.25\ Hz < f_1(i) \le 1.7\ Hz \\ \quad \| \ \dfrac{f_1(i) - 1.25\ Hz}{0.45\ Hz} \\ \text{else if } 1.7\ Hz < f_1(i) \le 2.1\ Hz \\ \quad \| \ 1 \\ \text{else if } 2.1\ Hz < f_1(i) \le 2.3\ Hz \\ \quad \| \ 1 - \dfrac{f_1(i) - 2.1\ Hz}{0.2\ Hz} \\ \text{else if } 2.3\ Hz < f_1(i) \le 2.5\ Hz \\ \quad \| \ 0 \\ \text{else if } 2.5\ Hz < f_1(i) \le 3.4\ Hz \\ \quad \| \ \dfrac{f_1(i) - 2.5\ Hz}{4 \cdot 0.9\ Hz} \\ \text{else if } 3.4\ Hz < f_1(i) \le 4.2\ Hz \\ \quad \| \ 0.25 \\ \text{else if } 4.2\ Hz < f_1(i) \le 4.6\ Hz \\ \quad \| \ 0.25 - \dfrac{f_1(i) - 4.2\ Hz}{4 \cdot 0.4\ Hz} \\ \text{else if } f_1(i) > 4.6\ Hz \\ \quad \| \ 0 \end{array} = \begin{bmatrix} 0 \\ 0 \end{bmatrix}$$

$j := 0..1$

$$\psi_{2_j} := \begin{array}{l} \text{if } f_2(j) \le 1.25\ Hz \\ \quad \| \ 0 \\ \text{else if } 1.25\ Hz < f_2(j) \le 1.7\ Hz \\ \quad \| \ \dfrac{f_2(j) - 1.25\ Hz}{0.45\ Hz} \\ \text{else if } 1.7\ Hz < f_2(j) \le 2.1\ Hz \\ \quad \| \ 1 \\ \text{else if } 2.1\ Hz < f_2(j) \le 2.3\ Hz \\ \quad \| \ 1 - \dfrac{f_2(j) - 2.1\ Hz}{0.2\ Hz} \\ \text{else if } 2.3\ Hz < f_2(j) \le 2.5\ Hz \\ \quad \| \ 0 \\ \text{else if } 2.5\ Hz < f_2(j) \le 3.4\ Hz \\ \quad \| \ \dfrac{f_2(j) - 2.5\ Hz}{4 \cdot 0.9\ Hz} \\ \text{else if } 3.4\ Hz < f_2(j) \le 4.2\ Hz \\ \quad \| \ 0.25 \\ \text{else if } 4.2\ Hz < f_2(j) \le 4.6\ Hz \\ \quad \| \ 0.25 - \dfrac{f_2(j) - 4.2\ Hz}{4 \cdot 0.4\ Hz} \\ \text{else if } f_2(j) > 4.6\ Hz \\ \quad \| \ 0 \end{array} = \begin{bmatrix} 0 \\ 0 \end{bmatrix}$$

$P_v := 280\ N$

$$q_{1.TC1.3} := b \cdot P_v \cdot n'_{TC1.3} \cdot \psi_1 = \begin{bmatrix} 0 \\ 0 \end{bmatrix} \frac{N}{m}$$

$$q_{2.TC1.3} := b \cdot P_v \cdot n'_{TC1.3} \cdot \psi_2 = \begin{bmatrix} 0 \\ 0 \end{bmatrix} \frac{N}{m}$$

$$q_{np.TC1.3} := b \cdot P_v \cdot n'_{TC1.3} \cdot \psi_{np} = \begin{bmatrix} 0 \\ 0 \end{bmatrix} \frac{N}{m}$$

$$a_{1.TC1.3} := \frac{1}{2 \cdot \xi_{damping.timber}} \cdot \frac{4 \cdot q_{1.TC1.3}}{\pi \cdot m_{TC}} = \begin{bmatrix} 0 \\ 0 \end{bmatrix} \frac{m}{s^2}$$

$$a_{2.TC1.3} := \frac{1}{2 \cdot \xi_{damping.timber}} \cdot \frac{4 \cdot q_{2.TC1.3}}{\pi \cdot m_{TC}} = \begin{bmatrix} 0 \\ 0 \end{bmatrix} \frac{m}{s^2}$$

$$a_{np.TC1.3} := \frac{1}{2 \cdot \xi_{damping.timber}} \cdot \frac{4 \cdot q_{np.TC1.3}}{\pi \cdot m_g} = \begin{bmatrix} 0 \\ 0 \end{bmatrix} \frac{m}{s^2}$$

if $a_{np.TC1.3}(l) \le 0.75 \frac{m}{s^2}$ $= \begin{bmatrix} \text{"OK"} \\ \text{"OK"} \end{bmatrix}$

"OK"

else

"Not OK"

if $a_{1.TC1.3}(j) \le 0.75 \frac{m}{s^2}$ $= \begin{bmatrix} \text{"OK"} \\ \text{"OK"} \end{bmatrix}$

"OK"

else

"Not OK"

The limit for acccelerations is chosen to 0.75 m/s^2 to be acceptable.

if $a_{2.TC1.3}(j) \le 0.75 \frac{m}{s^2}$ $= \begin{bmatrix} \text{"OK"} \\ \text{"OK"} \end{bmatrix}$

"OK"

else

"Not OK"

Comparison between plain and reinforced cross-section

Moment capacity

$$\frac{M_{Ed}}{M_{Rd\_w}} = 49.16\%$$

$$\frac{M_{Ed}}{M_{Rd}} = 17.37\%$$

Deflections

$$\frac{\delta_{plain}}{\delta_{max}} = 103.18\%$$

$$\frac{\delta_{reinforced}}{\delta_{max}} = 53.41\%$$

$f_{1.np} = 5.151\ Hz$

$f_{2.np} = 20.603\ Hz$

$\delta_{reinforced} = 26.704\ mm$

$M_{Rd} = 687.282\ kN \cdot m$

Shear capacity

$$\frac{\tau_{Ed}}{\tau_{Rd}} = 15.38\%$$

Glule line failure

$$\frac{\tau_{Ed.glue}}{\tau_{Rd}} = 0.9\%$$

Reduction in height

$h_{unreinforced} := 795\ mm$

$$1 - \frac{h_{reinforced}}{h_{unreinforced}} = 21.384\%$$

Calculation of apex stresses in a pre-cambered beam

$\alpha := \text{atan}\left(\frac{25\ mm}{10000\ mm}\right) = 0.143\ deg$ Angle of the beam

$r_{in} := 2020\ m$ Radius of the beam

$h_{ap} := h_{reinforced}$ Apex height

$k_5 := 0.2 \cdot \tan(\alpha) = 5 \cdot 10^{-4}$

$k_6 := 0.25 - 1.5 \cdot \tan(\alpha) + 2.6 \cdot \tan(\alpha)^2 = 0.246$

$k_7 := 2.1 \cdot \tan(\alpha) - 4 \cdot \tan(\alpha)^2 = 0.005$

$$k_p := k_5 + k_6 \cdot \left(\frac{h_{ap}}{r_{in}}\right) + k_7 \cdot \left(\frac{h_{ap}}{r_{in}}\right)^2 = 5.762 \cdot 10^{-4}$$

$\sigma_{t.90.d} := k_p \cdot \frac{M_{Ed}}{W_{y.w}} = 0.005\ MPa$ Tension perpendicular to grain

$k_{dis} := 1.4$ Factor considering the stress distribution in the apex zone

$V_{tot} := A_{timber} \cdot L = 2.645\ m^3$

$V_{ap} := \frac{\alpha \cdot \pi}{180} \cdot b \cdot \left(h_{ap}^2 + 2\ h_{ap} \cdot r_{in}\right) = 0.024\ m^3$ Stressed area of Apex

$f_{t.90.k} := 0.5\ MPa$ Tension capacity

$f_{t.90.d} := \frac{k_{mod.glulam} \cdot f_{t.90.k}}{\gamma_{glulam}} = 0.32\ MPa$ Design value

$k_{vol} := \left(\frac{0.01\ m^3}{V_{ap}}\right)^{0.2} = 0.842$ Considering the stressed volume compared to the total volume

$f_{t.90.d} := k_{dis} \cdot k_{vol} \cdot f_{t.90.d} = 0.377\ MPa$

```
if σt.90.d ≤ ft.90.d     = "OK"
  ‖ "OK"
else
  ‖ "Not OK"
```

Utilisation

$\frac{\sigma_{t.90.d}}{f_{t.90.d}} = 1.346\%$

B

Mathcad T-Beam

Calculation of cross-sectional capacity of CFRP reinforced T-beam

Material properties

Service class 3, according to swedish standards

Characterisic values Timber(GL28c, DoTS Volume 2 Table 3.4)

$f_{mk} := 28\ MPa$

$f_{ck} := 24\ MPa$

$f_{tk} := 19.5\ MPa$

$f_{vk} := 3.5\ MPa$

$f_{rk} := 1.2\ MPa$

$\rho_w := 420\ \frac{kg}{m^3}$ Mean density

$E_w := 10.4\ GPa$

$E_{mean} := 12.5\ GPa$

$\varepsilon_{c.el.gl} := \frac{f_{ck}}{E_w} = 2.308\ 10^{-3}$

$\varepsilon_{t.el.gl} := \frac{f_{tk}}{E_w} = 1.875\ 10^{-3}$

CFRP properties (S&P C laminat, product sheet)

$f_{t.cfrp} := 2800\ MPa$ Tensile strength

$f_{c.cfrp} := 1400\ MPa$ Compressive strength Assumption of half

$\rho_{cfrp} := 1600\ \frac{kg}{m^3}$ Density

$\gamma_{cfrp} := 1.0$ assuming certified manufacturer

$E_{cfrp} := 450\ GPa$

low = 205
mid = 300
high = 375
ultrahigh = 450

$\alpha := \frac{E_{cfrp}}{E_{mean}} = 36$

CFRP Properties (Fiberline, Product Sheet)

$f_{t.cfrp.fiberline} := 1640\ MPa$ Tensile strength

$f_{c.cfrp.fiberline} := 890\ MPa$ Compressive strength

$f_{m.cfrp.fiberline} := 900\ MPa$ Flexural strength

$f_{tt.cfrp.fiberline} := 18\ MPa$ Tensile transverse strength

$f_{ils.cfrp.fiberline} := 52\ MPa$ Inter laminar shear strength

$\rho_{cfrp.fiberline} := 1550\ \frac{kg}{m^3}$ Density

Beam geometry

$L := 20\ m$

$n_{laminations.w} := 10$ Number of laminations in web

$n_{laminations.f} := 5$ Number of laminations in flange

$h_{lamella} := 45\ mm$ Height of lamellas

$h_{last.lamella} := 15\ mm$ Height of sacrificial lamella

$h_w := (n_{laminations.w} - 1) \cdot h_{lamella} + h_{last.lamella} = 420\ mm$ Total web height

$t_f := (n_{laminations.f} - 1) \cdot h_{lamella} + h_{last.lamella} = 195\ mm$ Total flange height

$h_{tot} := h_w + t_f = 615\ mm$ Total height (plain timber)

$b_w := 215\ mm$

$b_f := 1.5\ m$ Assumption with two T-beams for the cross-section
3m wide walkway

$A_w := b_w \cdot h_w = 0.09\ m^2$

$A_f := b_f \cdot t_f = 0.293\ m^2$

$A_{timber} := A_w + A_f = 0.383\ m^2$

$b_{eff} := \min(b_f, 0.1 \cdot L + b_w, 25 \cdot t_f + b_w) = 1.5\ m$ Calculation of effective width of the flange

Carbon fibre geometry

The exterior timber part surrounding the CFRP-laminas on the sides (15 mm x h_cfrp) is exluded as it is assumed to have little effect on the overall behaviour.

$b_{c.cfrp} := 1.47\ m$ Assume that the CFRP is in the same level for the entire top flange (including the top of the web-beam)

$b_{t.cfrp} := 185\ mm$

$h_{cfrp} := 5\ mm$

$n_c := 1$ Number of laminations (comp) flange

$n_t := 8$ Number of laminations (tens) web

$A_{c.cfrp.i} := b_{c.cfrp} \cdot h_{cfrp} = (7.35 \cdot 10^3)\ mm^2$

$A_{t.cfrp.i} := b_{t.cfrp} \cdot h_{cfrp} = 925\ mm^2$

lever arms CFRP

$h_{reinforced} := h_w + n_t \cdot h_{cfrp} = 460\ mm$

$t_{reinforced} := t_f + n_c \cdot h_{cfrp} = 200\ mm$

$h_{tot.rf} := h_{reinforced} + t_{reinforced} = 660\ mm$

$y_c := h_{last.lamella} + \frac{h_{cfrp}}{2} \cdot n_c = 17.5\ mm$

$y_t := h_{tot.rf} - \left(h_{last.lamella} + \frac{h_{cfrp}}{2} \cdot n_t\right) = 625\ mm$

$A_{t.cfrp} := n_t \cdot A_{t.cfrp.i} = \left(7.4 \cdot 10^3\right)\ mm^2$ Area reinforcement on compression side

$A_{c.cfrp} := n_c \cdot A_{c.cfrp.i} = \left(7.35 \cdot 10^3\right)\ mm^2$ Area reinforcement on tension side

$A_{cfrp} := A_{t.cfrp} + A_{c.cfrp} = \left(1.475 \cdot 10^4\right)\ mm^2$ Total reinforcement area

Timber geometry

$A_{reinforced.w} := b_w \cdot h_{reinforced} = 0.099\ m^2$

$A_{reinforced.f} := b_{eff} \cdot t_{reinforced} = 0.3\ m^2$

$A_{reinforced} := A_{reinforced.w} + A_{reinforced.f} = 0.399\ m^2$

$\frac{A_{cfrp}}{A_{reinforced}} = 3.698\%$ Ratio reinforcement in cross section

Design Values Timber, values from DoTS volume 2

$k_{cr} := 0.67$ Reduction of shear capacity due to solar radiation and percipitation

$\gamma_{glulam} := 1.25$ Partial factor for material properties in glulam

$k_{def} := 2$ Factor considering long term effects, service class 3

$$k_h := \begin{cases} \text{if } h_w < 600\ mm: & \min\left(\left(\frac{600\ mm}{h_w}\right)^{0.1}, 1.1\right) \\ \text{else if } h_w \geq 600\ mm: & 1 \end{cases} = 1.036$$

Size factor, DoTS section 3.3 Volume 2

$k_{mod.glulam} := 0.8$ Factor considering duration of load and service class 3

$f_{md} := \frac{f_{mk} \cdot k_{mod.glulam}}{\gamma_{glulam}} = 17.92\ MPa$

$f_{cd} := \frac{f_{ck} \cdot k_{mod.glulam}}{\gamma_{glulam}} = 15.36\ MPa$

$$f_{td} := \frac{k_h \cdot f_{tk} \cdot k_{mod.glulam}}{\gamma_{glulam}} = 12.933\ MPa$$

$$f_{vd} := \frac{f_{vk} \cdot k_{mod.glulam}}{\gamma_{glulam}} = 2.24\ MPa$$

$$f_{rd} := \frac{f_{rk} \cdot k_{mod.glulam}}{\gamma_{glulam}} = 0.768\ MPa$$

$$E_{mean.fin.glulam} := \frac{E_{mean}}{1 + k_{def}} = 4.167\ GPa$$

$$E_{fin.glulam} := \frac{E_w}{1 + k_{def}} = 3.467\ GPa$$

Transformed area

$$A_{transformed} := A_{reinforced} + A_{cfrp} \cdot (\alpha - 1) = 0.915\ m^2$$

Loads

$g := 9.82\ \frac{m}{s^2}$ Gravitational constant

$g_k := \rho_w \cdot A_{timber} \cdot g + \rho_{cfrp} \cdot A_{cfrp} \cdot g = 1.811\ \frac{kN}{m}$ Self-weight

$q_k := 5\ \frac{kN}{m^2} \cdot b_{eff} = 7.5\ \frac{kN}{m}$ Distributed pedestrian load

$$M_{max} := \frac{(g_k + q_k) \cdot L^2}{8} = 465.529\ kN \cdot m$$

$q_{ULS} := 1.35 \cdot g_k + 1.5 \cdot q_k = 13.694\ \frac{kN}{m}$ Load combination according to ULS

$$M_{Ed} := \frac{q_{ULS} \cdot L^2}{8} = 684.714\ kN \cdot m$$

Resistance of cross section (plain timber)

$W_{y.w} := \frac{b_w \cdot h_w^2}{6} + \frac{b_{eff} \cdot t_f^2}{6} = 0.016\ m^3$ Oklart om det är rätt, hittar inget bra

$M_{Rd\_w} := W_{y.w} \cdot f_{md} = 283.624\ kN \cdot m$ Assume that it is braced against lateral torsional buckling. kcrit=1

Plain timber deflection

$\psi_{red} := 0.4$ Reduction of traffic load, Eurocode 1

$$\delta_{max} := \frac{L}{400} = 50\ mm$$

Maximum allowed deflection, according to Trafikverket Krav Brobyggande

$$y_{NA.plain} := \frac{A_w \cdot \left(t_f + \frac{h_w}{2}\right) + A_f \cdot \frac{t_f}{2}}{A_{timber}} = 0.17\ m$$

$$I_{plain} := \frac{b_f \cdot t_f^{\,3}}{12} + A_f \cdot \left(y_{NA.plain} - \frac{t_f}{2}\right)^2 + \frac{b_w \cdot h_w^{\,3}}{12} + A_w \cdot \left(y_{NA.plain} - t_f - \frac{h_w}{2}\right)^2 = \left(8.779 \cdot 10^9\right)\ mm^4$$

$$\delta_{plain} := \frac{5 \cdot \left(q_k \cdot \psi_{red}\right) \cdot L^4}{384 \cdot E_{mean.fin.glulam} \cdot I_{plain}} = 170.871\ mm$$

The influence of shear deformation on deflection is assumed to be small on the final deflection. Eurocode 1

Calculation of neutral axis

$$y_{NA} := \frac{A_{t.cfrp} \cdot y_t \cdot (\alpha - 1) + A_{c.cfrp} \cdot y_c \cdot (\alpha - 1) + A_{reinforced.w} \cdot \left(t_{reinforced} + \frac{h_{reinforced}}{2}\right) + A_{reinforced.f} \cdot \frac{t_{reinforced}}{2}}{A_{transformed}} = 261.054\ mm$$

if $y_{NA} < t_{reinforced}$
 "Neutral axis in the flange, NOK "
else
 "Neutral axis in the web, OK"

= "Neutral axis in the web, OK"

Resistance of cross section (CFRP reinforced)

$$\varepsilon_t := \varepsilon_{t.el.gl} = 1.875\ 10^{-3}$$

$$\varepsilon_c := \frac{\varepsilon_t \cdot y_{NA}}{h_{tot.rf} - y_{NA}} = 1.227\ 10^{-3}$$ $\varepsilon_c < \varepsilon_{c.el.gl} = 1$ ok!

$$\varepsilon_{t.cfrp} := \varepsilon_t \cdot \frac{\left(y_t - y_{NA}\right)}{h_{tot.rf} - y_{NA}} = 1.711\ 10^{-3}$$

$$\varepsilon_{c.cfrp} := \varepsilon_c \cdot \frac{\left(y_{NA} - y_c\right)}{y_{NA}} = 1.145\ 10^{-3}$$

$$F_{t.cfrp} := \varepsilon_{t.cfrp} \cdot E_{cfrp} \cdot A_{t.cfrp} = \left(5.696 \cdot 10^3\right)\ kN$$ $A_{t.cfrp} = 0.007\ m^2$

$$F_{c.cfrp} := \varepsilon_{c.cfrp} \cdot E_{cfrp} \cdot A_{c.cfrp} = \left(3.786 \cdot 10^3\right)\ kN$$ $A_{c.cfrp} = 0.007\ m^2$

Strain compatability compression

$$\varepsilon_{c.top.flange} := \frac{\left(y_{NA} - h_{last.lamella}\right) \cdot \varepsilon_c}{y_{NA}} = 1.156\ 10^{-3}$$

$$\varepsilon_{c.top.flange.mean} := \frac{\varepsilon_{c.top.flange} + \varepsilon_c}{2} = 1.192\ 10^{-3}$$

$$\varepsilon_{c.bottom.flange} := \frac{\left(y_{NA} - y_c - \frac{h_{cfrp}}{2} \cdot n_c\right) \cdot \varepsilon_c}{y_{NA}} = 1.133\ 10^{-3}$$

$$\varepsilon_{c.web} := \varepsilon_c \cdot \frac{\left(y_{NA} - t_{reinforced}\right)}{y_{NA}} = 2.869 \cdot 10^{-4}$$

$$\varepsilon_{c.bottom.flange.mean} := \frac{\varepsilon_{c.bottom.flange} + \varepsilon_{c.web}}{2} = 7.099 \cdot 10^{-4}$$

$$\varepsilon_{c.web.mean} := \frac{\varepsilon_{c.web}}{2} = 1.435 \cdot 10^{-4}$$

Strain compatability tension

$$\varepsilon_{t.edge} := \frac{\left(h_{tot.rf} - h_{last.lamella} - y_{NA}\right) \cdot \varepsilon_t}{h_{tot.rf} - y_{NA}} = 1.805\ 10^{-3}$$

$$\varepsilon_{t.edge.mean} := \frac{\varepsilon_{t.edge} + \varepsilon_t}{2} = 1.84\ 10^{-3}$$

$$\varepsilon_{t.mid} := \varepsilon_t \cdot \frac{\left(y_t - y_{NA} - \frac{h_{cfrp}}{2} \cdot n_t\right)}{h_{tot.rf} - y_{NA}} = 1.617\ 10^{-3}$$

$$\varepsilon_{t.mid.mean} := \frac{\varepsilon_{t.mid}}{2} = 8.083 \cdot 10^{-4}$$

$$F_{c.top.flange} := \varepsilon_{c.top.flange.mean} \cdot E_w \cdot \left(h_{last.lamella}\right) \cdot b_{eff} = 278.852\ kN$$

$$F_{c.bottom.flange} := \varepsilon_{c.bottom.flange.mean} \cdot E_w \cdot \left(t_{reinforced} - h_{last.lamella} - h_{cfrp} \cdot n_c\right) \cdot b_{eff} = \left(1.994 \cdot 10^3\right)\ kN$$

$$F_{c.web} := \varepsilon_{c.web.mean} \cdot E_w \cdot \left(y_{NA} - t_{reinforced}\right) \cdot b_w = 19.587\ kN$$

$$F_{t.edge} := \varepsilon_{t.edge.mean} \cdot E_w \cdot \left(h_{last.lamella}\right) \cdot b_w = 61.705\ kN$$

$$F_{t.mid} := \varepsilon_{t.mid.mean} \cdot E_w \cdot \left(y_t - y_{NA} - \frac{h_{cfrp}}{2} \cdot n_t \right) \cdot b_w = 621.597 \ kN$$

Check horizontal equilibrium

$$F_c := F_{c.top.flange} + F_{c.bottom.flange} + F_{c.cfrp} + F_{c.web} = \left(6.078 \cdot 10^3\right) \ kN \quad \text{Compression}$$

$$F_t := F_{t.mid} + F_{t.edge} + F_{t.cfrp} = \left(6.379 \cdot 10^3\right) \ kN \quad \text{Tension}$$

Moment capacity

Lever arms (distance from top)

$$z_1 := \frac{h_{last.lamella} \cdot \varepsilon_{c.top.flange} \cdot \frac{h_{last.lamella}}{2} + h_{last.lamella} \cdot \frac{\left(\varepsilon_c - \varepsilon_{c.top.flange}\right)}{2} \cdot \frac{h_{last.lamella}}{3}}{h_{last.lamella} \cdot \varepsilon_{c.top.flange} + h_{last.lamella} \cdot \frac{\left(\varepsilon_c - \varepsilon_{c.top.flange}\right)}{2}} = 7.426 \ mm$$

$$z_3 := \frac{\left(t_{reinforced} - h_{last.lamella} - h_{cfrp} \cdot n_c\right) \cdot \varepsilon_{c.bottom.flange} \cdot \left(\frac{\left(t_{reinforced} - h_{last.lamella} - h_{cfrp} \cdot n_c\right)}{2} + h_{last.lamella} + \frac{h_{cfrp}}{2} \cdot n_c \right) + \left(t_{reinforced} - h_{last.lamella} - h_{cfrp} \cdot n_c\right) \cdot \frac{\left(\varepsilon_{c.top.flange} - \varepsilon_{c.bottom.flange}\right)}{2} \cdot \left(\frac{\left(t_{reinforced} - h_{last.lamella} - h_{cfrp} \cdot n_c\right)}{3} + h_{last.lamella} + \frac{h_{cfrp}}{2} \cdot n_c \right)}{\left(t_{reinforced} - h_{last.lamella} - h_{cfrp} \cdot n_c\right) \cdot \varepsilon_{c.bottom.flange} + \left(t_{reinforced} - h_{last.lamella} - h_{cfrp} \cdot n_c\right) \cdot \frac{\left(\varepsilon_{c.top.flange} - \varepsilon_{c.bottom.flange}\right)}{2}} = 107.192 \ mm$$

$$z_4 := t_{reinforced} + \frac{1}{3} \cdot \left(y_{NA} - t_{reinforced}\right) = 220.351 \ mm$$

$$z_5 := y_{NA} + \frac{2}{3} \left(y_t - y_{NA} - \frac{h_{cfrp}}{2} \cdot n_t \right) = 490.351 \ mm$$

$$z_7 := y_t + \frac{h_{cfrp}}{2} + \frac{h_{last.lamella} \cdot \varepsilon_{t.edge} \cdot \frac{h_{last.lamella}}{2} + h_{last.lamella} \cdot \frac{\left(\varepsilon_t - \varepsilon_{t.edge}\right)}{2} \cdot \frac{2 \cdot h_{last.lamella}}{3}}{h_{last.lamella} \cdot \varepsilon_{t.edge} + h_{last.lamella} \cdot \frac{\left(\varepsilon_t - \varepsilon_{t.edge}\right)}{2}} = 635.048 \ mm$$

$$M_{Rd} := F_{c.top.flange} \cdot \left(z_7 - z_1\right) + F_{c.cfrp} \cdot \left(z_7 - y_c\right) + F_{c.bottom.flange} \cdot \left(z_7 - z_3\right) + F_{c.web} \cdot \left(z_7 - z_4\right) + F_{t.mid} \cdot \left(z_7 - z_5\right) + F_{t.cfrp} \cdot \left(z_7 - y_t\right) = \left(3.721 \cdot 10^3\right) \ kN \cdot m$$

Stiffness of cross section

$b_{fic.cfrp.c} := \alpha \cdot b_{c.cfrp} = 52.92\ m$ $\qquad$ $b_{fic.cfrp.t} := \alpha \cdot b_{t.cfrp} = 6.66\ m$

$$I_{centre.of.gravity} := \begin{bmatrix} \dfrac{b_f \cdot h_{last.lamella}^{\ 3}}{12} \\ \dfrac{b_{fic.cfrp.c} \cdot \left(h_{cfrp} \cdot n_c\right)^3}{12} \\ \dfrac{b_f \cdot \left(t_{reinforced} - h_{last.lamella} - h_{cfrp} \cdot n_c\right)^3}{12} \\ \dfrac{b_w \cdot \left(y_{NA} - t_{reinforced}\right)^3}{12} \\ \dfrac{b_w \cdot \left(y_t - y_{NA} - \dfrac{h_{cfrp}}{2} \cdot n_t\right)^3}{12} \\ \dfrac{b_{fic.cfrp.t} \cdot \left(h_{cfrp} \cdot n_t\right)^3}{12} \\ \dfrac{b_w \cdot h_{last.lamella}^{\ 3}}{12} \end{bmatrix} = \begin{bmatrix} 4.219 \cdot 10^{-7} \\ 5.513 \cdot 10^{-7} \\ 7.29 \cdot 10^{-4} \\ 4.078 \cdot 10^{-6} \\ 7.29 \cdot 10^{-4} \\ 3.552 \cdot 10^{-5} \\ 6.047 \cdot 10^{-8} \end{bmatrix} m^4$$

$$A := \begin{bmatrix} b_f \cdot h_{last.lamella} \\ b_{fic.cfrp.c} \cdot h_{cfrp} \cdot n_c \\ b_f \cdot \left(t_{reinforced} - h_{last.lamella} - h_{cfrp} \cdot n_c\right) \\ b_w \cdot \left(y_{NA} - t_{reinforced}\right) \\ b_w \cdot \left(y_t - y_{NA} - \dfrac{h_{cfrp}}{2} \cdot n_t\right) \\ b_{fic.cfrp.t} \cdot h_{cfrp} \cdot n_t \\ b_w \cdot h_{last.lamella} \end{bmatrix} = \begin{bmatrix} 0.023 \\ 0.265 \\ 0.27 \\ 0.013 \\ 0.074 \\ 0.266 \\ 0.003 \end{bmatrix} m^2$$

$$a := \begin{bmatrix} y_{NA} - \dfrac{h_{last.lamella}}{2} \\ y_{NA} - h_{last.lamella} - \dfrac{h_{cfrp}}{2} \cdot n_c \\ y_{NA} - \left(h_{last.lamella} + h_{cfrp} \cdot n_c + \dfrac{\left(t_{reinforced} - h_{last.lamella} - h_{cfrp} \cdot n_c\right)}{2}\right) \\ y_{NA} - t_{reinforced} - \dfrac{\left(y_{NA} - t_{reinforced}\right)}{2} \\ \mathrm{abs}\left(y_t - y_{NA} - \dfrac{h_{cfrp}}{2} \cdot n_t - y_{NA}\right) \\ \left(h_{tot.rf} - h_{last.lamella} - \dfrac{h_{cfrp}}{2} \cdot n_t - y_{NA}\right) - y_{NA} \\ h_{tot.rf} - \dfrac{h_{last.lamella}}{2} - y_{NA} \end{bmatrix} = \begin{bmatrix} 253.554 \\ 243.554 \\ 151.054 \\ 30.527 \\ 82.891 \\ 102.891 \\ 391.446 \end{bmatrix} mm$$

$$I := I_{centre.of.gravity} + \overrightarrow{A \cdot a^2} = \begin{bmatrix} 1.447 \\ 15.696 \\ 6.89 \\ 0.016 \\ 1.237 \\ 2.856 \\ 0.494 \end{bmatrix} 10^{-3}\ m^4$$

Application of steiners load

$$I_{tot} := \sum I = 28.636\ 10^{-3}\ m^4$$

$$EI_{tot} := E_{mean} \cdot I_{tot} = 357.954\ MN \cdot m^2$$

Transformed CFRP to equivalent timber initial stage

$$E_d I_{tot} := E_{mean.fin.glulam} \cdot I_{tot} = 119.318\ MN \cdot m^2$$

Transformed CFRP to equivalent timber final stage

Deflection of reinforced beam

$$\delta_{reinforced} := \frac{5 \cdot (\psi_{red} \cdot q_k) \cdot L^4}{384 \cdot E_d I_{tot}} = 52.381\ mm$$

Shear Capacity, section 6 DoTS volume 2

$$h_{te} := y_{NA} - t_{reinforced} = 61.054\ mm$$

$$a_{te} := \frac{h_{te}}{2} = 30.527\ mm$$

$$S_{xx} := A(0) \cdot a(0) + A(1) \cdot a(1) + A(2) \cdot a(2) + b_w \cdot h_{te} \cdot a_{te} = 111.335\ 10^{-3}\ m^3$$

$$V_{Ed} := q_{ULS} \cdot \frac{L}{2} = 136.943\ kN$$

$$\tau_{Ed} := \frac{S_{xx} \cdot V_{Ed}}{I_{tot} \cdot b_w} = 2.476\ MPa$$

$$V_{Rd} := \frac{2}{3} \cdot A_{timber} \cdot f_{vd} \cdot k_{cr} = 383.004\ kN$$

Dynamic loads

$$S := b_f \cdot L = 30\ m^2$$

Surface of the walkway

$$P := 700\ N$$

Body weight of a pedestrian

$$m_g := \frac{g_k}{g} = 184.376\ \frac{kg}{m}$$

$$M_g := \frac{L \cdot m_g}{2} = (1.844 \cdot 10^3)\ kg$$

Modal mass of the system

Traffic classes

$$TC := \begin{bmatrix} 0.2 \cdot \dfrac{1}{m^2} \\ 0.5 \cdot \dfrac{1}{m^2} \end{bmatrix} = \begin{bmatrix} 0.2 \\ 0.5 \end{bmatrix} \dfrac{1}{m^2}$$

Density of pedestrians according to traffic classes

Only calculating for traffic classes 2 and 3

$$d_{TC} := TC \cdot P = \begin{bmatrix} 0.14 \\ 0.35 \end{bmatrix} \dfrac{kN}{m^2}$$

$$m_{TC} := m_g + \dfrac{b_f \cdot d_{TC}}{g} = \begin{bmatrix} 205.761 \\ 237.838 \end{bmatrix} \dfrac{kg}{m}$$

$$f_{1.np} := \dfrac{1}{2 \cdot \pi} \cdot \dfrac{9.869}{L^2} \cdot \sqrt{\dfrac{EI_{tot}}{m_g}} = 5.471\ Hz$$

No pedestrians

$$f_{2.np} := \dfrac{1}{2 \cdot \pi} \cdot \dfrac{39.478}{L^2} \cdot \sqrt{\dfrac{EI_{tot}}{m_g}} = 21.887\ Hz$$

No pedestrians

$$f_{np} := \begin{bmatrix} f_{1.np} \\ f_{2.np} \end{bmatrix} = \begin{bmatrix} 5.471 \\ 21.887 \end{bmatrix} Hz$$

$I := 0..1$

According to Eurocode the eigenfrequency should be over 5 Hz, to avoid checks of accelerations.

```
if f_np(I) > 5 Hz
  ‖ "OK"
else
  ‖ "Check accelerations"
```

$$= \begin{bmatrix} \text{“OK”} \\ \text{“OK”} \end{bmatrix}$$

$$f_1 := \dfrac{1}{2 \cdot \pi} \cdot \dfrac{9.869}{L^2} \cdot \sqrt{\dfrac{EI_{tot}}{m_{TC}}} = \begin{bmatrix} 5.179 \\ 4.817 \end{bmatrix} Hz$$

With pedestrian masses

$$f_2 := \dfrac{1}{2 \cdot \pi} \cdot \dfrac{39.478}{L^2} \cdot \sqrt{\dfrac{EI_{tot}}{m_{TC}}} = \begin{bmatrix} 20.718 \\ 19.27 \end{bmatrix} Hz$$

With pedestrian masses

Determination of maximum acceleration

$\xi_{damping.timber} := 0.015$

1.5% according to JRC (most critical)
3% accordint to Setra

$$n'_{TC1.3} := \dfrac{10.8 \cdot \sqrt{\xi_{damping.timber} \cdot S \cdot TC(1)}}{S} = 0.171\ \dfrac{1}{m^2}$$

Table 4-8: Parameters for load model of TC1 to TC5

P [N]		
Vertical	Longitudinal	Lateral
280	140	35
Reduction coefficient ψ		

Vertical and longitudinal

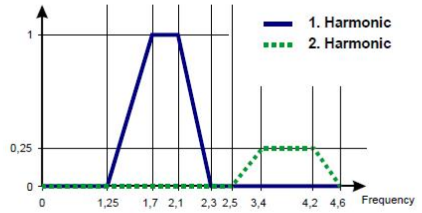

Lateral

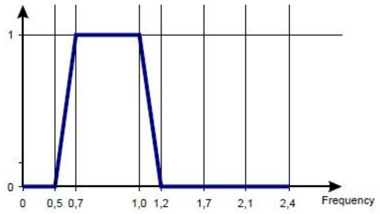

Equivalent number n' of pedestrians on the loaded surface S for load model of:		
TC1 to TC3	(density d < 1,0 P/m²):	$n' = \frac{10{,}8\sqrt{\xi \times n}}{S}$ [m⁻²]
TC4 and TC5	(density $d \geq$ 1,0 P/m²):	$n' = \frac{1{,}85\sqrt{n}}{S}$ [m⁻²]

without pedestrian masses

$$\psi_{np_l} := \begin{cases} 0 & \text{if } f_{np}(l) \le 1.25\ Hz \\ \dfrac{f_{np}(l) - 1.25\ Hz}{0.45\ Hz} & \text{else if } 1.25\ Hz < f_{np}(l) \le 1.7\ Hz \\ 1 & \text{else if } 1.7\ Hz < f_{np}(l) \le 2.1\ Hz \\ 1 - \dfrac{f_{np}(l) - 2.1\ Hz}{0.2\ Hz} & \text{else if } 2.1\ Hz < f_{np}(l) \le 2.3\ Hz \\ 0 & \text{else if } 2.3\ Hz < f_{np}(l) \le 2.5\ Hz \\ \dfrac{f_{np}(l) - 2.5\ Hz}{4 \cdot 0.9\ Hz} & \text{else if } 2.5\ Hz < f_{np}(l) \le 3.4\ Hz \\ 0.25 & \text{else if } 3.4\ Hz < f_{np}(l) \le 4.2\ Hz \\ 0.25 - \dfrac{f_{np}(l) - 4.2\ Hz}{4 \cdot 0.4\ Hz} & \text{else if } 4.2\ Hz < f_{np}(l) \le 4.6\ Hz \\ 0 & \text{else if } f_{np}(l) > 4.6\ Hz \end{cases} = \begin{bmatrix} 0 \\ 0 \end{bmatrix}$$

$i := 0..1$

$$\psi_{1_i} := \begin{array}{l} \text{if } f_1(i) \le 1.25\ Hz \\ \quad \| \ 0 \\ \text{else if } 1.25\ Hz < f_1(i) \le 1.7\ Hz \\ \quad \| \ \dfrac{f_1(i) - 1.25\ Hz}{0.45\ Hz} \\ \text{else if } 1.7\ Hz < f_1(i) \le 2.1\ Hz \\ \quad \| \ 1 \\ \text{else if } 2.1\ Hz < f_1(i) \le 2.3\ Hz \\ \quad \| \ 1 - \dfrac{f_1(i) - 2.1\ Hz}{0.2\ Hz} \\ \text{else if } 2.3\ Hz < f_1(i) \le 2.5\ Hz \\ \quad \| \ 0 \\ \text{else if } 2.5\ Hz < f_1(i) \le 3.4\ Hz \\ \quad \| \ \dfrac{f_1(i) - 2.5\ Hz}{4 \cdot 0.9\ Hz} \\ \text{else if } 3.4\ Hz < f_1(i) \le 4.2\ Hz \\ \quad \| \ 0.25 \\ \text{else if } 4.2\ Hz < f_1(i) \le 4.6\ Hz \\ \quad \| \ 0.25 - \dfrac{f_1(i) - 4.2\ Hz}{4 \cdot 0.4\ Hz} \\ \text{else if } f_1(i) > 4.6\ Hz \\ \quad \| \ 0 \end{array} = \begin{bmatrix} 0 \\ 0 \end{bmatrix}$$

$j := 0..1$

$$\psi_{2_j} := \begin{array}{l} \text{if } f_2(j) \le 1.25\ Hz \\ \quad \| \ 0 \\ \text{else if } 1.25\ Hz < f_2(j) \le 1.7\ Hz \\ \quad \| \ \dfrac{f_2(j) - 1.25\ Hz}{0.45\ Hz} \\ \text{else if } 1.7\ Hz < f_2(j) \le 2.1\ Hz \\ \quad \| \ 1 \\ \text{else if } 2.1\ Hz < f_2(j) \le 2.3\ Hz \\ \quad \| \ 1 - \dfrac{f_2(j) - 2.1\ Hz}{0.2\ Hz} \\ \text{else if } 2.3\ Hz < f_2(j) \le 2.5\ Hz \\ \quad \| \ 0 \\ \text{else if } 2.5\ Hz < f_2(j) \le 3.4\ Hz \\ \quad \| \ \dfrac{f_2(j) - 2.5\ Hz}{4 \cdot 0.9\ Hz} \\ \text{else if } 3.4\ Hz < f_2(j) \le 4.2\ Hz \\ \quad \| \ 0.25 \\ \text{else if } 4.2\ Hz < f_2(j) \le 4.6\ Hz \\ \quad \| \ 0.25 - \dfrac{f_2(j) - 4.2\ Hz}{4 \cdot 0.4\ Hz} \\ \text{else if } f_2(j) > 4.6\ Hz \\ \quad \| \ 0 \end{array} = \begin{bmatrix} 0 \\ 0 \end{bmatrix}$$

$P_v := 280\ N$

$$q_{1.TC1.3} := b_f \cdot P_v \cdot n'_{TC1.3} \cdot \psi_1 = \begin{bmatrix} 0 \\ 0 \end{bmatrix} \frac{kg}{s^2}$$

$$q_{2.TC1.3} := b_f \cdot P_v \cdot n'_{TC1.3} \cdot \psi_2 = \begin{bmatrix} 0 \\ 0 \end{bmatrix} \frac{kg}{s^2}$$

$$q_{np.TC1.3} := b_f \cdot P_v \cdot n'_{TC1.3} \cdot \psi_{np} = \begin{bmatrix} 0 \\ 0 \end{bmatrix} \frac{kg}{s^2}$$

$$a_{1.TC1.3} := \frac{1}{2 \cdot \xi_{damping.timber}} \cdot \frac{4 \cdot q_{1.TC1.3}}{\pi \cdot m_{TC}} = \begin{bmatrix} 0 \\ 0 \end{bmatrix} \frac{m}{s^2}$$

$$a_{2.TC1.3} := \frac{1}{2 \cdot \xi_{damping.timber}} \cdot \frac{4 \cdot q_{2.TC1.3}}{\pi \cdot m_{TC}} = \begin{bmatrix} 0 \\ 0 \end{bmatrix} \frac{m}{s^2}$$

$$a_{np.TC1.3} := \frac{1}{2 \cdot \xi_{damping.timber}} \cdot \frac{4 \cdot q_{np.TC1.3}}{\pi \cdot m_g} = \begin{bmatrix} 0 \\ 0 \end{bmatrix} \frac{m}{s^2}$$

$$\text{if } a_{1.TC1.3}(j) \le 0.75\ \frac{m}{s^2} \;\; \| \text{“OK”} \;\; \text{else} \;\; \| \text{“Not OK”} = \begin{bmatrix} \text{“OK”} \\ \text{“OK”} \end{bmatrix}$$

The limit for acccelerations is chosen to 0.75 m/s^2 to be acceptable.

$$\text{if } a_{2.TC1.3}(j) \le 0.75\ \frac{m}{s^2} \;\; \| \text{“OK”} \;\; \text{else} \;\; \| \text{“Not OK”} = \begin{bmatrix} \text{“OK”} \\ \text{“OK”} \end{bmatrix}$$

$$\text{if } a_{np.TC1.3}(l) \le 0.75\ \frac{m}{s^2} \;\; \| \text{“OK”} \;\; \text{else} \;\; \| \text{“Not OK”} = \begin{bmatrix} \text{“OK”} \\ \text{“OK”} \end{bmatrix}$$

Comparison between plain and reinforced cross-section

$$\frac{M_{Ed}}{M_{Rd\_w}} = 241.416\%$$

$$\frac{\delta_{plain}}{\delta_{max}} = 341.742\%$$

$$f_{1.np} = 5.471\ Hz$$

$$M_{Rd} = 3.721\ MN \cdot m$$

$$\frac{M_{Ed}}{M_{Rd}} = 18.403\%$$

$$\frac{\delta_{reinforced}}{\delta_{max}} = 104.762\%$$

$$\delta_{reinforced} = 52.381\ mm$$

$$\frac{V_{Ed}}{V_{Rd}} = 35.755\%$$

C

Mathcad Stress-laminated Deck

Calculation of cross-sectional capacity of CFRP reinforced Stress-laminated plate. The pretensioning force is assumed to be sufficient for full interaction between the beams.

Material properties

Service class 3, according to swedish standards

Characterisic values Timber(GL28c, DoTS Volume 2 Table 3.4)

$f_{mk} := 28\ MPa$

$f_{ck} := 24\ MPa$

$f_{tk} := 19.5\ MPa$

$f_{c.90.k} := 2.5\ MPa$

$f_{vk} := 3.5\ MPa$

$f_{rk} := 1.2\ MPa$

$\rho_w := 420\ \frac{kg}{m^3}$ Mean density

$E_w := 10.4\ GPa$

$E_{mean} := 12.5\ GPa$

$\varepsilon_{c.el.gl} := \frac{f_{ck}}{E_w} = 2.308\ 10^{-3}$

$\varepsilon_{t.el.gl} := \frac{f_{tk}}{E_w} = 1.875\ 10^{-3}$

CFRP properties (S&P C laminat, product sheet)

$f_{t.cfrp} := 2800\ MPa$ Tensile strength

$f_{c.cfrp} := 1400\ MPa$ Compressive strength Assumption of half

$\rho_{cfrp} := 1600\ \frac{kg}{m^3}$ Density

$\gamma_{cfrp} := 1.0$ assuming certified manufacturer

$E_{cfrp} := 300\ GPa$

low = 205
mid = 300
high = 375
ultrahigh = 450

$\alpha := \frac{E_{cfrp}}{E_{mean}} = 24$

CFRP Properties (Fiberline, Product Sheet)

$f_{t.cfrp.fiberline} := 1640\ MPa$ Tensile strength

$f_{c.cfrp.fiberline} := 890\ MPa$ Compressive strength

$f_{m.cfrp.fiberline} := 900\ MPa$ Flexural strength

$f_{tt.cfrp.fiberline} := 18\ MPa$ Tensile transverse strength

$f_{ils.cfrp.fiberline} := 52\ MPa$ Inter laminar shear strength

$\rho_{cfrp.fiberline} := 1550\ \frac{kg}{m^3}$ Density

Plate geometry

$L := 20\ m$

$h_{lamella} := 45\ mm$ Thickness of lamellas

$h_{last.lamella} := 15\ mm$ Thickness of sacrificial lamella

$n_{laminations} := 17$ Number of laminations

$h_{plain} := \left(n_{laminations} - 2\right) \cdot h_{lamella} + 2 \cdot h_{last.lamella} = 705\ mm$

$b := 3\ m$ Assumed width of the bridge

$A_w := b \cdot h_{plain} = 2.115\ m^2$

Carbon fibre geometry

The exterior timber part surrounding the CFRP-laminas on the sides (15 mm x h_cfrp) is exluded as it is assumed to have little effect on the overall behaviour.

$b_{cfrp} := 2.58\ m$ CFRP through the entire width

$h_{cfrp} := 3\ mm$

$A_{i.cfrp} := b_{cfrp} \cdot h_{cfrp} = 0.008\ m^2$

$n_c := 1$ Number of laminations (comp)

$n_t := 1$ Number of laminations (tens)

lever arms CFRP

$h_{reinforced} := h_{plain} + \left(n_c + n_t\right) \cdot h_{cfrp} = 711\ mm$ Reinforced height

$y_c := h_{last.lamella} + \frac{h_{cfrp}}{2} \cdot n_c = 16.5\ mm$ Compression lever arm

$y_t := h_{reinforced} - \left(h_{last.lamella} + \frac{h_{cfrp}}{2} \cdot n_t\right) = 694.5\ mm$ Tension lever arm

$A_{t.cfrp} := n_t \cdot A_{i.cfrp} = \left(7.74 \cdot 10^3\right)\ mm^2$ Area reinforcement on compression side

$A_{c.cfrp} := n_c \cdot A_{i.cfrp} = \left(7.74 \cdot 10^3\right)\ mm^2$ Area reinforcement on tension side

$A_{cfrp} := A_{t.cfrp} + A_{c.cfrp} = \left(1.548 \cdot 10^4\right)\ mm^2$ Total reinforcement area

Timber geometry

$$A_{reinforced} := b \cdot h_{reinforced} = 2.133\ m^2$$

$$\frac{A_{cfrp}}{A_{reinforced}} = 0.726\%$$

Ratio reinforcement in cross section

Design Values Timber, values from DoTS volume 2

$$k_{cr} := 0.67$$

Reduction of shear capacity due to solar radiation and percipitation

$$\gamma_{glulam} := 1.25$$

Partial factor for material properties in glulam

$$k_{def} := 2$$

Factor considering long term effects, service class 3

$$k_h := \begin{cases} \text{if } h_{plain} < 600\ mm \\ \quad \min\left(\left(\frac{600\ mm}{h_{plain}}\right)^{0.1}, 1.1\right) \\ \text{else if } h_{plain} \geq 600\ mm \\ \quad 1 \end{cases} = 1$$

Size factor, section 3.3 DoTS Volume 2

$$k_{mod.glulam} := 0.8$$

Factor considering duration of load and service class 3

$$k_{c.90} := 1$$

Support condition factor, according to section 5.2 DoTS

$$f_{md} := \frac{k_h \cdot f_{mk} \cdot k_{mod.glulam}}{\gamma_{glulam}} = 17.92\ MPa$$

$$f_{cd} := \frac{f_{ck} \cdot k_{mod.glulam}}{\gamma_{glulam}} = 15.36\ MPa$$

$$f_{c.90.d} := \frac{k_{c.90} \cdot k_{mod.glulam} \cdot f_{c.90.k}}{\gamma_{glulam}} = 1.6\ MPa$$

$$f_{td} := \frac{k_h \cdot f_{tk} \cdot k_{mod.glulam}}{\gamma_{glulam}} = 12.48\ MPa$$

$$f_{vd} := \frac{f_{vk} \cdot k_{mod.glulam}}{\gamma_{glulam}} = 2.24\ MPa$$

$$f_{rd} := \frac{f_{rk} \cdot k_{mod.glulam}}{\gamma_{glulam}} = 0.768\ MPa$$

$$E_{mean.fin.glulam} := \frac{E_{mean}}{1 + k_{def}} = 4.167\ GPa$$

$$E_{fin.glulam} := \frac{E_w}{1 + k_{def}} = 3.467\ GPa$$

Transformed area

$$A_{transformed} := A_{reinforced} + A_{cfrp} \cdot (\alpha - 1) = 2.489\ m^2$$

Loads

Service vehicle

$$Q_1 := \frac{80}{2}\ kN = 40\ kN$$

$$Q_2 := \frac{40}{2}\ kN = 20\ kN$$

$$b_{axel} := 1.3\ m$$

$$s_{axel} := 3\ m$$

$$A_{wheel} := 0.2 \cdot 0.2\ m^2 = 0.04\ m^2$$

$$a_1 := 6.7\ m$$

$$a_2 := a_1 - s_{axel} = 3.7\ m$$

$$a_{sv} := \frac{L}{2} - 3\ m = 7\ m$$

$$b_{sv} := L - a_{sv} = 13\ m$$

Self-weights

$$g := 9.82\ \frac{m}{s^2}$$ Gravitational constant

$$g_{railing} := 0.5\ \frac{kN}{m}$$ Added weight of railings

$$g_{prestressing} := 0.5\ \frac{kN}{m}$$ Added weight of prestressing bars

$$g_{walkway} := 0.8\ \frac{kN}{m^2} \cdot b = 2.4\ \frac{kN}{m}$$ Added weight of walkway cover (asphalt)

$$g_k := \rho_w \cdot A_w \cdot g + \rho_{cfrp} \cdot A_{cfrp} \cdot g + 2 \cdot g_{railing} + g_{prestressing} + g_{walkway} = 12.866\ \frac{kN}{m}$$

$$q_k := 5\ \frac{kN}{m^2} \cdot b = 15\ \frac{kN}{m}$$ Distributed load from pedestrians

Design load

$$M_{max} := \frac{(g_k + q_k) \cdot L^2}{8} + \frac{Q_1 \cdot L}{4} + \frac{Q_2 \cdot a_{sv} \cdot b_{sv}}{L} = 1.684\ MN \cdot m$$

$$q_{ULS} := 1.35 \cdot g_k + 1.5 \cdot q_k = 39.87\ \frac{kN}{m}$$

Load combination according to ULS

$$M_{Ed} := \frac{q_{ULS} \cdot L^2}{8} + \frac{Q_1 \cdot L}{4} + \frac{Q_2 \cdot a_{sv} \cdot b_{sv}}{L} = 2.284\ MN \cdot m$$

Resistance of cross section (unreinforced plate)

$$W_{y.w} := \frac{b \cdot h_{plain}^{\ 2}}{6} = 0.249\ m^3$$

$$F_t := \varepsilon_{t.el.gl} \cdot E_w \cdot \frac{b \cdot h_{plain}}{4} = \left(1.031 \cdot 10^4\right)\ kN$$

$$M_{Rd\_w} := W_{y.w} \cdot f_{md} = 4.4533\ MN \cdot m$$

$$M := F_t \cdot \frac{2}{3} \cdot h_{plain} = 4.846\ MN \cdot m$$

Plain plate deflection

$$\delta_{max} := \frac{L}{400} = 50\ mm$$

Maximum allowed deflection, according to Trafikverket Krav Brobyggande

$$\psi_{red} := 0.4$$

Reduction of traffic load, Eurocode 1

The deflections are split not effecting each other, according to Table 5.1 Eurocode 1

$$\delta_{plain} := \frac{5 \cdot \left(q_k \cdot \psi_{red}\right) \cdot L^4}{384 \cdot E_{mean.fin.glulam} \cdot \frac{b \cdot \left(h_{plain}\right)^3}{12}} = 34.246\ mm$$

The influence of shear deformation on deflection is assumed to be small on the final deflection. Eurocode 1

$$\delta_{plain.service} := \psi_{red} \cdot Q_1 \cdot \frac{a_1 \cdot L^2}{48 \cdot E_{mean} \cdot \frac{b \cdot \left(h_{plain}\right)^3}{12}} \cdot \left(3 - \frac{4 \cdot a_1^{\ 2}}{L^2}\right) + \psi_{red} \cdot Q_2 \cdot \frac{a_2 \cdot L^2}{48 \cdot E_{mean} \cdot \frac{b \cdot \left(h_{plain}\right)^3}{12}} \cdot \left(3 - \frac{4 \cdot a_2^{\ 2}}{L^2}\right) = 2.726\ mm$$

Calculation of neutral axis

$$y_{NA} := \frac{A_{t.cfrp} \cdot y_t \cdot (\alpha - 1) + A_{c.cfrp} \cdot y_c \cdot (\alpha - 1) + A_{reinforced} \cdot \frac{h_{reinforced}}{2}}{A_{transformed}} = 355.5\ mm$$

Stiffness of cross section

$b_{fic.cfrp} := \alpha \cdot b_{cfrp} = 61.92\ m$ equivalent transformed length

$$I_{centre.of.gravity} := \begin{bmatrix} \dfrac{b \cdot h_{last.lamella}^{3}}{12} \\ \dfrac{b_{fic.cfrp} \cdot \left(h_{cfrp} \cdot n_c\right)^{3}}{12} \\ \dfrac{b \cdot \left(h_{reinforced} - 2 \cdot h_{last.lamella} - h_{cfrp} \cdot n_c - h_{cfrp} \cdot n_t\right)^{3}}{12} \\ \dfrac{b_{fic.cfrp} \cdot \left(h_{cfrp} \cdot n_t\right)^{3}}{12} \\ \dfrac{b \cdot h_{last.lamella}^{3}}{12} \end{bmatrix} = \begin{bmatrix} 8.438 \cdot 10^{-7} \\ 1.393 \cdot 10^{-7} \\ 0.077 \\ 1.393 \cdot 10^{-7} \\ 8.438 \cdot 10^{-7} \end{bmatrix} m^{4}$$

$$A := \begin{bmatrix} b \cdot h_{last.lamella} \\ b_{fic.cfrp} \cdot h_{cfrp} \cdot n_c \\ b \cdot \left(h_{reinforced} - 2 \cdot h_{last.lamella} - h_{cfrp} \cdot n_c - h_{cfrp} \cdot n_t\right) \\ b_{fic.cfrp} \cdot h_{cfrp} \cdot n_t \\ b \cdot h_{last.lamella} \end{bmatrix} = \begin{bmatrix} 0.045 \\ 0.186 \\ 2.025 \\ 0.186 \\ 0.045 \end{bmatrix} m^{2}$$

$$a := \begin{bmatrix} y_{NA} - \dfrac{h_{last.lamella}}{2} \\ y_{NA} - h_{last.lamella} - \dfrac{h_{cfrp}}{2} \cdot n_c \\ \mathrm{abs}\left(\dfrac{h_{reinforced}}{2} - y_{NA}\right) \\ h_{reinforced} - h_{last.lamella} - \dfrac{h_{cfrp}}{2} \cdot n_t - y_{NA} \\ h_{reinforced} - \dfrac{h_{last.lamella}}{2} - y_{NA} \end{bmatrix} = \begin{bmatrix} 348 \\ 339 \\ 0 \\ 339 \\ 348 \end{bmatrix} mm$$

$$I := I_{centre.of.gravity} + \overrightarrow{A \cdot a^{2}} = \begin{bmatrix} 5.451 \\ 21.348 \\ 76.887 \\ 21.348 \\ 5.451 \end{bmatrix} 10^{-3}\ m^{4}$$

$$I_{tot} := \sum I = 130.483\ 10^{-3}\ m^{4}$$

$EI_{tot} := E_{mean} \cdot I_{tot} = \left(1.631 \cdot 10^3\right)\ MN \cdot m^2$ Transformed CFRP to equivalent timber initial stage

$E_d I_{tot} := E_{mean.fin.glulam} \cdot I_{tot} = 543.681\ MN \cdot m^2$ Transformed CFRP to equivalent timber final stage

Resistance of cross section (CFRP reinforced)

$\varepsilon_t := \varepsilon_{t.el.gl} = 1.875\ 10^{-3}$

$$\varepsilon_c := \frac{\varepsilon_t \cdot y_{NA}}{h_{reinforced} - y_{NA}} = 1.875\ 10^{-3} \qquad \varepsilon_c < \varepsilon_{c.el.gl} = 1 \qquad \text{ok!}$$

$$\varepsilon_{t.cfrp} := \varepsilon_t \cdot \frac{\left(y_t - y_{NA}\right)}{h_{reinforced} - y_{NA}} = 1.788\ 10^{-3}$$

$$\varepsilon_{c.cfrp} := \varepsilon_c \cdot \frac{\left(y_{NA} - y_c\right)}{y_{NA}} = 1.788\ 10^{-3}$$

$$F_{t.cfrp} := \varepsilon_{t.cfrp} \cdot E_{cfrp} \cdot A_{t.cfrp} = \left(4.152 \cdot 10^3\right)\ kN$$

$$F_{c.cfrp} := \varepsilon_{c.cfrp} \cdot E_{cfrp} \cdot A_{c.cfrp} = \left(4.152 \cdot 10^3\right)\ kN$$

Strain compatability compression

$$\varepsilon_{c.edge} := \frac{\left(y_{NA} - h_{last.lamella}\right) \cdot \varepsilon_c}{y_{NA}} = 1.796\ 10^{-3}$$

$$\varepsilon_{c.edge.mean} := \frac{\varepsilon_{c.edge} + \varepsilon_c}{2} = 1.835\ 10^{-3}$$

$$\varepsilon_{c.mid} := \frac{\left(y_{NA} - y_c - \frac{h_{cfrp}}{2} \cdot n_c\right) \cdot \varepsilon_c}{y_{NA}} = 1.78\ 10^{-3}$$

$$\varepsilon_{c.mid.mean} := \frac{\varepsilon_{c.mid}}{2} = 8.9 \cdot 10^{-4}$$

Strain compatability tension

$$\varepsilon_{t.edge} := \frac{\left(h_{reinforced} - h_{last.lamella} - y_{NA}\right) \cdot \varepsilon_t}{h_{reinforced} - y_{NA}} = 1.796\ 10^{-3}$$

$$\varepsilon_{t.edge.mean} := \frac{\varepsilon_{t.edge} + \varepsilon_t}{2} = 1.835\ 10^{-3}$$

$$\varepsilon_{t.mid} := \varepsilon_t \cdot \frac{\left(y_t - y_{NA} - \frac{h_{cfrp}}{2} \cdot n_t\right)}{h_{reinforced} - y_{NA}} = 1.78\ 10^{-3}$$

$$\varepsilon_{t.mid.mean} := \frac{\varepsilon_{t.mid}}{2} = 8.9 \cdot 10^{-4}$$

$$F_{c.edge} := \varepsilon_{c.edge.mean} \cdot E_w \cdot \left(h_{last.lamella}\right) \cdot b = 858.987 \ kN$$

$$F_{c.mid} := \varepsilon_{c.mid.mean} \cdot E_w \cdot \left(y_{NA} - y_c - \frac{h_{cfrp}}{2} \cdot n_c\right) \cdot b = \left(9.372 \cdot 10^3\right) \ kN$$

$$F_{t.edge} := \varepsilon_{t.edge.mean} \cdot E_w \cdot \left(h_{last.lamella}\right) \cdot b = 858.987 \ kN$$

$$F_{t.mid} := \varepsilon_{t.mid.mean} \cdot E_w \cdot \left(y_t - y_{NA} - \frac{h_{cfrp}}{2} \cdot n_t\right) \cdot b = \left(9.372 \cdot 10^3\right) \ kN$$

Check horizontal equilibrium

$F_{c.edge} + F_{c.mid} + F_{c.cfrp} = 14.383 \ MN$ Compression

$F_{t.mid} + F_{t.edge} + F_{t.cfrp} = 14.383 \ MN$ Tension

Moment capacity

Lever arms (distance from top)

$$z_1 := \frac{h_{last.lamella} \cdot \varepsilon_{c.edge} \cdot \frac{h_{last.lamella}}{2} + h_{last.lamella} \cdot \frac{\left(\varepsilon_c - \varepsilon_{c.edge}\right)}{2} \cdot \frac{h_{last.lamella}}{3}}{h_{last.lamella} \cdot \varepsilon_{c.edge} + h_{last.lamella} \cdot \frac{\left(\varepsilon_c - \varepsilon_{c.edge}\right)}{2}} = 7.446 \ mm$$

$$z_3 := y_c + \frac{h_{cfrp}}{2} + \frac{1}{3} \cdot \left(y_{NA} - \left(y_c + \frac{h_{cfrp}}{2} \cdot n_c\right)\right) = 130.5 \ mm$$

$$z_4 := y_{NA} + \frac{2}{3} \left(y_t - y_{NA} - \frac{h_{cfrp}}{2} \cdot n_t\right) = 580.5 \ mm$$

$$z_6 := y_t + \frac{h_{cfrp}}{2} + \frac{h_{last.lamella} \cdot \varepsilon_{t.edge} \cdot \frac{h_{last.lamella}}{2} + h_{last.lamella} \cdot \frac{\left(\varepsilon_t - \varepsilon_{t.edge}\right)}{2} \cdot \frac{2 \cdot h_{last.lamella}}{3}}{h_{last.lamella} \cdot \varepsilon_{t.edge} + h_{last.lamella} \cdot \frac{\left(\varepsilon_t - \varepsilon_{t.edge}\right)}{2}} = 703.554 \ mm$$

$$M_{Rd} := F_{c.edge} \cdot \left(z_6 - z_1\right) + F_{c.cfrp} \cdot \left(z_6 - y_c\right) + F_{c.mid} \cdot \left(z_6 - z_3\right) + F_{t.mid} \cdot \left(z_6 - z_4\right) + F_{t.cfrp} \cdot \left(z_6 - y_t\right) = 10.012 \ MN \cdot m$$

Deflection of reinforced beam

$$\delta_{reinforced} := \frac{5 \cdot (\psi_{red} \cdot q_k) \cdot L^4}{384 \cdot E_d I_{tot}} = 22.991 \ mm$$

$$\delta_{reinforced.service} := \psi_{red} \cdot Q_1 \cdot \frac{a_1 \cdot L^2}{48 \cdot E_d I_{tot}} \cdot \left(3 - \frac{4 \cdot a_1^2}{L^2}\right) + \psi_{red} \cdot Q_2 \cdot \frac{a_2 \cdot L^2}{48 \cdot E_d I_{tot}} \cdot \left(3 - \frac{4 \cdot a_2^2}{L^2}\right) = 5.491 \ mm$$

Shear Capacity, section 6 DoTS volume 2

$$h_{te} := y_{NA} - h_{last.lamella} - h_{cfrp} \cdot n_c = 337.5 \ mm$$

$$a_{te} := \frac{h_{te}}{2} = 168.75 \ mm$$

$$S_{xx} := A(0) \cdot a(0) + A(1) \cdot a(1) + b \cdot h_{te} \cdot a_{te} = 249.492 \ 10^{-3} \ m^3$$

$$V_{Ed} := q_{ULS} \cdot \frac{L}{2} + Q_1 + \frac{Q_2 \cdot s_{axel}}{L} = 441.695 \ kN$$

$$\tau_{Ed} := \frac{S_{xx} \cdot V_{Ed}}{I_{tot} \cdot b} = 0.282 \ MPa$$

Dynamic loads

Eigenfrequencies and accelerations are only calculated in vertical direction, lateral direction has been neglected due to the high amount of available stiffness in that direction.

$S := b \cdot L = 60 \ m^2$ — Surface of the walkway

$P := 700 \ N$ — Body weight of a pedestrian

$$m_g := \frac{g_k}{g} = (1.31 \cdot 10^3) \ \frac{kg}{m}$$

$$M_g := \frac{L \cdot m_g}{2} = (1.31 \cdot 10^4) \ kg$$

Modal mass of the system

Traffic classes

$$TC := \begin{bmatrix} 0.2 \cdot \frac{1}{m^2} \\ 0.5 \cdot \frac{1}{m^2} \end{bmatrix} = \begin{bmatrix} 0.2 \\ 0.5 \end{bmatrix} \frac{1}{m^2}$$

Density of pedestrians according to traffic classes

Only calculating for traffic classes 2 and 3

$$d_{TC} := TC \cdot P = \begin{bmatrix} 0.14 \\ 0.35 \end{bmatrix} \frac{kN}{m^2}$$

$$m_{TC} := m_g + \frac{b \cdot d_{TC}}{g} = \begin{bmatrix} 1.353 \cdot 10^3 \\ 1.417 \cdot 10^3 \end{bmatrix} \frac{kg}{m}$$

$$f_{1.np} := \frac{1}{2 \cdot \pi} \cdot \frac{9.869}{L^2} \cdot \sqrt{\frac{EI_{tot}}{m_g}} = 4.381\ Hz$$

No pedestrians

$$f_{2.np} := \frac{1}{2 \cdot \pi} \cdot \frac{39.478}{L^2} \cdot \sqrt{\frac{EI_{tot}}{m_g}} = 17.526\ Hz$$

No pedestrians

$$f_{np} := \begin{bmatrix} f_{1.np} \\ f_{2.np} \end{bmatrix} = \begin{bmatrix} 4.381 \\ 17.526 \end{bmatrix} Hz$$

$$l := 0..1$$

$$\begin{array}{l} \text{if } f_{np}(l) > 5\ Hz \\ \quad \| \text{"OK"} \\ \text{else} \\ \quad \| \text{"Check accelerations"} \end{array} = \begin{bmatrix} \text{"Check accelerations"} \\ \text{"OK"} \end{bmatrix}$$

According to Eurocode the eigenfrequency should be over 5 Hz, to avoid checks of accelerations.

$$f_1 := \frac{1}{2 \cdot \pi} \cdot \frac{9.869}{L^2} \cdot \sqrt{\frac{EI_{tot}}{m_{TC}}} = \begin{bmatrix} 4.311 \\ 4.213 \end{bmatrix} Hz$$

With pedestrian masses

$$f_2 := \frac{1}{2 \cdot \pi} \cdot \frac{39.478}{L^2} \cdot \sqrt{\frac{EI_{tot}}{m_{TC}}} = \begin{bmatrix} 17.247 \\ 16.852 \end{bmatrix} Hz$$

With pedestrian masses

Determination of maximum acceleration

$$\xi_{damping.timber} := 0.015$$

1.5% according to JRC (most critical)
3% accordint to Setra

$$n'_{TC1.3} := \frac{10.8 \cdot \sqrt{\xi_{damping.timber} \cdot S \cdot TC(1)}}{S} = 0.121\ \frac{1}{m^2}$$

Table 4-8: Parameters for load model of TC1 to TC5

P [N]		
Vertical	Longitudinal	Lateral
280	140	35
Reduction coefficient ψ		
Vertical and longitudinal 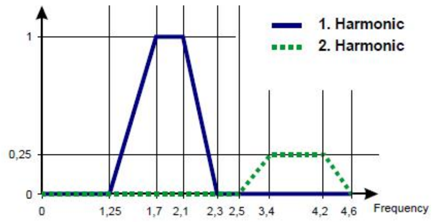		Lateral 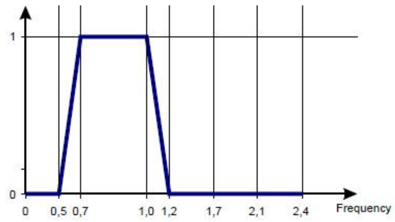
Equivalent number n' of pedestrians on the loaded surface S for load model of:		
TC1 to TC3 (density d < 1,0 P/m²):	$n' = \frac{10.8\sqrt{\xi \times n}}{S}$ [m⁻²]	
TC4 and TC5 (density $d \geq$ 1,0 P/m²):	$n' = \frac{1.85\sqrt{n}}{S}$ [m⁻²]	

Without pedestrian masses

$$\psi_{np_l} := \begin{cases} 0 & \text{if } f_{np}(l) \leq 1.25\ Hz \\ \dfrac{f_{np}(l) - 1.25\ Hz}{0.45\ Hz} & \text{else if } 1.25\ Hz < f_{np}(l) \leq 1.7\ Hz \\ 1 & \text{else if } 1.7\ Hz < f_{np}(l) \leq 2.1\ Hz \\ 1 - \dfrac{f_{np}(l) - 2.1\ Hz}{0.2\ Hz} & \text{else if } 2.1\ Hz < f_{np}(l) \leq 2.3\ Hz \\ 0 & \text{else if } 2.3\ Hz < f_{np}(l) \leq 2.5\ Hz \\ \dfrac{f_{np}(l) - 2.5\ Hz}{4 \cdot 0.9\ Hz} & \text{else if } 2.5\ Hz < f_{np}(l) \leq 3.4\ Hz \\ 0.25 & \text{else if } 3.4\ Hz < f_{np}(l) \leq 4.2\ Hz \\ 0.25 - \dfrac{f_{np}(l) - 4.2\ Hz}{4 \cdot 0.4\ Hz} & \text{else if } 4.2\ Hz < f_{np}(l) \leq 4.6\ Hz \\ 0 & \text{else if } f_{np}(l) > 4.6\ Hz \end{cases} = \begin{bmatrix} 0.137 \\ 0 \end{bmatrix}$$

$$i := 0..1$$

$$\psi_{1_i} := \begin{cases} 0 & \text{if } f_1(i) \le 1.25\ Hz \\ \dfrac{f_1(i) - 1.25\ Hz}{0.45\ Hz} & \text{else if } 1.25\ Hz < f_1(i) \le 1.7\ Hz \\ 1 & \text{else if } 1.7\ Hz < f_1(i) \le 2.1\ Hz \\ 1 - \dfrac{f_1(i) - 2.1\ Hz}{0.2\ Hz} & \text{else if } 2.1\ Hz < f_1(i) \le 2.3\ Hz \\ 0 & \text{else if } 2.3\ Hz < f_1(i) \le 2.5\ Hz \\ \dfrac{f_1(i) - 2.5\ Hz}{4 \cdot 0.9\ Hz} & \text{else if } 2.5\ Hz < f_1(i) \le 3.4\ Hz \\ 0.25 & \text{else if } 3.4\ Hz < f_1(i) \le 4.2\ Hz \\ 0.25 - \dfrac{f_1(i) - 4.2\ Hz}{4 \cdot 0.4\ Hz} & \text{else if } 4.2\ Hz < f_1(i) \le 4.6\ Hz \\ 0 & \text{else if } f_1(i) > 4.6\ Hz \end{cases} = \begin{bmatrix} 0.18 \\ 0.242 \end{bmatrix}$$

$j := 0..1$

$$\psi_{2_j} := \begin{array}{l} \text{if } f_2(j) \le 1.25\ Hz \\ \quad \| \ 0 \\ \text{else if } 1.25\ Hz < f_2(j) \le 1.7\ Hz \\ \quad \| \ \dfrac{f_2(j) - 1.25\ Hz}{0.45\ Hz} \\ \text{else if } 1.7\ Hz < f_2(j) \le 2.1\ Hz \\ \quad \| \ 1 \\ \text{else if } 2.1\ Hz < f_2(j) \le 2.3\ Hz \\ \quad \| \ 1 - \dfrac{f_2(j) - 2.1\ Hz}{0.2\ Hz} \\ \text{else if } 2.3\ Hz < f_2(j) \le 2.5\ Hz \\ \quad \| \ 0 \\ \text{else if } 2.5\ Hz < f_2(j) \le 3.4\ Hz \\ \quad \| \ \dfrac{f_2(j) - 2.5\ Hz}{4 \cdot 0.9\ Hz} \\ \text{else if } 3.4\ Hz < f_2(j) \le 4.2\ Hz \\ \quad \| \ 0.25 \\ \text{else if } 4.2\ Hz < f_2(j) \le 4.6\ Hz \\ \quad \| \ 0.25 - \dfrac{f_2(j) - 4.2\ Hz}{4 \cdot 0.4\ Hz} \\ \text{else if } f_2(j) > 4.6\ Hz \\ \quad \| \ 0 \end{array} = \begin{bmatrix} 0 \\ 0 \end{bmatrix}$$

$P_v := 280\ N$

$$q_{1.TC1.3} := b \cdot P_v \cdot n'_{TC1.3} \cdot \psi_1 = \begin{bmatrix} 18.294 \\ 24.553 \end{bmatrix} \frac{kg}{s^2}$$

$$q_{2.TC1.3} := b \cdot P_v \cdot n'_{TC1.3} \cdot \psi_2 = \begin{bmatrix} 0 \\ 0 \end{bmatrix} \frac{kg}{s^2}$$

$$q_{np.TC1.3} := b \cdot P_v \cdot n'_{TC1.3} \cdot \psi_{np} = \begin{bmatrix} 13.869 \\ 0 \end{bmatrix} \frac{kg}{s^2}$$

$$a_{1.TC1.3} := \frac{1}{2 \cdot \xi_{damping.timber}} \cdot \frac{4 \cdot q_{1.TC1.3}}{\pi \cdot m_{TC}} = \begin{bmatrix} 0.574 \\ 0.735 \end{bmatrix} \frac{m}{s^2}$$

$$a_{2.TC1.3} := \frac{1}{2 \cdot \xi_{damping.timber}} \cdot \frac{4 \cdot q_{2.TC1.3}}{\pi \cdot m_{TC}} = \begin{bmatrix} 0 \\ 0 \end{bmatrix} \frac{m}{s^2}$$

$$a_{np.TC1.3} := \frac{1}{2 \cdot \xi_{damping.timber}} \cdot \frac{4 \cdot q_{np.TC1.3}}{\pi \cdot m_g} = \begin{bmatrix} 0.449 \\ 0 \end{bmatrix} \frac{m}{s^2}$$

$$\text{if } a_{1.TC1.3}(j) \le 0.75\ \frac{m}{s^2} \;\Vert\; \text{“OK”} \quad \text{else} \;\Vert\; \text{“Not OK”} = \begin{bmatrix} \text{“OK”} \\ \text{“OK”} \end{bmatrix}$$

The limit for acccelerations is chosen to 0.75 m/s^2 to be acceptable.

$$\text{if } a_{2.TC1.3}(j) \le 0.75\ \frac{m}{s^2} \;\Vert\; \text{“OK”} \quad \text{else} \;\Vert\; \text{“Not OK”} = \begin{bmatrix} \text{“OK”} \\ \text{“OK”} \end{bmatrix}$$

$$\text{if } a_{np.TC1.3}(l) \le 0.75\ \frac{m}{s^2} \;\Vert\; \text{“OK”} \quad \text{else} \;\Vert\; \text{“Not OK”} = \begin{bmatrix} \text{“OK”} \\ \text{“OK”} \end{bmatrix}$$

Calculate necessary pre-stressing force for stress-laminated deck.

$b_t := b - b_{axel} = 1.7\ m$

Assume it is acting in the middle of the bridge

$$M_T := \frac{q_{ULS} \cdot b^2}{8} + 2 \cdot \frac{Q_1 \cdot b_{axel} \cdot b_t}{L} = 53.693\ kN \cdot m$$

$$V_T := \frac{q_{ULS} \cdot b}{2} + 2 \cdot \frac{Q_1}{2} = 99.804\ kN$$

$\mu_{timber} := 0.3$

0.29-0.34

$$F_{ps.M} := \frac{6 \cdot M_T}{h_{reinforced}} = 0.453\ MN$$

$$F_{ps.V} := \frac{3 \cdot V_T}{2 \cdot \mu_{timber}} = 0.499\ MN$$

$F_{ps} := \max\left(F_{ps.M}, F_{ps.V}\right) = 0.499\ MN$

Ekholms rapport

Calculate necessary bearing length

$l_b := 260\ mm$

Assumed starting value

$$\sigma_{c.90.d} := \frac{V_{Ed}}{b \cdot l_b} = 0.566\ MPa$$

According to Equation 4.22 STDtE5

$$\text{if } f_{c.90.d} > \sigma_{c.90.d} \;\|\; \text{“OK”} \;\text{else}\; \|\; \text{“Increase support length”} = \text{“OK”}$$

Comparison between plain and reinforced cross-section

Moment capacity

$$\frac{M_{Ed}}{M_{Rd\_w}} = 51.298\%$$

$$\frac{M_{Ed}}{M_{Rd}} = 22.818\%$$

Deflections

$$\frac{\delta_{plain}}{\delta_{max}} = 68.493\% \qquad \frac{\delta_{plain.service}}{\delta_{max}} = 5.452\%$$

$$\frac{\delta_{reinforced}}{\delta_{max}} = 45.983\% \qquad \frac{\delta_{reinforced.service}}{\delta_{max}} = 10.981\%$$

Shear Capacity

$$\frac{\tau_{Ed}}{k_{cr} \cdot f_{vd}} = 18.758\%$$

Reduction in height

$h_{unreinforced} := 840\ mm$ 24 lamellas

$$1 - \frac{h_{reinforced}}{h_{unreinforced}} = 15.357\%$$

D

Mathcad NSM Beam

Material properties

Service class 3, according to swedish standards

Characterisic values Timber(GL28c, DoTS Volume 2 Table 3.4)

$f_{mk} := 28\ MPa$

$f_{ck} := 24\ MPa$

$f_{c.90.k} := 2.5\ MPa$

$f_{tk} := 19.5\ MPa$

$f_{vk} := 3.5\ MPa$

$f_{rk} := 1.2\ MPa$

$\rho_w := 420\ \frac{kg}{m^3}$ Mean density

$E_w := 10.4\ GPa$

$E_{mean} := 12.5\ GPa$

$\varepsilon_{c.el.gl} := \frac{f_{ck}}{E_w} = 2.308 \cdot 10^{-3}$

$\varepsilon_{t.el.gl} := \frac{f_{tk}}{E_w} = 1.875 \cdot 10^{-3}$

CFRP properties (S&P C laminat, product sheet)

$f_{t.cfrp} := 2800\ MPa$ Tensile strength

$f_{c.cfrp} := 1400\ MPa$ Compressive strength Assumption of half

$\rho_{cfrp} := 1600\ \frac{kg}{m^3}$ Density

$\gamma_{cfrp} := 1.0$ assuming certified manufacturer

$E_{cfrp} := 300\ GPa$

low = 205
mid = 300
high = 375
ultrahigh = 450

$\alpha := \frac{E_{cfrp}}{E_{mean}} = 24$

Beam geometry

Carbon fibre geometry

$b_{cfrp} := 2.6\ mm$

$h_{cfrp} := 30\ mm$

$A_{i.cfrp} := b_{cfrp} \cdot h_{cfrp} = 78\ mm^2$

$n_c := 4$ Number of laminations (comp)

$n_t := 4$ Number of laminations (tens)

$h_{last.lamella} := 15\ mm$

$n_{laminations} := 15$

$L := 20\ m$

$h := (n_{laminations} - 2) \cdot 45\ mm + 2 \cdot h_{last.lamella} = 615\ mm$

$b := 215\ mm$

$A_{gross} := b \cdot h = (1.322 \cdot 10^5)\ mm^2$

Distance to reinforcement

$y_c := h_{last.lamella} + \frac{h_{cfrp}}{2} = 30\ mm$

$y_t := h - \left(h_{last.lamella} + \frac{h_{cfrp}}{2}\right) = 585\ mm$

$A_{t.cfrp} := n_t \cdot A_{i.cfrp} = 312\ mm^2$ Area reinforcement on compression side

$A_{c.cfrp} := n_c \cdot A_{i.cfrp} = 312\ mm^2$ Area reinforcement on tension side

$A_{cfrp} := A_{t.cfrp} + A_{c.cfrp} = 624\ mm^2$ Total reinforcement area

$\frac{A_{cfrp}}{A_{gross}} = 0.472\%$

Ratio reinforcement in cross section

Timber geometry

$A_{timber} := b \cdot h - A_{cfrp} = (1.316 \cdot 10^5)\ mm^2$

Design Values Timber, values from DoTS volume 2

$k_{cr} := 0.67$ Reduction of shear capacity due to solar radiation and percipitation

$\gamma_{glulam} := 1.25$ Partial factor for material properties in glulam

$k_{def} := 2$ Factor considering long term effects, service class 3

$$k_h := \begin{cases} \min\left(\left(\frac{600\ mm}{h}\right)^{0.1}, 1.1\right) & \text{if } h < 600\ mm \\ 1 & \text{else if } h \geq 600\ mm \end{cases} = 1$$

Size factor, DoTS section 3.3 Volume 2

$k_{mod.glulam} := 0.8$ Factor considering duration of load and service class 3

$k_{c.90} := 1$ Support condition factor, according to section 5.2 DoTS

$$f_{md} := \frac{k_h \cdot f_{mk} \cdot k_{mod.glulam}}{\gamma_{glulam}} = 17.92\ MPa$$

$$f_{cd} := \frac{f_{ck} \cdot k_{mod.glulam}}{\gamma_{glulam}} = 15.36\ MPa$$

$$f_{c.90.d} := \frac{k_{c.90} \cdot k_{mod.glulam} \cdot f_{c.90.k}}{\gamma_{glulam}} = 1.6\ MPa$$

$$f_{td} := \frac{f_{tk} \cdot k_{mod.glulam}}{\gamma_{glulam}} = 12.48\ MPa$$

$$f_{vd} := \frac{f_{vk} \cdot k_{mod.glulam}}{\gamma_{glulam}} = 2.24\ MPa$$

$$f_{rd} := \frac{f_{rk} \cdot k_{mod.glulam}}{\gamma_{glulam}} = 0.768\ MPa$$

$$E_{mean.fin} := \frac{E_{mean}}{1 + k_{def}} = 4.167\ GPa$$

Transformed area

$$A_{transformed} := A_{gross} + A_{cfrp} \cdot (\alpha - 1) = \left(1.466 \cdot 10^5\right)\ mm^2$$

Loads

$$g := 9.82\ \frac{m}{s^2}$$ Gravitational constant

$$g_k := \rho_w \cdot A_{timber} \cdot g + \rho_{cfrp} \cdot A_{cfrp} \cdot g = 0.553\ \frac{kN}{m}$$ Self-weight

$$q_k := 5\ \frac{kN}{m^2} \cdot b = 1.075\ \frac{kN}{m}$$ Distributed pedestrian load

$$M_{max} := \frac{(g_k + q_k) \cdot L^2}{8} = 81.379\ kN \cdot m$$

$$q_{ULS} := 1.35 \cdot g_k + 1.5 \cdot q_k = 2.358\ \frac{kN}{m}$$ Load combination according to ULS

$$M_{Ed} := \frac{q_{ULS} \cdot L^2}{8} = 117.924\ kN \cdot m$$

Resistance of cross section (plain timber)

$$W_{y.w} := \frac{b \cdot h^2}{6} = 0.014\ m^3$$

Assume that it is braced against lateral torsional buckling. kcrit=1

$$M_{Rd\_w} := W_{y.w} \cdot f_{md} = 242.871\ kN \cdot m$$

Plain timber deflection

$\psi_{red} := 0.4$

Reduction of traffic load, Eurocode 1

$\delta_{max} := \frac{L}{400} = 50\ mm$

Maximum allowed deflection, according to Trafikverket Krav Brobyggande

$$\delta_{plain} := \frac{5 \cdot (\psi_{red} \cdot q_k) \cdot L^4}{384 \cdot E_{mean.fin} \cdot \frac{b \cdot h^3}{12}} = 51.589\ mm$$

The influence of shear deformation on deflection is assumed to be small on the final deflection. Eurocode 1

Calculation of neutral axis

$$y_{NA} := \frac{A_{t.cfrp} \cdot y_t \cdot (\alpha - 1) + A_{c.cfrp} \cdot y_c \cdot (\alpha - 1) + A_{gross} \cdot \frac{h}{2}}{A_{transformed}} = 307.5\ mm$$

Stiffness of cross section

$b_{fic.cfrp} := \alpha \cdot b_{cfrp} = 62.4\ mm$

$$I_{gross} := \frac{b \cdot h^3}{12} = 0.004\ m^4$$

$$I_{c.holes} := (\alpha - 1)\ n_c \cdot \frac{b \cdot {h_{cfrp}}^3}{12} = (4.451 \cdot 10^{-5})\ m^4$$

$$I_{t.holes} := (\alpha - 1) \cdot n_t \cdot \frac{b \cdot {h_{cfrp}}^3}{12} = (4.451 \cdot 10^{-5})\ m^4$$

$$a_{gross} := y_{NA} - \frac{h}{2} = 0\ mm$$

$$a_{c.cfrp} := y_{NA} - h_{last.lamella} - \frac{h_{cfrp}}{2} = 277.5\ mm$$

$$a_{t.cfrp} := h - h_{last.lamella} - \frac{h_{cfrp}}{2} - y_{NA} = 277.5\ mm$$

$$I_{tot} := I_{gross} + I_{c.holes} + I_{t.holes} + A_{gross} \cdot {a_{gross}}^2 + (\alpha - 1)\left(A_{c.cfrp} \cdot {a_{c.cfrp}}^2 + A_{t.cfrp} \cdot {a_{t.cfrp}}^2\right) = 0.005\ m^4$$

$EI_{tot} := E_{mean} \cdot I_{tot} = 67.022\ MN \cdot m^2$

$E_d I_{tot} := E_{mean.fin} \cdot I_{tot} = 22.341\ MN \cdot m^2$

Resistance of cross section (CFRP reinforced)

$\varepsilon_t := \varepsilon_{t.el.gl} = 1.875 \cdot 10^{-3}$

$\varepsilon_c := \dfrac{\varepsilon_t \cdot y_{NA}}{h - y_{NA}} = 1.875 \cdot 10^{-3}$ $\qquad \varepsilon_c < \varepsilon_{c.el.gl} = 1$ $\qquad$ ok!

Strain compatability compression

$$\varepsilon_{c.cfrp.edge} := \varepsilon_c \cdot \frac{\left(y_{NA} - h_{last.lamella}\right)}{y_{NA}} = 1.784 \cdot 10^{-3}$$

$$\varepsilon_{c.cfrp.mid} := \varepsilon_c \cdot \frac{\left(y_{NA} - h_{last.lamella} - h_{cfrp}\right)}{y_{NA}} = 1.601 \cdot 10^{-3}$$

$$\varepsilon_{c.cfrp} := 0.5 \cdot \left(\varepsilon_{c.cfrp.edge} + \varepsilon_{c.cfrp.mid}\right) = 1.692 \cdot 10^{-3}$$

Strain compatability tension

$$\varepsilon_{t.cfrp.mid} := \left(h - y_{NA} - h_{last.lamella} - h_{cfrp}\right) \frac{\varepsilon_t}{h - y_{NA}} = 1.601 \cdot 10^{-3}$$

$$\varepsilon_{t.cfrp.edge} := \left(h - y_{NA} - h_{last.lamella}\right) \frac{\varepsilon_t}{h - y_{NA}} = 1.784 \cdot 10^{-3}$$

$$\varepsilon_{t.cfrp} := 0.5 \cdot \left(\varepsilon_{t.cfrp.mid} + \varepsilon_{t.cfrp.edge}\right) = 1.692 \cdot 10^{-3}$$

Section forces

$$F_{c.edge} := 0.5 \cdot \left(\varepsilon_{c.cfrp.edge} + \varepsilon_c\right) \cdot E_w \cdot h_{last.lamella} \cdot b = 61.354\ kN$$

$$F_{c.w.cfrp} := \varepsilon_{c.cfrp} \cdot E_w \cdot h_{cfrp} \cdot \left(b - n_c \cdot b_{cfrp}\right) = 108.014\ kN$$

$$F_{c.mid} := 0.5 \cdot \varepsilon_{c.cfrp.mid} \cdot E_w \cdot \left(y_{NA} - h_{cfrp} - h_{last.lamella}\right) \cdot b = 469.739\ kN$$

$$F_{t.mid} := 0.5 \cdot \varepsilon_{t.cfrp.mid} \cdot E_w \cdot \left(h - y_{NA} - h_{last.lamella} - h_{cfrp}\right) \cdot b = 469.739\ kN$$

$$F_{t.w.cfrp} := \varepsilon_{t.cfrp} \cdot E_w \cdot h_{cfrp} \cdot \left(b - n_t \cdot b_{cfrp}\right) = 108.014\ kN$$

$$F_{t.edge} := 0.5 \cdot \left(\varepsilon_{t.cfrp.edge} + \varepsilon_t\right) \cdot E_w \cdot h_{last.lamella} \cdot b = 61.354\ kN$$

$$F_{t.cfrp} := \varepsilon_{t.cfrp} \cdot E_{cfrp} \cdot A_{t.cfrp} = 158.378\ kN$$

$$F_{c.cfrp} := \varepsilon_{c.cfrp} \cdot E_{cfrp} \cdot A_{c.cfrp} = 158.378\ kN$$

Check horizontal equilibrium

$F_{c.edge} + F_{c.w.cfrp} + F_{c.mid} + F_{c.cfrp} = 797.484\ kN$ Compression

$F_{t.edge} + F_{t.w.cfrp} + F_{t.mid} + F_{t.cfrp} = 797.484\ kN$ Tension

Moment capacity

Lever arms (distance from top)

$$z_1 := \frac{h_{last.lamella} \cdot \varepsilon_{c.cfrp.edge} \cdot \dfrac{h_{last.lamella}}{2} + h_{last.lamella} \cdot \dfrac{(\varepsilon_c - \varepsilon_{c.cfrp.edge})}{2} \cdot \dfrac{h_{last.lamella}}{3}}{h_{last.lamella} \cdot \varepsilon_{c.cfrp.edge} + h_{last.lamella} \cdot \dfrac{(\varepsilon_c - \varepsilon_{c.cfrp.edge})}{2}} = 7.438\ mm$$

$$z_2 := h_{last.lamella} + \frac{h_{cfrp} \cdot \varepsilon_{c.cfrp.mid} \cdot \dfrac{h_{cfrp}}{2} + h_{cfrp} \cdot \dfrac{(\varepsilon_{c.cfrp.edge} - \varepsilon_{c.cfrp.mid})}{2} \cdot \dfrac{h_{cfrp}}{3}}{h_{cfrp} \cdot \varepsilon_{c.cfrp.mid} + h_{cfrp} \cdot \dfrac{(\varepsilon_{c.cfrp.edge} - \varepsilon_{c.cfrp.mid})}{2}} = 29.73\ mm$$

$$z_3 := h_{last.lamella} + h_{cfrp} + \frac{1}{3} \cdot (y_{NA} - (h_{last.lamella} + h_{cfrp})) = 132.5\ mm$$

$$z_4 := y_{NA} + \frac{2}{3}(h - y_{NA} - h_{cfrp} - h_{cfrp}) = 472.5\ mm$$

$$z_5 := h - h_{last.lamella} - \frac{h_{cfrp} \cdot \varepsilon_{t.cfrp.mid} \cdot \dfrac{h_{cfrp}}{2} + h_{cfrp} \cdot \dfrac{(\varepsilon_{t.cfrp.edge} - \varepsilon_{t.cfrp.mid})}{2} \cdot \dfrac{h_{cfrp}}{3}}{h_{cfrp} \cdot \varepsilon_{t.cfrp.mid} + h_{cfrp} \cdot \dfrac{(\varepsilon_{t.cfrp.edge} - \varepsilon_{t.cfrp.mid})}{2}} = 585.27\ mm$$

$$z_6 := h - \frac{h_{last.lamella} \cdot \varepsilon_{t.cfrp.edge} \cdot \dfrac{h_{last.lamella}}{2} + h_{last.lamella} \cdot \dfrac{(\varepsilon_t - \varepsilon_{t.cfrp.edge})}{2} \cdot \dfrac{h_{last.lamella}}{3}}{h_{last.lamella} \cdot \varepsilon_{t.cfrp.edge} + h_{last.lamella} \cdot \dfrac{(\varepsilon_t - \varepsilon_{t.cfrp.edge})}{2}} = 607.563\ mm$$

$$M_{Rd} := F_{c.edge} \cdot (z_6 - z_1) + (F_{c.cfrp} + F_{c.w.cfrp}) \cdot (z_6 - z_2) + F_{c.mid} \cdot (z_6 - z_3) + F_{t.mid} \cdot (z_6 - z_4) + (F_{t.cfrp} + F_{t.w.cfrp}) \cdot (z_6 - z_5) = 483.288\ kN \cdot m$$

Deflection of beam

$$\delta_{reinforced} := \frac{5 \cdot \psi_{red} \cdot q_k \cdot L^4}{384 \cdot E_d I_{tot}} = 40.099 \ mm$$

Shear Capacity, section 6 DoTS volume 2

$$h_{te} := y_{NA} - h_{last.lamella} - h_{cfrp} \cdot n_c = 172.5 \ mm$$

$$a_{te} := \frac{h_{te}}{2} = 86.25 \ mm$$

$$S_{xx} := \frac{h}{2} \cdot b \cdot \left(y_{NA} - \frac{h}{2}\right) + A_{c.cfrp} \cdot \left(y_{NA} - \frac{h}{2}\right) + b \cdot h_{te} \cdot a_{te} = 3.199\ 10^{-3} \ m^3$$

$$V_{Ed} := \left(q_{ULS}\right) \cdot \frac{L}{2} = 23.585 \ kN$$

$$\tau_{Ed} := \frac{S_{xx} \cdot V_{Ed}}{I_{tot} \cdot b} = 0.065 \ MPa$$

$$\tau_{Rd} := k_{cr} \cdot f_{vd} = 1.501 \ MPa$$

Dynamiska laster

$$S := b \cdot L = 4.3 \ m^2$$

$$P := 700 \ N$$

$$m_g := \frac{g_k}{g} = 56.271 \ \frac{kg}{m}$$

$$M_g := L \cdot m_g = \left(1.125 \cdot 10^3\right) \ kg$$

Traffic classes

$$d_{TC} := \begin{bmatrix} 0.2 \cdot \frac{P}{m^2} \\ 0.5 \cdot \frac{P}{m^2} \\ 1.0 \cdot \frac{P}{m^2} \\ 1.5 \cdot \frac{P}{m^2} \end{bmatrix} = \begin{bmatrix} 0.14 \\ 0.35 \\ 0.7 \\ 1.05 \end{bmatrix} \ \frac{kN}{m^2}$$

$$m_{TC} := m_g + \frac{b \cdot d_{TC}}{g} = \begin{bmatrix} 59.336 \\ 63.934 \\ 71.597 \\ 79.26 \end{bmatrix} \ \frac{kg}{m}$$

$$f_1 := \frac{1}{2 \cdot \pi} \cdot \frac{9.869}{L^2} \cdot \sqrt{\frac{EI_{tot}}{m_{TC}(2)}} = 3.799\ Hz$$

$$f_2 := \frac{1}{2 \cdot \pi} \cdot \frac{39.478}{L^2} \cdot \sqrt{\frac{EI_{tot}}{m_{TC}(2)}} = 15.198\ Hz$$

Comparison between plain and reinforced cross-section

Moment capacity

$$\frac{M_{Ed}}{M_{Rd\_w}} = 48.55\%$$

$$\frac{M_{Ed}}{M_{Rd}} = 24.4\%$$

Deflections

$$\frac{\delta_{plain}}{\delta_{max}} = 103.18\%$$

$$\frac{\delta_{reinforced}}{\delta_{max}} = 80.2\%$$

Shear capacity

$$\frac{\tau_{Ed}}{\tau_{Rd}} = 4.36\%$$

Reduction in height

$$h_{unreinforced} := 795\ mm$$

$$1 - \frac{h}{h_{unreinforced}} = 22.642\%$$

E

Python Script Pre-cambered Beam

```python
##############################################################################
### Appendix E: Pre-cambered beam script
### Authors: Adam Lennell and Christoffer Jonsson
### Last changed: 2019-06
##############################################################################

from part import *
from material import *
from section import *
from assembly import *
from step import *
from interaction import *
from load import *
from mesh import *
from optimization import *
from job import *
from sketch import *
from visualization import *
from connectorBehavior import *
from math import *

from abaqus import *
from abaqusConstants import *
from caeModules import *
from driverUtils import executeOnCaeStartup

# 'runModel' is a function where the input variables can be altered for the
# beam to have desired geometry
#
# preCamber - Amount of pre-camber [m]
# spanLength - Length of the span [m]
# noLamellas - Number of timber lamellas à 45 mm, excluding the two exterior lamellas
# CFRPHeight - Thickness of the CFRP lamina [m]
#
#
def runModel(preCamber, spanLength, noLamellas, CFRPHeight):

    myModel = mdb.Model('Model-1')

#-------------------- Generate model name ------------------------------------
    preCamberStr = str(preCamber*1000)
    cStr = preCamberStr[0:(len(preCamberStr)-2)]
    modelName = 'Camber' + cStr+ 'mm'

#-------------------- Input data --------------------------------------------
    lamellaHeight = 0.045

    width = 0.215
    CFRPWidth = 0.185
    extHeightInitial = 0.015
    extHeight = extHeightInitial+CFRPHeight
    midHeight = lamellaHeight*noLamellas
    totalHeight = 2*extHeight+midHeight

    # Support width
    l_sup = 0.1
    supHeight = 0.2

    # Total length of beam
    beamLength = spanLength+l_sup

    # Camber radius
    r = (pow(beamLength/2,2)+pow(preCamber,2))/(2*preCamber)

    # Material data
    densTimb = 420.0
    E1 = 0.7e9
    E2 = 12.6e9
    E3 = 0.37e9
    G12 = 0.72e9
    G13 = 0.03e9
    G23 = 0.35e9
```

```python
    ny12 = 0.03
    ny13 = 0.35
    ny23 = 0.04

    densCFRP = 1600.0
    E_CFRP = 300e9
    nyCFRP = 0.3

    # Load combination factors
    gamma_selfweight = 1.2
    gamma_traffic = 1.5
    gamma_temp = 1.5

    # Variable load and impulse load
    q_k = gamma_traffic*5000 # [N/m2]
    a_k = 100  # [N]

    # Tempartures
    startTemp = gamma_temp*20
    maxTemp = gamma_temp*40
    minTemp = gamma_temp*-20

    # Temperature expansion coefficients
    alpha_CFRP = -1e-06
    alpha_timber = 5e-06

    # Mesh sizes
    coarseSize = 0.04
    fineSize = 0.02

    # Part of beam that will be occupied by fine mesh
    meshPartition = 0.05

    # Initiate instance objects vector
    instanceObjects = []

    #-------------- Create parts ----------------------------------------------

    # Mid part
    timberProfile = myModel.ConstrainedSketch(name='__profile__', sheetSize=beamLength)
    timberProfile.Arc3Points( point1=(0.0, 0.0),
        point2=(beamLength, 0.0), point3=(beamLength/2, preCamber))

    timberProfile.linearPattern(angle1=0.0, angle2=
        90.0, geomList=(
        timberProfile.geometry.findAt((beamLength/2, preCamber),
        ), ), number1=1, number2=2, spacing1=1.0, spacing2=midHeight)

    timberProfile.Line(point1=(0.0, midHeight), point2=(0.0, 0.0))
    timberProfile.Line(point1=(beamLength, midHeight), point2=(beamLength, 0.0))

    timberPart = myModel.Part(dimensionality=THREE_D, name='mid', type=
        DEFORMABLE_BODY)
    timberPart.BaseSolidExtrude(depth=width, sketch=timberProfile)
    del timberProfile

    # CFRP part
    CFRPProfile = myModel.ConstrainedSketch(name='__profile__', sheetSize=beamLength)
    CFRPProfile.Arc3Points( point1=(0.0, 0.0),
        point2=(beamLength, 0.0), point3=(beamLength/2, preCamber))

    CFRPProfile.linearPattern(angle1=0.0, angle2=
        90.0, geomList=(
        CFRPProfile.geometry.findAt((beamLength/2, preCamber),
        ), ), number1=1, number2=2, spacing1=1.0, spacing2=CFRPHeight)

    CFRPProfile.Line(point1=(0.0, CFRPHeight), point2=(0.0, 0.0))
    CFRPProfile.Line(point1=(beamLength, CFRPHeight), point2=(beamLength, 0.0))

    CFRPPart = myModel.Part(dimensionality=THREE_D, name='CFRP', type=DEFORMABLE_BODY)
    CFRPPart.BaseSolidExtrude(depth=CFRPWidth, sketch=CFRPProfile)
```

```
        del CFRPProfile

        # Exterior parts
        extProfile = myModel.ConstrainedSketch(name='__profile__', sheetSize=beamLength)
        extProfile.Arc3Points( point1=(0.0, 0.0),
            point2=(beamLength, 0.0), point3=(beamLength/2, preCamber))

        extProfile.linearPattern(angle1=0.0, angle2=
            90.0, geomList=(
            extProfile.geometry.findAt((beamLength/2, preCamber),
            ), ), number1=1, number2=2, spacing1=1.0, spacing2=extHeight)

        extProfile.Line(point1=(0.0, extHeight), point2=(0.0, 0.0))
        extProfile.Line(point1=(beamLength, extHeight), point2=(beamLength, 0.0))

        extPartUpper = myModel.Part(dimensionality=THREE_D, name='Exterior upper',
        type=DEFORMABLE_BODY)
        extPartUpper.BaseSolidExtrude(depth=width, sketch=extProfile)
        del extProfile

        # Create another exterior part by copying the first one
        extPartLower = myModel.Part(name='Exterior lower', objectToCopy=extPartUpper)

        ############## Cut holes for CFRP in exterior parts ##############

        # Upper: Create sweep path for hole for CFRP
        sweepPath = myModel.ConstrainedSketch(gridSpacing=1.0, name='__sweep__',
            sheetSize=40.0, transform=extPartUpper.MakeSketchTransform(
            sketchPlane=extPartUpper.faces.findAt((0.001, extHeight/2, width), ),
            sketchPlaneSide=SIDE1, sketchUpEdge=extPartUpper.edges.findAt(
            (0.0, extHeight/2, width), ), sketchOrientation=LEFT, origin=(0.0, 0.0, 0.0)))
        extPartUpper.projectReferencesOntoSketch(filter=COPLANAR_EDGES, sketch=sweepPath)
        sweepPath.Arc3Points(point1=(0.0, 0.0),
            point2=(beamLength, 0.0), point3=(beamLength/2, preCamber))

        # Upper: Create profile for CFRP hole
        p = myModel.ConstrainedSketch(gridSpacing=0.01, name='__profile__',
            sheetSize=0.43, transform=
            extPartUpper.MakeSketchTransform(
            sketchPlane=extPartUpper.faces.findAt((0.0,
            extHeight/2, width/2), ), sketchPlaneSide=SIDE1,
            sketchUpEdge=extPartUpper.edges.findAt((0.0,
            extHeight/2, width), ), sketchOrientation=RIGHT, origin=(0.0, 0.0, 0.0)))
        extPartUpper.projectReferencesOntoSketch(filter=COPLANAR_EDGES, sketch=p)
        p.rectangle(point1=(0.015, 0.0), point2=(0.200, CFRPHeight))

        # Upper: Cut hole for CFRP
        extPartUpper.CutSweep(pathOrientation=LEFT, sketchOrientation=RIGHT,
            path=sweepPath, profile=p,
            pathPlane=extPartUpper.faces.findAt((0.001, extHeight/2, width), ),
            pathUpEdge=extPartUpper.edges.findAt((0.0, extHeight/2, width), ),
            sketchPlane=extPartUpper.faces.findAt((0.0, extHeight/2, width/2), ),
            sketchUpEdge=extPartUpper.edges.findAt((0.0, extHeight/2, width),))
        del sweepPath
        del p

        # Lower: Create sweep path for hole for CFRP
        sweepPath = myModel.ConstrainedSketch(gridSpacing=1.0, name='__sweep__',
            sheetSize=40.0, transform=extPartLower.MakeSketchTransform(
            sketchPlane=extPartLower.faces.findAt((0.001, extHeight/2, width), ),
            sketchPlaneSide=SIDE1, sketchUpEdge=extPartLower.edges.findAt(
            (0.0, extHeight/2, width), ), sketchOrientation=LEFT, origin=(0.0, 0.0, 0.0)))
        extPartLower.projectReferencesOntoSketch(filter=COPLANAR_EDGES, sketch=sweepPath)
        sweepPath.Arc3Points(point1=(0.0, 0.0),
            point2=(beamLength, 0.0), point3=(beamLength/2, preCamber))

        # Lower: Create profile for CFRP hole
        p = myModel.ConstrainedSketch(gridSpacing=0.01, name='__profile__',
            sheetSize=0.43, transform=
            extPartLower.MakeSketchTransform(
            sketchPlane=extPartLower.faces.findAt((0.0,
            extHeight/2, width/2), ), sketchPlaneSide=SIDE1,
```

```
            sketchUpEdge=extPartLower.edges.findAt((0.0,
            extHeight/2, width), ), sketchOrientation=RIGHT, origin=(0.0, 0.0, 0.0)))
        extPartLower.projectReferencesOntoSketch(filter=COPLANAR_EDGES, sketch=p)
        p.rectangle(point1=(0.015, extHeight-CFRPHeight), point2=(0.200, extHeight+0.1))

        # Lower: Cut hole for CFRP
        extPartLower.CutSweep(pathOrientation=LEFT, sketchOrientation=RIGHT,
            path=sweepPath, profile=p,
            pathPlane=extPartLower.faces.findAt((0.001, extHeight/2, width), ),
            pathUpEdge=extPartLower.edges.findAt((0.0, extHeight/2, width), ),
            sketchPlane=extPartLower.faces.findAt((0.0, extHeight/2, width/2), ),
            sketchUpEdge=extPartLower.edges.findAt((0.0, extHeight/2, width),))
        del sweepPath
        del p

        # Support beam - beam element to accurately model the boundary conditions
        beamSketch = myModel.ConstrainedSketch(name='__profile__', sheetSize=200.0)
        beamSketch.Line(point1=(0.0, 0.0), point2=(0.0, supHeight))
        beamPart = myModel.Part(dimensionality=THREE_D, name='SupportBeam', type=DEFORMABLE_BODY)
        beamPart.BaseWire(sketch=beamSketch)
        del beamSketch

        #-------------- Create materials ---------------------------------------------------
        timberMaterial = myModel.Material(name='Timber')
        timberMaterial.Density(table=((densTimb, ), ))
        timberMaterial.Elastic(table=((E1, E2, E3, ny12, ny13, ny23, G12, G13, G23), ),
            type=ENGINEERING_CONSTANTS)
        timberMaterial.Expansion(table=((alpha_timber, ), ))

        CFRPMaterial = myModel.Material(name='CFRP')
        CFRPMaterial.Density(table=((densCFRP,),))
        CFRPMaterial.Elastic(table=((E_CFRP, nyCFRP),))
        CFRPMaterial.Expansion(table=((alpha_CFRP, ), ))

        supportMaterial = myModel.Material(name='Support')
        supportMaterial.Elastic(table=((1e15, nyCFRP),))
        supportMaterial.Density(table=((0.001,),))

        #-------------- Define local orientation of timber with cylindrical coordinates------
        import regionToolset
        # Middle Part
        v1 = timberPart.vertices

        timberPart.DatumCsysByThreePoints(point1=v1.findAt(coordinates=(0.0, 0.0, 0.0)),
            point2=v1.findAt(coordinates=(beamLength, 0.0, 0.0)), name='CylCSYS',
            coordSysType=CYLINDRICAL, origin=(beamLength/2, preCamber-r, 0.0))

        c1 = timberPart.cells
        cells1 = c1.findAt(((0.0, 0.0, 0.0), ))
        reg1 = regionToolset.Region(cells=cells1)
        orientation1 = timberPart.datums[2]

        timberPart.MaterialOrientation(region=reg1, orientationType=SYSTEM, axis=AXIS_3,
            localCsys=orientation1)

        # Upper Part
        v2 = extPartUpper.vertices
        extPartUpper.DatumCsysByThreePoints(point1=v2.findAt(coordinates=(0.0, 0.0, 0.0)),
            point2=v2.findAt(coordinates=(beamLength, 0.0, 0.0)), name='CylCSYS',
            coordSysType=CYLINDRICAL, origin=(beamLength/2, preCamber-r, 0.0))

        c2 = extPartUpper.cells
        cells2 = c2.findAt(((0.0, 0.0, 0.0), ))
        reg2 = regionToolset.Region(cells=cells2)
        orientation2 = extPartUpper.datums[3]

        extPartUpper.MaterialOrientation(region=reg2, orientationType=SYSTEM, axis=AXIS_3,
```

```
        localCsys=orientation2)

    # Lower Part
    v3 = extPartLower.vertices
    extPartLower.DatumCsysByThreePoints(point1=v3.findAt(coordinates=(0.0, 0.0, 0.0)),
        point2=v3.findAt(coordinates=(beamLength, 0.0, 0.0)), name='CylCSYS',
        coordSysType=CYLINDRICAL, origin=(beamLength/2, preCamber-r, 0.0))

    c = extPartLower.cells
    cells = c.findAt(((0.0, 0.0, 0.0), ))
    reg = regionToolset.Region(cells=cells)
    orientation = extPartLower.datums[3]

    extPartLower.MaterialOrientation(region=reg, orientationType=SYSTEM, axis=AXIS_3,
        localCsys=orientation)

    # Add orientation of support beam
    beamPart.assignBeamSectionOrientation(method=N1_COSINES,
        n1=(0.0, 0.0, -1.0), region=Region(
        edges=beamPart.edges.findAt(((0.0, supHeight/2,
        0.0), ), )))
    #-------------- Assign materials to section -----------------------------------------
    myModel.HomogeneousSolidSection(material='Timber', name='TimberSec')
    myModel.HomogeneousSolidSection(material='CFRP', name='CFRPSec')
    myModel.CircularProfile(name='BeamProfile', r=0.01)
    myModel.BeamSection(consistentMassMatrix=False, integration=
        DURING_ANALYSIS, material='Support', name='SupportSec',
        poissonRatio=0.0, profile='BeamProfile', temperatureVar=LINEAR)

    #-------------- Assigns cfrp section to cfrp sheet
    CFRPPart.SectionAssignment(region=Region(cells=CFRPPart.cells.findAt(
        ((0.0, 0.0, 0.0), ), )), sectionName='CFRPSec',
        thicknessAssignment=FROM_SECTION)

    #-------------- Assigns timber section to timber lamellas
    timberPart.SectionAssignment(region=Region(cells=timberPart.cells.findAt(
        ((0.0, 0.0, 0.0), ), )), sectionName='TimberSec',
        thicknessAssignment=FROM_SECTION)

    extPartUpper.SectionAssignment(region=Region(cells=extPartUpper.cells.findAt(
        ((0.0, 0.0, 0.0), ), )), sectionName='TimberSec',
        thicknessAssignment=FROM_SECTION)

    extPartLower.SectionAssignment(region=Region(cells=extPartLower.cells.findAt(
        ((0.0, 0.0, 0.0), ), )), sectionName='TimberSec',
        thicknessAssignment=FROM_SECTION)

    beamPart.SectionAssignment(region=Region(edges=beamPart.edges.findAt(
        ((0.0, supHeight/2, 0.0), ), )), sectionName='SupportSec',
        thicknessAssignment=FROM_SECTION)

    #-------------- Create instances with cfrp sheet and timber lamella and create assembly ---------------
    myAssembly = myModel.rootAssembly
    myAssembly.DatumCsysByDefault(CARTESIAN)

    CFRPInstance = myAssembly.Instance(dependent=OFF, name='CFRP sheet', part=CFRPPart)
    timberInstance = myAssembly.Instance(dependent=OFF, name='Wood lamella', part=timberPart)
    extInstanceUpper = myAssembly.Instance(dependent=OFF, name='Outer lamella top', part=extPartUpper)
    extInstanceLower = myAssembly.Instance(dependent=OFF, name='Outer lamella bottom', part=extPartLower)
    supInstance = myAssembly.Instance(dependent=OFF, name='Left support', part=beamPart)

    #-------------- Assemble ---------------------------------------------------------------------------

```

```python
        # First lamella from bottom
        instanceObjects.append(extInstanceLower)

        # CFRP
        myAssembly.translate(instanceList=('CFRP sheet', ),
            vector=(0.0, extHeightInitial, 0.015))
        instanceObjects.append(CFRPInstance)

        # Middle Part
        myAssembly.translate(instanceList=('Wood lamella', ),
            vector=(0.0, extHeight, 0.0))
        instanceObjects.append(timberInstance)

        # CFRP
        myAssembly.LinearInstancePattern(instanceList=('CFRP sheet', ), number1=1, number2=2,
            spacing1=0, spacing2=CFRPHeight+midHeight, direction1=(0.0, 0.0,
            0.0), direction2=(0.0, 1.0, 0.0))
        instanceObjects.append(myAssembly.instances['CFRP sheet-lin-1-2'])

        # Last wood lamella
        myAssembly.translate(instanceList=('Outer lamella top', ),
            vector=(0.0, midHeight+extHeight, 0.0))
        instanceObjects.append(myAssembly.instances['Outer lamella top'])

        # Left support
        myAssembly.translate(instanceList=('Left support', ),
            vector=(l_sup/2, -supHeight, width/2))
        instanceObjects.append(myAssembly.instances['Left support'])

        # Right support
        myAssembly.LinearInstancePattern(instanceList=('Left support', ), number1=2, number2=1,
            spacing1=spanLength, spacing2=0.0, direction1=(1.0, 0.0,
            0.0), direction2=(0.0, 0.0, 0.0))
        instanceObjects.append(myAssembly.instances['Left support-lin-2-1'])

        #-------------- Create coordinate vector for instances -----------------------------------------------
        instanceCoordinates = []
        instanceCoordinates.append((0.0, 0.0, 0.0))
        instanceCoordinates.append((0.0, extHeightInitial, 0.015))
        instanceCoordinates.append((0.0, extHeight, 0.0))
        instanceCoordinates.append((0.0, extHeight+midHeight, 0.015))
        instanceCoordinates.append((0.0, extHeight+CFRPHeight+midHeight, 0.0))

        #-------------- Creates step ----------------------------------------------------------------
        myModel.StaticStep(name='Self-weight', nlgeom=OFF,
            previous='Initial')

        myModel.StaticStep(name='Traffic', nlgeom=OFF, previous='Self-weight')

        # Create initial field for temperature at the region for all the model
        reg = regionToolset.Region(cells=instanceObjects[0].cells.findAt((instanceCoordinates[0] , ), ) +\
            instanceObjects[1].cells.findAt((instanceCoordinates[1] , ), ) +\
            instanceObjects[2].cells.findAt((instanceCoordinates[2] , ), ) +\
            instanceObjects[3].cells.findAt((instanceCoordinates[3] , ), ) +\
            instanceObjects[4].cells.findAt((instanceCoordinates[4] , ), ))
        myModel.Temperature(createStepName='Initial',
            crossSectionDistribution=CONSTANT_THROUGH_THICKNESS, distributionType=
            UNIFORM, magnitudes=(startTemp, ), name='Start Temperature', region=reg)

        myModel.StaticStep(name='CoolDown', previous='Traffic')
        myModel.Temperature(createStepName='CoolDown',
            crossSectionDistribution=CONSTANT_THROUGH_THICKNESS, distributionType=
            UNIFORM, magnitudes=(maxTemp, ), name='MaxTemperature', region=reg)

        # Put field output requests
        myModel.fieldOutputRequests['F-Output-1'].setValues(variables=(
```

```
            'S', 'U'))

        #-------------- Apply load to step -----------------------------------------------------------
        myModel.Gravity(comp2=-9.82*gamma_selfweight, createStepName='Self-weight', name='Gravity')

        myModel.Pressure(name='Variable load', createStepName='Traffic', magnitude=q_k,
            region=Region(side1Faces=instanceObjects[4].faces.findAt((
            (beamLength/2, totalHeight+preCamber, width/2), ), )))

        #-------------- Creates tie between materials by partiotioning the assembly -----------------
        p1 = myAssembly.DatumPlaneByPrincipalPlane(offset=0.015, principalPlane=XYPLANE)
        p2 = myAssembly.DatumPlaneByPrincipalPlane(offset=0.2, principalPlane=XYPLANE)

        f = instanceObjects[2].faces

        faceCoord1 = (l_sup, totalHeight-extHeight, width/2)
        faceCoord2 = (l_sup, extHeight, width/2)
        e1 = f.getClosest(coordinates=(faceCoord1, ))
        e2 = f.getClosest(coordinates=(faceCoord2, ))

        myAssembly.PartitionFaceByDatumPlane(datumPlane=myAssembly.datums[p1.id], faces=
            instanceObjects[2].faces.findAt(e1[0][0].pointOn) +\
            instanceObjects[2].faces.findAt(e2[0][0].pointOn))

        faceCoord1 = (l_sup, totalHeight-extHeight, width/2)
        faceCoord2 = (l_sup, extHeight, width/2)
        e1 = f.getClosest(coordinates=(faceCoord1, ))
        e2 = f.getClosest(coordinates=(faceCoord2, ))

        myAssembly.PartitionFaceByDatumPlane(datumPlane=myAssembly.datums[p2.id], faces=
            instanceObjects[2].faces.findAt(e1[0][0].pointOn) +\
            instanceObjects[2].faces.findAt(e2[0][0].pointOn))

        # Add ties between timber lamellas and CFRP
        for x in range(1, 5):
            tieCoord = (beamLength/2, instanceCoordinates[x][1]+preCamber, width/2)

            f = instanceObjects[x].faces
            e = f.getClosest(coordinates=(tieCoord,))
            slaveReg = regionToolset.Region(faces=instanceObjects[x].faces.findAt(e[0][0].pointOn))

            f = instanceObjects[x-1].faces
            e = f.getClosest(coordinates=(tieCoord,))
            masterReg = regionToolset.Region(faces=instanceObjects[x-1].faces.findAt(e[0][0].pointOn))

            myModel.Tie(name='Constraint-' + str(x), master=masterReg, slave=slaveReg)

        #-------------- Create partitions for boundaries and mesh -----------------------------------
        # Partition x-coord
        leftEdge = beamLength*meshPartition
        rightEdge = beamLength-beamLength*meshPartition
        leftSupport = l_sup
        rightSupport = beamLength-l_sup

        # Create datum planes for partitions
        meshPartition1 = myAssembly.DatumPlaneByPrincipalPlane(offset=leftEdge, principalPlane=YZPLANE)
        meshPartition2 = myAssembly.DatumPlaneByPrincipalPlane(offset=rightEdge, principalPlane=YZPLANE)
        supportPartition1 = myAssembly.DatumPlaneByPrincipalPlane(offset=leftSupport, principalPlane=YZPLANE)
        supportPartition2 = myAssembly.DatumPlaneByPrincipalPlane(offset=rightSupport, principalPlane=YZPLANE)

        # Extract datum ids
        index1 = meshPartition1.id
```

```
        index2 = meshPartition2.id
        index3 = supportPartition1.id
        index4 = supportPartition2.id

        # Partition cells by the datum planes for denser mesh
        myAssembly.PartitionCellByDatumPlane(cells=
            instanceObjects[0].cells.findAt((instanceCoordinates[0] , ), ) +\
            instanceObjects[1].cells.findAt((instanceCoordinates[1] , ), ) +\
            instanceObjects[2].cells.findAt((instanceCoordinates[2] , ), ) +\
            instanceObjects[3].cells.findAt((instanceCoordinates[3] , ), ) +\
            instanceObjects[4].cells.findAt((instanceCoordinates[4] , ), ),
            datumPlane = myAssembly.datums[index2])

        myAssembly.PartitionCellByDatumPlane(cells=
            instanceObjects[0].cells.findAt((instanceCoordinates[0] , ), ) +\
            instanceObjects[1].cells.findAt((instanceCoordinates[1] , ), ) +\
            instanceObjects[2].cells.findAt((instanceCoordinates[2] , ), ) +\
            instanceObjects[3].cells.findAt((instanceCoordinates[3] , ), ) +\
            instanceObjects[4].cells.findAt((instanceCoordinates[4] , ), ),
            datumPlane = myAssembly.datums[index1])

        # Partition faces by the datum planes for boundary conditions
        myAssembly.PartitionCellByDatumPlane(cells=
            instanceObjects[0].cells.findAt(((0.0, 0.0, 0.0) , ), ),
            datumPlane = myAssembly.datums[index3])

        myAssembly.PartitionCellByDatumPlane(cells=
            instanceObjects[0].cells.findAt(((beamLength, 0.0, 0.0) , ), ),
            datumPlane = myAssembly.datums[index4])

        #-------------- Tie support to beam --------------------------------------------------------------
        f = instanceObjects[0].faces

        # Left support, center of face coordinates
        x_face = l_sup/2
        y_face = preCamber-r+sqrt(pow(r,2)-pow((beamLength-l_sup)/2,2))
        z_face = width/2

        e = f.getClosest(coordinates=((x_face, y_face, z_face),))
        supportSet1 = myAssembly.Set(faces=instanceObjects[0].faces.findAt(e[0][0].pointOn), name='Left support')

        myModel.Tie(adjust=OFF, master=Region(
            vertices=instanceObjects[5].vertices.findAt(((l_sup/2, 0.0, width/2), ), )),
            name='Left Support Tie', positionToleranceMethod=SPECIFIED, positionTolerance=width,
            slave=supportSet1, thickness=ON, tieRotations=ON)

        # Right support, center of face coordinates
        x_face = beamLength-l_sup/2

        e = f.getClosest(coordinates=((x_face, y_face, z_face),))
        supportSet2 = myAssembly.Set(faces=instanceObjects[0].faces.findAt(e[0][0].pointOn), name='Right support')

        myModel.Tie(adjust=OFF, master=Region(
            vertices=instanceObjects[6].vertices.findAt(((beamLength-l_sup/2, 0.0, width/2), ), )),
            name='Right Support Tie', positionToleranceMethod=SPECIFIED, positionTolerance=width,
            slave=supportSet2, thickness=ON, tieRotations=ON)

        #-------------- Boundary conditions --------------------------------------------------------------
        # Left boundary
        myModel.DisplacementBC(amplitude=UNSET, createStepName='Initial',
            distributionType=UNIFORM, name='Left support', region=Region(
            vertices=instanceObjects[5].vertices.findAt(((l_sup/2, -supHeight, width/2), ), )),
```

```
        u1=SET, u2=SET, u3=UNSET, ur1=UNSET, ur2=UNSET, ur3=UNSET)

    myModel.DisplacementBC(amplitude=UNSET, createStepName='Initial',
        distributionType=UNIFORM, name='Left z', region=Region(
        vertices = instanceObjects[5].edges.findAt(((l_sup/2, 0.0, width/2), ), )),
        u1=UNSET, u2=UNSET, u3=SET, ur1=UNSET, ur2=UNSET, ur3=UNSET)

    # Right boundary
    myModel.DisplacementBC(amplitude=UNSET, createStepName='Initial',
        distributionType=UNIFORM, name='Right support', region=Region(
        vertices=instanceObjects[6].vertices.findAt(((beamLength-l_sup/2, -supHeight, width/2), ), )),
        u1=UNSET, u2=SET, u3=UNSET, ur1=UNSET, ur2=UNSET, ur3=UNSET)

    myModel.DisplacementBC(amplitude=UNSET, createStepName='Initial',
        distributionType=UNIFORM, name='Right z', region=Region(
        edges = instanceObjects[6].edges.findAt(((beamLength-l_sup/2, 0.0, width/2), ), )),
        u1=UNSET, u2=UNSET, u3=SET, ur1=UNSET, ur2=UNSET, ur3=UNSET)

    #----------------- Mesh controls ---------------------------------------------------------
    myAssembly.PartitionFaceByAuto(face=instanceObjects[0].faces.findAt(coordinates=(0.0, extHeight/2, width/2)))
    myAssembly.PartitionFaceByAuto(face=instanceObjects[4].faces.findAt(coordinates=(0.0, totalHeight-extHeight/2, width/2)))
    myAssembly.PartitionFaceByAuto(face=instanceObjects[0].faces.findAt(coordinates=(beamLength, extHeight/2, width/2)))
    myAssembly.PartitionFaceByAuto(face=instanceObjects[4].faces.findAt(coordinates=(beamLength, totalHeight-extHeight/2, width/2)))


    # Seed the coarse size to the whole assembly
    myAssembly.seedPartInstance(
        deviationFactor=0.001, minSizeFactor=0.0001, regions=(
        instanceObjects), size=coarseSize)


    # Seed finer mesh at the ends of the beam
    delta = 1.0 # Margin for bounding box
    endEdges = []
    for i in myAssembly.instances.keys():
        for j in myAssembly.instances[i].edges.getByBoundingBox(
                0.0-delta, 0.0-delta, 0.0-delta, leftEdge+delta, totalHeight+delta, width+delta):
            endEdges.append(j)


    for i in myAssembly.instances.keys():
        for j in myAssembly.instances[i].edges.getByBoundingBox(
                rightEdge-delta,0.0-delta,0.0-delta,beamLength+delta,totalHeight+delta,width+delta):
            endEdges.append(j)


    myAssembly.seedEdgeBySize(constraint=FINER,
        deviationFactor=0.001, edges=
        endEdges, minSizeFactor=0.0001, size=fineSize)


    #----------------- Generate mesh -------------------------------------------------------
    myAssembly.generateMesh(regions=instanceObjects)

    #----------------- Create job ----------------------------------------------------------
    myJob = mdb.Job(name='Static' + modelName, model='Model-1')
```

```
    myJob.setValues(description='', memoryUnits=PERCENTAGE, memory=50, numCpus=1,
    numDomains=1)
    myJob.setValues(queue='BrigadePlusQueue')
    myJob.submit(datacheckJob=False)
    myJob.waitForCompletion()

    #--------------------- Output
    ------------------------------------------------------------
    myVp = session.Viewport(name='Viewport: 1', origin=(0.0, 0.0), width=40.02,
    height=40.0)
    myVp.makeCurrent()
    myVp.maximize()

    executeOnCaeStartup()
    odbName = 'Static' + modelName
    o1 = session.openOdb(name='C:/BRIGADE Plus Work Directory/' + odbName + '.odb')

    myVp.setValues(displayedObject=o1)

    #--------------Create paths for output
    -----------------------------------------------
    myVp.odbDisplay.display.setValues(plotState=(CONTOURS_ON_UNDEF, ))

    longPathTop = session.Path(name=('LongCFRPTop'+ modelName),
    type=CIRCUMFERENTIAL, expression=(
        (0, totalHeight-extHeightInitial, width/2),
        (beamLength/2, totalHeight+preCamber-extHeightInitial, width/2),
        (beamLength, totalHeight-extHeightInitial, width/2)),
        circleDefinition=POINT_ARC, numSegments=500, startAngle=0,
        endAngle=(180/pi)*2*atan((beamLength/2)/(r-preCamber)),
        radius=CIRCLE_RADIUS)

    longPathTop2 = session.Path(name=('LongCFRPTop2'+ modelName),
    type=CIRCUMFERENTIAL, expression=(
        (0, totalHeight-extHeight, width/2),
        (beamLength/2, totalHeight+preCamber-extHeight, width/2),
        (beamLength, totalHeight-extHeight, width/2)),
        circleDefinition=POINT_ARC, numSegments=500, startAngle=0,
        endAngle=(180/pi)*2*atan((beamLength/2)/(r-preCamber)),
        radius=CIRCLE_RADIUS)

    middlePath = session.Path(name=('LongMiddle'+modelName), type=CIRCUMFERENTIAL,
    expression=(
        (0, totalHeight/2, width/2),
        (beamLength/2, totalHeight/2+preCamber, width/2),
        (beamLength, totalHeight/2, width/2)),
        circleDefinition=POINT_ARC, numSegments=500, startAngle=0,
        endAngle=(180/pi)*2*atan((beamLength/2)/(r-preCamber)),
        radius=CIRCLE_RADIUS)

    longPathBottom = session.Path(name=('LongCFRPBottom' + modelName),
    type=CIRCUMFERENTIAL, expression=(
        (0, extHeightInitial, width/2),
        (beamLength/2, extHeightInitial+preCamber, width/2),
        (beamLength, extHeightInitial, width/2)),
        circleDefinition=POINT_ARC, numSegments=500, startAngle=0,
        endAngle=(180/pi)*2*atan((beamLength/2)/(r-preCamber)),
        radius=CIRCLE_RADIUS)

    longPathBottom2 = session.Path(name=('LongCFRPBottom2' + modelName),
    type=CIRCUMFERENTIAL, expression=(
        (0, extHeight, width/2),
        (beamLength/2, extHeight+preCamber, width/2),
        (beamLength, extHeight, width/2)),
        circleDefinition=POINT_ARC, numSegments=500, startAngle=0,
        endAngle=(180/pi)*2*atan((beamLength/2)/(r-preCamber)),
        radius=CIRCLE_RADIUS)

    transPathEdge = session.Path(name=('TransShear' + modelName), type=POINT_LIST,
        expression=((beamLength*0.0025, 0.0, width/2), (beamLength*0.0025,
        preCamber+totalHeight, width/2)))

```

```
    transPathMiddle = session.Path(name=('TransShearMiddle' + modelName),
    type=POINT_LIST,
        expression=((beamLength/2, 0.0, width/2), (beamLength/2,
        preCamber+totalHeight, width/2)))

    #--------------------- Create stress plots
    ---------------------------------------------
    myVp.odbDisplay.setPrimaryVariable(variableLabel='S',
    outputPosition=INTEGRATION_POINT,
        refinement=(COMPONENT, 'S22'), )

    myDataTransEdge = session.XYDataFromPath(name = ('TransSupport' + modelName),
    path=transPathEdge, includeIntersections=True,
        projectOntoMesh=False, pathStyle=PATH_POINTS, numIntervals=30,
        projectionTolerance=0, shape=UNDEFORMED, labelType=TRUE_DISTANCE)

    myDataTransMid = session.XYDataFromPath(name = ('TransMid' + modelName),
    path=transPathMiddle, includeIntersections=True,
        projectOntoMesh=False, pathStyle=PATH_POINTS, numIntervals=30,
        projectionTolerance=0, shape=UNDEFORMED, labelType=TRUE_DISTANCE)

    myVp.odbDisplay.setPrimaryVariable(
       variableLabel='S', outputPosition=INTEGRATION_POINT, refinement=(COMPONENT,
       'S12'), )

    leaf = dgo.LeafFromPartInstance(partInstanceName=('CFRP sheet-lin-1-2', ))
    myVp.odbDisplay.displayGroup.remove(leaf=leaf)
    leaf = dgo.LeafFromPartInstance(partInstanceName=('CFRP sheet', ))
    myVp.odbDisplay.displayGroup.remove(leaf=leaf)

    myData1 = session.XYDataFromPath(name='TopTop Shear' + modelName,
    path=longPathTop, includeIntersections=True,
        projectOntoMesh=False, pathStyle=PATH_POINTS,
        projectionTolerance=0, shape=UNDEFORMED, labelType=TRUE_DISTANCE)

    myData2 = session.XYDataFromPath(name='TopBottom Shear' + modelName,
    path=longPathTop2, includeIntersections=True,
        projectOntoMesh=False, pathStyle=PATH_POINTS,
        projectionTolerance=0, shape=UNDEFORMED, labelType=TRUE_DISTANCE)

    myData3 = session.XYDataFromPath(name='BottomBottom Shear' + modelName,
    path=longPathBottom, includeIntersections=True,
        projectOntoMesh=False, pathStyle=PATH_POINTS,
        projectionTolerance=0, shape=UNDEFORMED, labelType=TRUE_DISTANCE)

    myData4 = session.XYDataFromPath(name='BottomTop Shear' + modelName,
    path=longPathBottom2, includeIntersections=True,
        projectOntoMesh=False, pathStyle=PATH_POINTS,
        projectionTolerance=0, shape=UNDEFORMED, labelType=TRUE_DISTANCE)

    myData5 = session.XYDataFromPath(name='Middle Shear' + modelName,
    path=middlePath, includeIntersections=True,
        projectOntoMesh=False, pathStyle=PATH_POINTS,
        projectionTolerance=0, shape=UNDEFORMED, labelType=TRUE_DISTANCE)

    #--------------------- Extract data to text files
    ---------------------------------
    session.writeXYReport('TopTop' + modelName + '.txt', xyData=myData1)
    session.writeXYReport('TopBottom' + modelName + '.txt', xyData=myData2)
    session.writeXYReport('BottomBottom' + modelName + '.txt', xyData=myData3)
    session.writeXYReport('BottomTop' + modelName + '.txt', xyData=myData4)

    session.writeXYReport('S22 middle' + modelName + '.txt', xyData=myDataTransMid)

# Input variables to the funtion 'runModel'
noL = 12
l = 20
cHeight = 0.005

# Loop for pre-camber cases 25, 50, 75, .... , 250 mm
for x in range(1,11):
    pC = 0.025*x
```

```
    runModel(pC, l, noL, cHeight)
```